

UNCLASSIFIED

AD NUMBER

AD918677

LIMITATION CHANGES

TO:

Approved for public release; distribution is unlimited.

FROM:

Distribution authorized to U.S. Gov't. agencies only; Test and Evaluation; JAN 1974. Other requests shall be referred to Air Force Rocket Propulsion Lab., Edwards AFB, CA.

AUTHORITY

AFRPL ltr 13 May 1966

THIS PAGE IS UNCLASSIFIED

**THIS REPORT HAS BEEN DELIMITED
AND CLEARED FOR PUBLIC RELEASE
UNDER DOD DIRECTIVE 5200.20 AND
NO RESTRICTIONS ARE IMPOSED UPON
ITS USE AND DISCLOSURE.**

DISTRIBUTION STATEMENT A

**APPROVED FOR PUBLIC RELEASE;
DISTRIBUTION UNLIMITED.**

AD 918 677

AUTHORITY:

AERPL etc.,

13 May 86



AFRPL-TR-72-112

DEVELOPMENT OF LARGE DIAMETER HIGH CHAMBER PRESSURE THROAT INSERT MATERIALS

Volume III

Vapor Deposition of Pyrolytic Graphite Coatings For Large Diameter Throat Inserts

Final Report

Contract F04611-70-C-0009

Period Covered

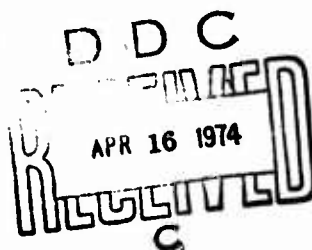
15 February 1970 to 1 September 1972

Author:

Kenneth E. Undercoffer

1974

AFRPL-TR-72-112



Prepared by:

ATLANTIC RESEARCH CORPORATION
5390 CHEROKEE AVE.
ALEXANDRIA, VIRGINIA 22314

AIR FORCE ROCKET PROPULSION LABORATORY
DIRECTOR OF SCIENCE AND TECHNOLOGY

Air Force Systems Command
Edwards, California

AD918677

UNCLASSIFIED

SECURITY CLASSIFICATION OF THIS PAGE (When Data Entered)

REPORT DOCUMENTATION PAGE		READ INSTRUCTIONS BEFORE COMPLETING FORM
1. REPORT NUMBER AFRPL-TR-72-112	2. GOVT ACCESSION NO.	3. RECIPIENT'S CATALOG NUMBER
4. TITLE (and Subtitle) Development of Large Diameter High-Chamber Pressure Throat Insert Materials. Volume III - Vapor Deposition of Pyrolytic Graphite Coatings for Large Diameter Throat Inserts		5. TYPE OF REPORT & PERIOD COVERED Final - 15 February 1970 to 1 September 1972
7. AUTHOR(s) Kenneth E. Undercoffer		6. PERFORMING ORG. REPORT NUMBER 42-5489
9. PERFORMING ORGANIZATION NAME AND ADDRESS Atlantic Research Corporation 5390 Cherokee Avenue Alexandria, Virginia 22314		8. CONTRACT OR GRANT NUMBER(s) F04611-70-C-0009
11. CONTROLLING OFFICE NAME AND ADDRESS Air Force Rocket Propulsion Laboratory Director of Laboratories Edwards, CA 93523; Air Force Systems Command, United States Air Force		10. PROGRAM ELEMENT, PROJECT, TASK AREA & WORK UNIT NUMBERS BPSN: 623059 Project No.: 3059 Prog. Elem. No: 6.23.02F
14. MONITORING AGENCY NAME & ADDRESS (if different from Controlling Office) Commander, DCASD Baltimore Building 22, Fort Holabird Baltimore, Maryland 21219		12. REPORT DATE January 1974
		13. NUMBER OF PAGES 105
		15. SECURITY CLASS. (of this report) UNCLASSIFIED
		15a. DECLASSIFICATION/DOWNGRADING SCHEDULE
16. DISTRIBUTION STATEMENT (of this Report) Distribution limited to U.S. Government agencies only; Test and Evaluation data, January 1974. Other requests for this document must be referred to AFRPL (STINFO/DOZ), Edwards, CA 93523		
17. DISTRIBUTION STATEMENT (of the abstract entered in Block 20, if different from Report)		
18. SUPPLEMENTARY NOTES		
19. KEY WORDS (Continue on reverse side if necessary and identify by block number) Vapor Deposition Pyrolytic Graphite Coatings Rocket Nozzles		
20. ABSTRACT (Continue on reverse side if necessary and identify by block number) Volume III - Describes the development of a process for coating large diameter rocket nozzle throat inserts with pyrolytic graphite. Inserts with throat diameters of 7.0, 10.6, 12.45 and 13.0 inches were fabricated.		

DD FORM 1473

1 JAN 73

EDITION OF 1 NOV 65 IS OBSOLETE

UNCLASSIFIED

SECURITY CLASSIFICATION OF THIS PAGE (When Data Entered)

REPORT INFORMATION PAGE	
1. REPORT NUMBER	
2. REPORT DATE	
3. REPORT TYPE AND PERIOD	
4. AUTHOR	
5. PERFORMING ORGANIZATION NAME(S) AND ADDRESS(ES)	
6. PERFORMING ORGANIZATION REPORT NUMBER	
7. AUTHORING OR PERFORMING ORGANIZATION	
8. PERFORMING ORGANIZATION	
9. PERFORMING ORGANIZATION	
10. PERFORMING ORGANIZATION	
11. PERFORMING ORGANIZATION	
12. PERFORMING ORGANIZATION	
13. PERFORMING ORGANIZATION	
14. PERFORMING ORGANIZATION	
15. PERFORMING ORGANIZATION	
16. PERFORMING ORGANIZATION	
17. PERFORMING ORGANIZATION	
18. PERFORMING ORGANIZATION	
19. PERFORMING ORGANIZATION	
20. PERFORMING ORGANIZATION	
21. PERFORMING ORGANIZATION	
22. PERFORMING ORGANIZATION	
23. PERFORMING ORGANIZATION	
24. PERFORMING ORGANIZATION	
25. PERFORMING ORGANIZATION	
26. PERFORMING ORGANIZATION	
27. PERFORMING ORGANIZATION	
28. PERFORMING ORGANIZATION	
29. PERFORMING ORGANIZATION	
30. PERFORMING ORGANIZATION	
31. PERFORMING ORGANIZATION	
32. PERFORMING ORGANIZATION	
33. PERFORMING ORGANIZATION	
34. PERFORMING ORGANIZATION	
35. PERFORMING ORGANIZATION	
36. PERFORMING ORGANIZATION	
37. PERFORMING ORGANIZATION	
38. PERFORMING ORGANIZATION	
39. PERFORMING ORGANIZATION	
40. PERFORMING ORGANIZATION	
41. PERFORMING ORGANIZATION	
42. PERFORMING ORGANIZATION	
43. PERFORMING ORGANIZATION	
44. PERFORMING ORGANIZATION	
45. PERFORMING ORGANIZATION	
46. PERFORMING ORGANIZATION	
47. PERFORMING ORGANIZATION	
48. PERFORMING ORGANIZATION	
49. PERFORMING ORGANIZATION	
50. PERFORMING ORGANIZATION	
51. PERFORMING ORGANIZATION	
52. PERFORMING ORGANIZATION	
53. PERFORMING ORGANIZATION	
54. PERFORMING ORGANIZATION	
55. PERFORMING ORGANIZATION	
56. PERFORMING ORGANIZATION	
57. PERFORMING ORGANIZATION	
58. PERFORMING ORGANIZATION	
59. PERFORMING ORGANIZATION	
60. PERFORMING ORGANIZATION	
61. PERFORMING ORGANIZATION	
62. PERFORMING ORGANIZATION	
63. PERFORMING ORGANIZATION	
64. PERFORMING ORGANIZATION	
65. PERFORMING ORGANIZATION	
66. PERFORMING ORGANIZATION	
67. PERFORMING ORGANIZATION	
68. PERFORMING ORGANIZATION	
69. PERFORMING ORGANIZATION	
70. PERFORMING ORGANIZATION	
71. PERFORMING ORGANIZATION	
72. PERFORMING ORGANIZATION	
73. PERFORMING ORGANIZATION	
74. PERFORMING ORGANIZATION	
75. PERFORMING ORGANIZATION	
76. PERFORMING ORGANIZATION	
77. PERFORMING ORGANIZATION	
78. PERFORMING ORGANIZATION	
79. PERFORMING ORGANIZATION	
80. PERFORMING ORGANIZATION	
81. PERFORMING ORGANIZATION	
82. PERFORMING ORGANIZATION	
83. PERFORMING ORGANIZATION	
84. PERFORMING ORGANIZATION	
85. PERFORMING ORGANIZATION	
86. PERFORMING ORGANIZATION	
87. PERFORMING ORGANIZATION	
88. PERFORMING ORGANIZATION	
89. PERFORMING ORGANIZATION	
90. PERFORMING ORGANIZATION	
91. PERFORMING ORGANIZATION	
92. PERFORMING ORGANIZATION	
93. PERFORMING ORGANIZATION	
94. PERFORMING ORGANIZATION	
95. PERFORMING ORGANIZATION	
96. PERFORMING ORGANIZATION	
97. PERFORMING ORGANIZATION	
98. PERFORMING ORGANIZATION	
99. PERFORMING ORGANIZATION	
100. PERFORMING ORGANIZATION	

SUPPLEMENTAL TO T211 **TABLE OF CONTENTS**

	Page
I INTRODUCTION	1
II OBJECTIVE	1
III SCOPE	1
IV CONCLUSION	2
V GENERAL COATING PROCEDURES	3
VI COATING DEVELOPMENT	11
1. 7.0-INCH NOZZLE THROAT INSERTS	11
2. 10.6-INCH NOZZLE THROAT INSERTS	54
3. 13.0-INCH NOZZLE THROAT INSERTS	60
4. 12.45-INCH NOZZLE THROAT INSERTS	76
VII DISCUSSION	97

LIST OF ILLUSTRATIONS

Figure		Page
1	Large Nozzle Deposition Assembly	4
2	Water-Cooled Copper Injector for Large Nozzle Deposition	5
3	Relationship of Process Gas Flow Rate to Coating Surface Temperature (Coating thickness ~50 mils)	7
4	As Deposited 7.0-inch Throat Insert No. 6300-1 (Coating surface stains are superficial)	12
5	Coating Microstructure of 7.0-inch Throat Insert No. 6300-39, Entrance End View, X60	13
6	Coating Microstructure of 7.0-inch Throat Insert No. 6300-9, Exit End View, X60	13
7	Coating Microstructure of 7.0-inch Throat Insert No. 6300-32, Entrance End View, 135X	14
8	7.0-inch Nozzle Throat Insert Substrate Configurations 1 and 1A	23
9	7.0-inch Nozzle Throat Insert Substrate Configuration 2 (Including groove modifications)	24
10	7.0-inch Nozzle Throat Insert Substrate Configuration 3	25
11	7.0-inch Injector Tip Configuration 1	27
12	7.0-inch Injector Tip Configuration 2	28
13	7.0-inch Injector Tip Configuration 3	29
14	Deposition Chamber Geometry of Run No. 6000-1	30
15	Deposition Chamber Geometry of Run No. 6300-1	32
16	Deposition Chamber Geometry of Run No. 6300-2	33
17	Deposition Chamber Geometry of Run No's. 6302-3 and 6300-4	34

LIST OF ILLUSTRATIONS (continued)

Figure		Page
18	Deposition Chamber Geometry of Run No's 6300-5 and 6300-6	36
19	Deposition Chamber Geometry of Run No. 6300-7	37
20	Deposition Chamber Geometry of Run No. 6300-8	38
21	Deposition Chamber Geometry of Run No's 6300-9 and 6300-10	40
22	Deposition Chamber Geometry of Run No's 6300-11 thru 6300-16	41
23	Deposition Chamber Geometry of Run No's 6300-17 thru 6300-19 and Run No. 6300-30	42
24	Deposition Chamber Geometry of Run No. 6300-20	44
25	Deposition Chamber Geometry of Run No. 6300-21	45
26	Deposition Chamber Geometry of Run No. 6300-22	46
27	Deposition Chamber Geometry of Run No. 6300-23	47
28	Deposition Chamber Geometry of Run No. 6300-24	48
29	Deposition Chamber Geometry of Run No. 6300-25	49
30	Deposition Chamber Geometry of Run No. 6300-26	50
31	Deposition Chamber Geometry of Run No. 6300-27	51
32	Deposition Chamber Geometry of Run No. 6300-28	52
33	Deposition Chamber Geometry of Run No. 6300-29	53
34	Deposition Chamber Geometry of Run No. 6300-31	55
35	Deposition Chamber Geometry of Run No's 6300-32 thru 6300-45	56
36	10.6-inch Nozzle Throat Insert Substrate Configuration	59
37	Deposition Chamber Geometry of Run No. 7300-1	61

LIST OF ILLUSTRATIONS (continued)

Figure		Page
38	Deposition Chamber Geometry of Run No. 7300-2	62
39	Deposition Chamber Geometry of Run No. 7300-3	63
40	13.0-inch Nozzle Throat Insert Substrate Configuration 1	66
41	Deposition Chamber Geometry of Run No. 8300-1	67
42	Deposition Chamber Geometry of Run No. 8300-2	69
43	Deposition Chamber Geometry of Run No's 8300-3 and 8300-4	70
44	Deposition Chamber Geometry of Run No. 8300-5	71
45	Deposition Chamber Geometry of Run No's 8300-6, 8300-7 and 8300-8	73
46	Deposition Chamber Geometry of Run No. 8300-9	74
47	Deposition Chamber Geometry of Run No. 8300-10	75
48	Deposition Chamber Geometry Run No's 8300-11 and 8300-12	77
49	12.45-inch Throat Insert No. 8300-24, Entrance End View	78
50	Coating Microstructure of 12.45-inch Insert No. 8300-21, Entrance End, 60X	79
51	Coating Microstructure of 12.45-inch Insert No. 8300-21, Exit End, 60X	79
52	Injector Tip Configuration Utilized for Runs 8300-13 thru 8300-15 (Plenum diameter 0.343) and Runs 8300-16 thru 8300-18 (Plenum diameter as shown)	82
53	Injector Tip Configuration Utilized for Runs 8300-19 thru 8300-26	83
54	12.45-inch Nozzle Throat Insert Substrate Configuration 1 (Including groove modifications)	85
55	Deposition Chamber Geometry of Run No's 8300-13, 8300-15 (Mandrel removed) and 8300-16	87

LIST OF ILLUSTRATIONS (continued)

Figure		Page
56	Deposition Chamber Geometry of Run No. 8300-14	88
57	Deposition Chamber Geometry of Run No's 8300-17 and 8300-18 (Injector lowered 1/4 inch)	90
58	Deposition Chamber Geometry of Run No's 8300-19 (Mandrel position indicated by broken line), 8300-20 and 8300-21	91
59	Deposition Chamber Geometry of Run No. 8300-22	93
60	Deposition Chamber Geometry of Run No. 8300-23	94
61	Deposition Chamber Geometry of Run No's 8300-24, 8300-25 and 8300-26 (Injector lowered 1/4 inch)	95

LIST OF TABLES

Table		Page
I	Coating Index System	8
II	7.0-Inch Nozzle Throat Insert Deposition Conditions	15
III	7.0-Inch Nozzle Throat Insert Substrate and Coating Data	19
IV	7.0-Inch Nozzle Throat Insert Substrate Dimensional Changes After Coating	26
V	10.6-Inch Nozzle Throat Insert Deposition Conditions	57
VI	10.6-Inch Nozzle Throat Insert Substrate and Coating Data	58
VII	13.0-Inch Nozzle Throat Insert Deposition Conditions	64
VIII	13.0-Inch Nozzle Throat Insert Substrate and Coating Data	65
IX	12.45-Inch Nozzle Throat Insert Deposition Conditions	80
X	12.45-Inch Nozzle Throat Insert Substrate and Coating Data	81
XI	12.45-Inch Nozzle Throat Insert Substrate Dimensional Data	86
XII	Nominal Process Conditions for Large Nozzle Deposition Runs	98

SECTION I

INTRODUCTION

Techniques for the fabrication of pyrolytic graphite coated rocket nozzle components were developed by Atlantic Research for AFRPL under several prior contracts. During these programs pyrolytic graphite coated nozzle throat inserts were fabricated and test fired in throat sizes up to 2.3 inches. Electrode grade AGSR graphite was the established substrate material. The successful performance of these parts indicated that a scale-up in size was warranted to determine the suitability of the PG-coated AGSR system in larger sizes. This is Volume III of a three-volume report and contains a description of the deposition process development.

Volume I contains the analysis of the five 7.0-inch throat diameter test firings conducted at AFRPL.

Volume II describes the nondestructive testing of the PG-coated throat inserts, the design analysis of the 7-inch PG coated throat, and the design analysis of the 7-inch nozzle package. Also included are details of the nozzle fabrication and the post-firing analysis of the ablative components.

SECTION II

OBJECTIVE

The basic objective of this phase of the program was to develop techniques for the fabrication of pyrolytic graphite coated nozzle throat inserts with throat diameters of 7.0, 10.6, and 12.45 inches. Five 7.0-inch throat diameter inserts were to be fabricated for test firing at AFRPL.

SECTION III

SCOPE

Coating techniques were developed for the fabrication of nozzle throat inserts with throat diameters of 7.0, 10.6, 12.45, and 13.0 inches.

Very coarse-grained AGSR graphite was utilized as the basic substrate material. Five 7.0-inch-diameter nozzle throat inserts were fabricated and test fired.

SECTION IV

CONCLUSION

Large diameter pyrolytic graphite components can be fabricated using techniques established during this program. Reproducibility was demonstrated in the 7.0-inch size and, with a statistically significant number of runs, could probably be demonstrated in the larger sizes. Indications are that AGSR graphite is not an ideal substrate material for large diameter parts and other graphitic materials with lower coefficients of thermal expansion should be investigated as potential substrate materials.

SECTION V

GENERAL COATING PROCEDURES

The large nozzle deposition runs were conducted in a 20-inch diameter induction furnace, heated by a 100 kW, 10 kHz, A_j Motor Generator.

The graphite substrate to be coated was placed inside a graphite canister using contoured graphite fixtures to direct the deposition gases onto the substrate and out of the deposition chamber. A generalized view of the large nozzle deposition assembly is shown in Figure 1.

In most of the runs a contoured graphite mandrel was utilized to reduce the free volume within the center of the deposition chamber. Several different mandrel configurations were tried for each of the three substrate sizes. The initial mandrel designs utilized holes drilled in the base to pass the exhaust gases from the deposition chamber to the furnace exhaust tube. This system was unsatisfactory because the holes plugged during deposition. Slots were tried to increase the gas exhaust area but these also clogged. The problem was finally solved by setting the mandrel on one-half-inch-diameter posts.

Commercial grade methane was the carbonaceous gas and was diluted with nitrogen to 1.9-5.1 volume percent before introduction into the furnace. This gas enters the furnace through a water-cooled, multiple-holed injector, as shown in Figure 2. A small amount of nitrogen was introduced into the annular area around the injector to prevent back-flow of the gases between the injector and the graphite entrance section.

Deposition temperature was monitored on the canister backside with a Leeds & Northrup Model 8632F optical pyrometer and controlled manually by adjusting the power input from the motor generator.

Because deposition temperatures are routinely measured on the canister backside, the recorded temperature is less than the temperature of the deposition surface which determines the characteristics of the coating. This difference is caused by the cooling effect of the process gas on the coating surface and increases with coating thickness because of the low conductivity of the coating in the "c" direction.

For small substrates and low gas flow rates, this temperature difference is believed to be negligible. However, because of the increased gas flow rates used during fabrication of large nozzles, the thermal gradient, between the deposition surface and the outside surface of the deposition chamber, becomes significant. To determine the magnitude of this gradient, a previously coated 7.0-inch nozzle (55 mils of PG at throat) was assembled using the deposition chamber geometry established for the last fourteen runs of the 7.0-inch series. Two holes were drilled through the deposition chamber and into the coating at the nozzle throat plane. The first penetrated the canister, substrate and coating to within 5 mils of the coating inner surface. The second penetrated the canister and the substrate to the substrate/coating interface. A second sight tube was added to the furnace, which lined up with these holes. The previously used sight tube plane was 6 inches above the substrate throat plane. The furnace was then heated to deposition temperature. Temperatures were recorded at the substrate throat plane, 5 mils from the coating surface, at the substrate/coating interface, and on the canister backside. The canister backside temperature was also recorded using the original sight tube.

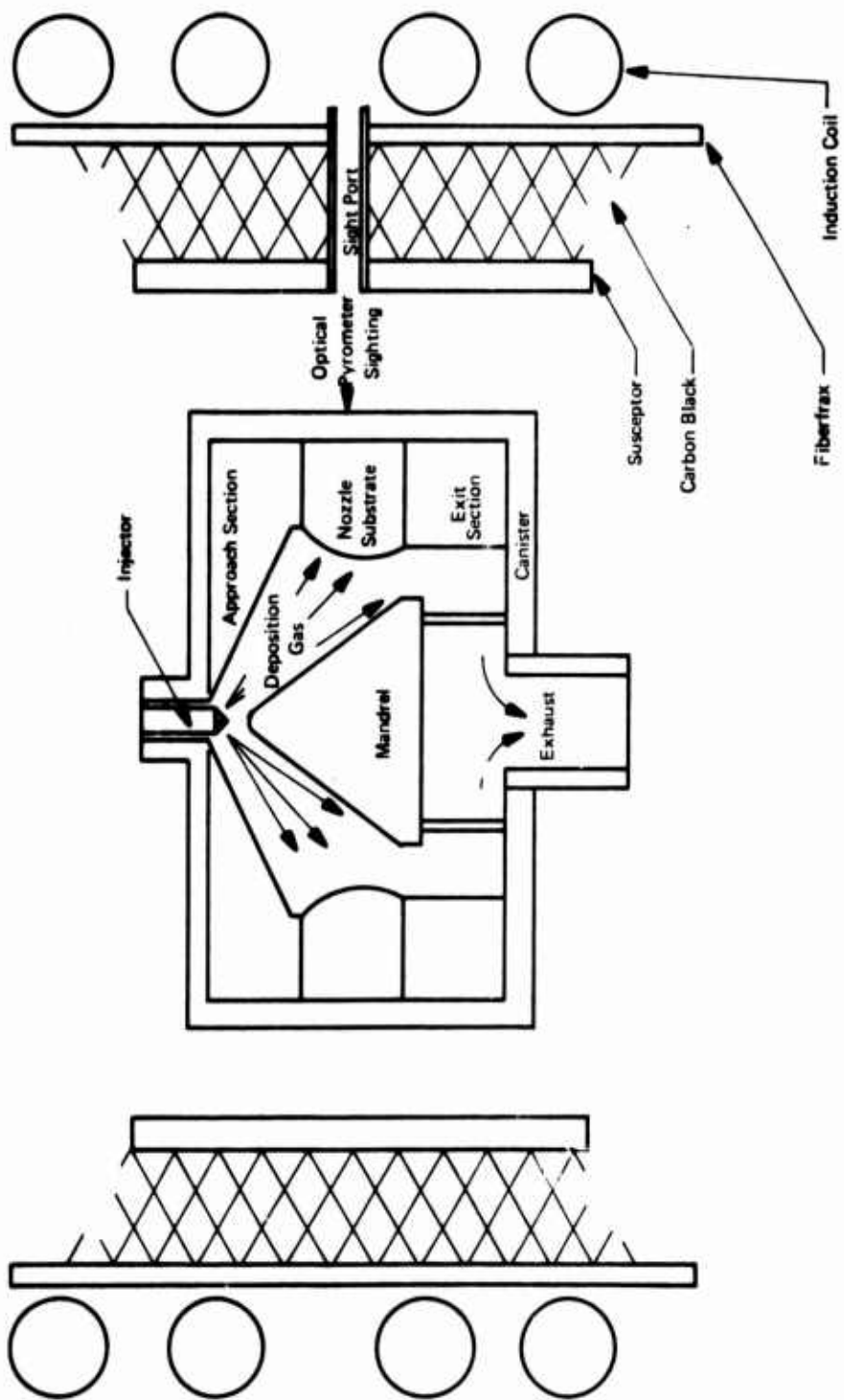


Figure 1. Large Nozzle Deposition Assembly.

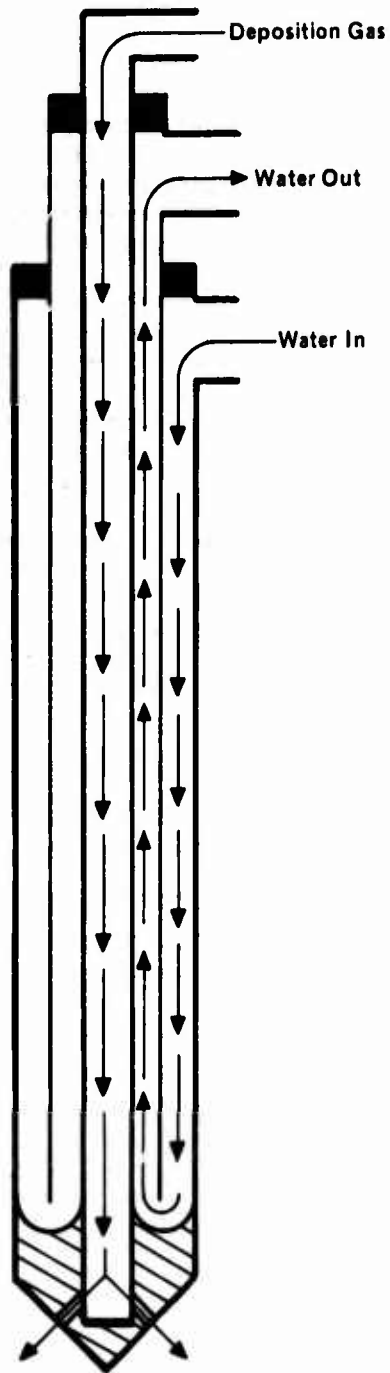


Figure 2. Water-Cooled Copper Injector for Large Nozzle Deposition.

Measurements were made at five different nitrogen gas flow rates, the highest of which was that used for Runs 6300-32 through 6300-45. Methane was introduced for a brief period, at the highest of the gas flow rates, to determine its cooling effect. The methane addition lowered the coating surface temperature approximately 20°F, immediately upon introduction. Its exact effect on the thermal gradient could not be determined because if the flow was maintained for an extended period, the PG thickness would have increased significantly.

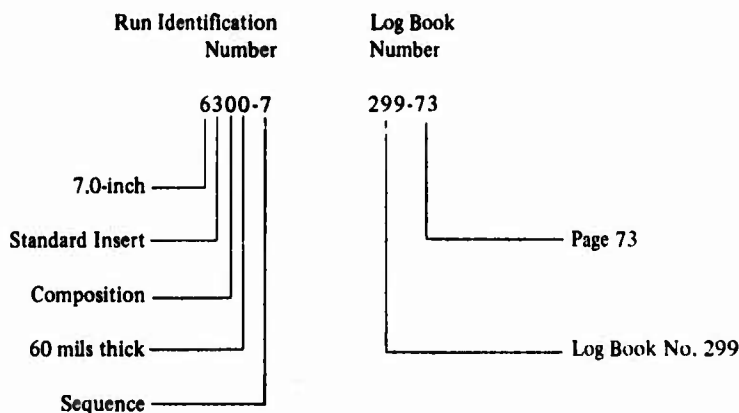
An average canister backside temperature decrease of 30°F was measured between the new sight tube, installed at the throat plane, and the original sight tube 6 inches above, indicating that the upper part of the deposition chamber runs slightly lower in temperature than the middle.

The thermal gradient between the coating surface and the coating interface averaged about 90°F. This indicates that the temperature should be slowly increased by this amount during the run to maintain a constant temperature at the coating surface.

The overall thermal gradient between the coating surface and the deposition chamber backside varied with the nitrogen flow rate as shown in Figure 3.

These data show that for a starting temperature reading of 4100°F on the canister backside, and with the temperature slowly increased to 4200°F throughout the run, the deposition surface temperature will be 3800°F. This procedure was used for all 7.0-inch deposition runs after 6300-37 and all 12.45-inch deposition runs after 8300-22.

A coating index system was utilized to define the type of part fabricated and the major coating characteristics. This is shown in Table I. For cataloging purposes, the parts were given sequential numbers based on the first 2 digits only. A second series of numbers denotes the deposition log book number. An example of the system as used in this report is:



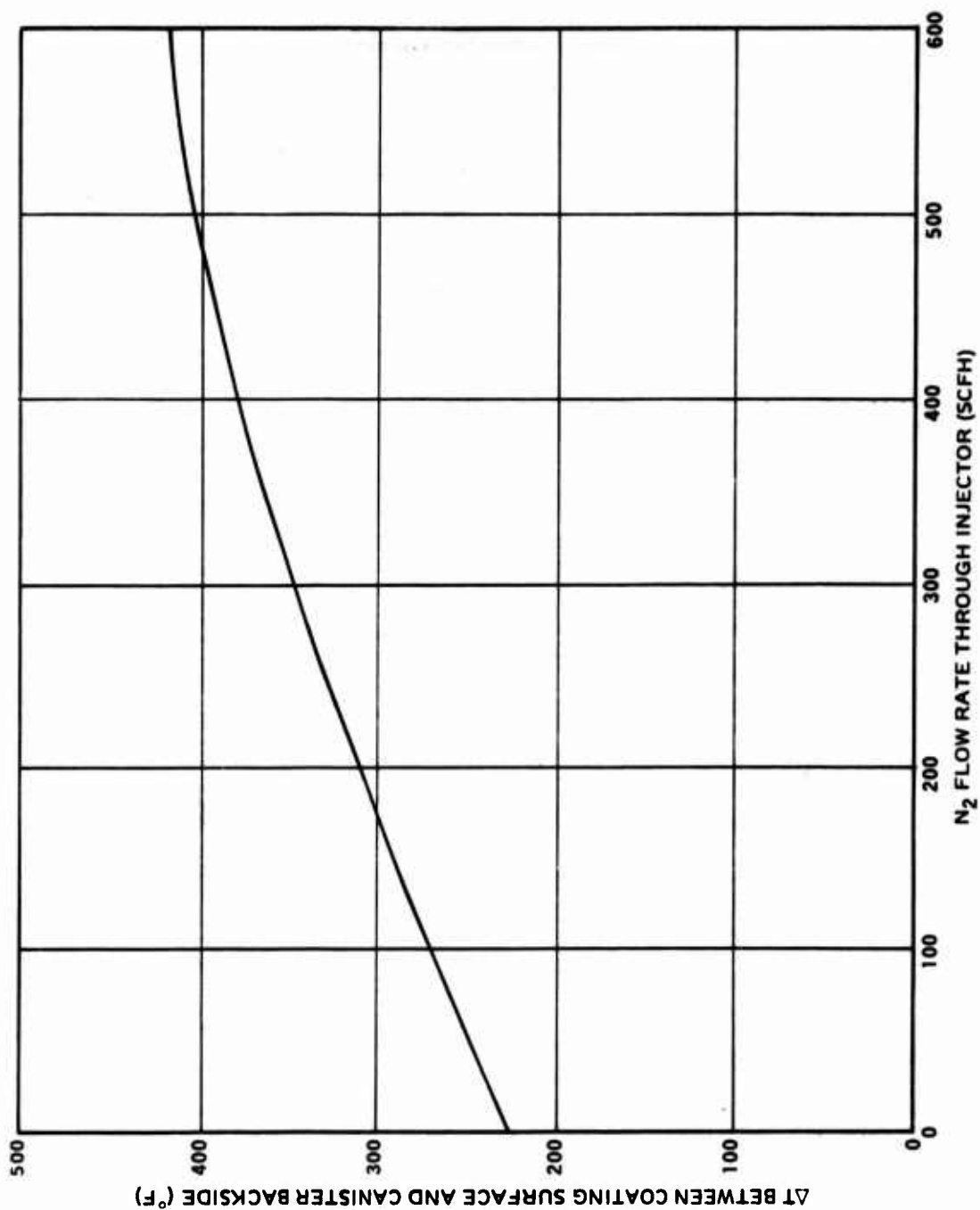


Figure 3. Relationship of Process Gas Flow Rate to Coating Surface Temperature
(Coating thickness ~ 50 mils).

Table I. Coating Index System.

Description of Part	Digit			
	1st	2nd	3rd	4th
NOMINAL SIZE				
7.0	6			
10.0	7			
13.0	8			
SHAPE				
Cylindrical		0		
Standard Insert		3		
Wraparound — Large Radius		4		
Wraparound — Small Radius		5		
Entrance Approach		7		
Exit Section		9		
NOMINAL COMPOSITION				
Pyrolytic Graphite (Unalloyed)			0	
8% SiC			1	
15% SiC			2	
25% SiC			3	
Graded Coating			5	
NOMINAL THICKNESS (mils)				
50 (0/75)				0
100 (75/125)				2
150 (125/175)				4
200 (175/250)				6
250 and Beyond				8

Volumes I and II of this report utilize the Log Book No. only and these should be utilized for cross-referencing.

All of the substrates coated were fabricated from Union Carbide Grade AGSR graphite. A number of these substrates utilized material which had been annealed at 5400°F for two hours.

Most of the substrates were fabricated from 24-inch-diameter billets which have a maximum grain size of 0.25 inch. This is an extruded, electrode-grade graphite with a Young's Modulus¹ of 0.5×10^6 psi in both the with grain and against grain directions. The CTE¹ is $1.2 \times 10^{-6}/^\circ\text{C}$ in the with grain direction and $1.9 \times 10^{-6}/^\circ\text{C}$ in the against grain direction. This material, designated AGSR-VCG, was selected because its against grain CTE approaches that of PG in the "ab" plane more nearly than that of any other bulk graphite and for its low modulus of elasticity. The low CTE reduces the coating/substrate stresses induced during cooldown from deposition temperature and the reduced modulus allows the substrate to distort to further relieve these stresses. In the past AGSR-VCG has proven to be a useful substrate material for PG-coated nozzles up to 2.3-inch throat diameter.

Because of its porosity and large grain size, very coarse grained AGSR graphite has an extremely rough surface finish after machining. If a PG coating is applied to this type of surface, it tends to follow and exaggerate the roughness. Where the coating wraps around the edges of an open pore, large growth cone angles occur. The resultant large growth cones induce severe localized stresses within the coating and serve as loci for delaminations. To eliminate this problem requires the following pretreatment of the substrate surface before the PG coating is applied:

- a. Apply a coating of Union Carbide C-34 cement to the surface to be coated.
- b. Wipe off all excess coating with a dry, lint-free rag leaving cement in the pores only.
- c. Cure at 100°C for 1-2 hours.
- d. Recoat surface with a thin, uniform layer of cement.
- e. Cure at 120-130°C for 16 hours.
- f. Bake part in an inert atmosphere at 4000°F for two hours to carbonize C-34 and remove residual volatiles from graphite.
- g. Remove excess coating with medium grit emery cloth by carefully exposing substrate material without exposing new voids. No patches of cement can be present as the PG will debond from the substrate in these areas.

¹AFML-TR-67-113

A few preliminary 7.0-inch deposition runs were conducted utilizing material cut from 12-inch-diameter AGSR billets and these are indicated by the designation AGSR-CG. The maximum grain size of this material is 0.06 inch. The Young's Modulus¹ is 1.2×10^6 psi in the with grain direction and 0.8×10^6 psi in the against grain direction. The CTE¹ is $1.9 \times 10^{-6}/^\circ\text{C}$ in the with grain direction and $3.0 \times 10^{-6}/^\circ\text{C}$ in the against grain direction. Because of its higher modulus and CTE, the finer grained AGSR-CG is inferior as a substrate material for PG. It is, however, less porous and requires no surface pretreatment before coating. Therefore, it makes an ideal, low-cost substrate material for preliminary test deposition runs.

To permit removal of the coated substrate from the deposition assembly after coating, release grooves were machined into the fixtures where they mated with the substrate. These grooves were 0.050/0.070-inch wide and from 0.100/0.300 inch in radial depth. In most cases, the coating did not bridge the release gap and the substrate was easily removed from the assembly. In cases where the coating did bridge the gap, coating delaminations occurred because of the CTE mismatch between the HLM fixture and the adjacent AGSR substrate. This was easily remedied by increasing the groove width.

The coated substrates were prepared for inspection by facing 90 mills of material from each end on a lathe using conventional techniques. The exposed coating ends were polished, successively, with 240, 320, 400 and finally 600 grit emery cloth. The coating ends were then micropolished with a water suspension of 1-micron aluminum oxide polishing compound. Microscopic examination of the polished coating ends was conducted with a Zeiss Binocular Microscope at a magnification of 120-600X. Parts were rejected, for firing, if they contained circumferential delaminations more than 3-5 growth cones in length. The coating surface was inspected visually using the alcohol wipe technique to locate exposed surface cracks. The surface was also examined for nodules. Any nodules more than 1/8 inch in diameter or raised more than 1/16 inch above the coating surface were cause for rejection, if the part was being considered for test firing.

United Technology Corporation, under subcontract to Atlantic Research, investigated advanced techniques for nondestructive testing of both coated and uncoated substrates. The principal advanced techniques studied were acoustic emission and spectral audiosonic prints. In addition, UTC utilized ultrasonics, X-ray, and alcohol wipe techniques in pursuit of NDT studies. The results of this investigation are documented in Volume II.

¹AFML-TR-67-113

SECTION VI

COATING DEVELOPMENT

1. 7.0-INCH NOZZLE THROAT INSERTS

One 7.0-inch cylindrical and forty-five 7.0-inch nozzle throat insert fabrication runs were conducted. Five of these inserts were utilized for motor test firing. AFRPL firing data is presented in Volume I.

Figure 4 shows an as-deposited 7.0-inch throat insert. Typical coating microstructures, observed at the substrate ends, are shown in Figures 5, 6 and 7.

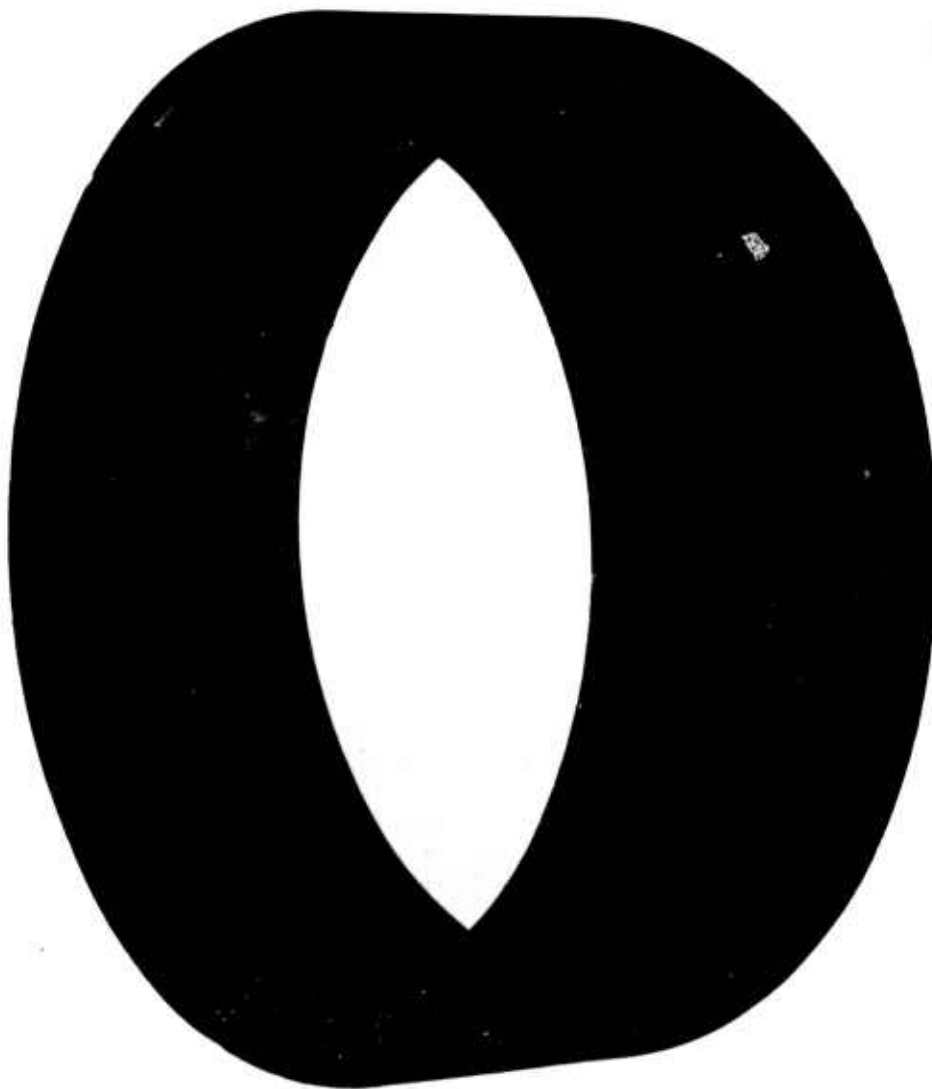
Deposition conditions are shown in Table II. Coating and substrate data are shown in Table III.

Three basic substrate configurations were utilized. The first of these was of a preliminary design and is shown in Figure 8. The second is shown in Figure 9 and is the configuration utilized for Test Firings SN-1, SN-2 and SN-3. The third configuration, shown in Figure 10, was similar to the second. The radii of curvature of the entrance and exit ends were increased, and the throat diameter was decreased to compensate for the after-coating dimensional changes which occur because of coating thickness variations and substrate dimensional changes. This third design was utilized for the throat inserts fired in SN-4 and SN-5.

Substrate dimensions were recorded before and after deposition for seven of the latter runs to determine the amount of substrate deformation caused by substrate/coating CTE mismatch. These data are summarized in Table IV. In all cases, the substrate outside diameter increased significantly after deposition. The two substrates on which the thinnest coating was applied showed the least amount of expansion, as would be expected. Length change dimensions were recorded in only three cases and no meaningful conclusions could be derived from them.

Four injector tip configurations were utilized. The first three of these are shown in Figures 11, 12 and 13. The fourth configuration was like the second except a second row of 16 holes was drilled below the first at an angle of 45 degrees to the injector axis. The particular configuration utilized for each run is marked on the injector tip in the deposition chamber geometry drawings.

Run 6000-1 was conducted utilizing a 7.0-inch I.D. X 7.45-inch-long cylindrical substrate. This run served to establish preliminary deposition gas flow rates, and to determine the impingement pattern of the injector. The deposition chamber geometry is shown in Figure 14. After deposition, the wall thickness was measured along three axial lines 120 degrees apart at 1/2-inch intervals along the length of the cylinder. The coating thickness profile was determined by averaging the three readings taken at each of the 1/2-inch stages. This profile is included in Figure 14.



12157
25339



Figure 4. As Deposited 7.0-inch Throat Insert No. 6300-1 (Coating surface stains are superficial).

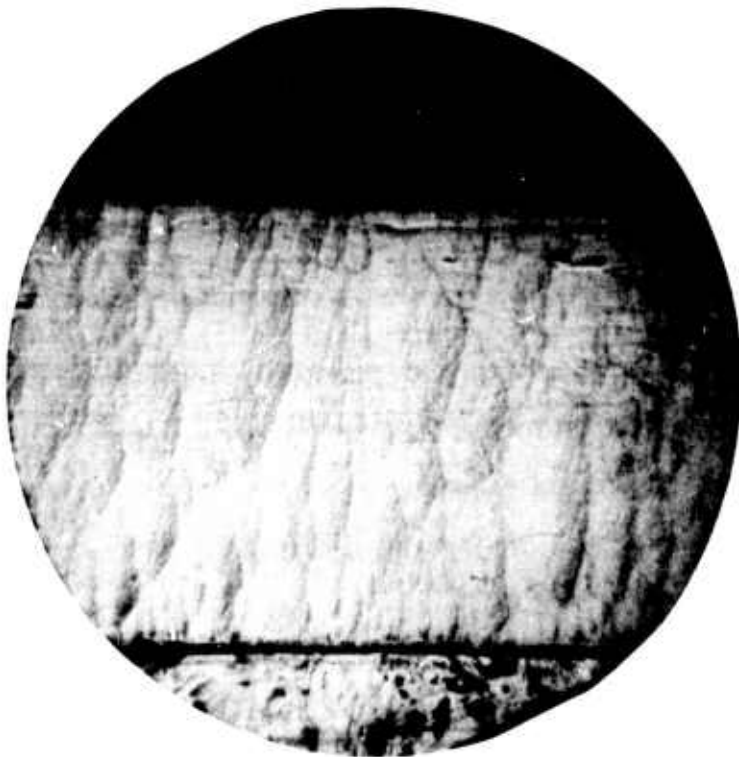
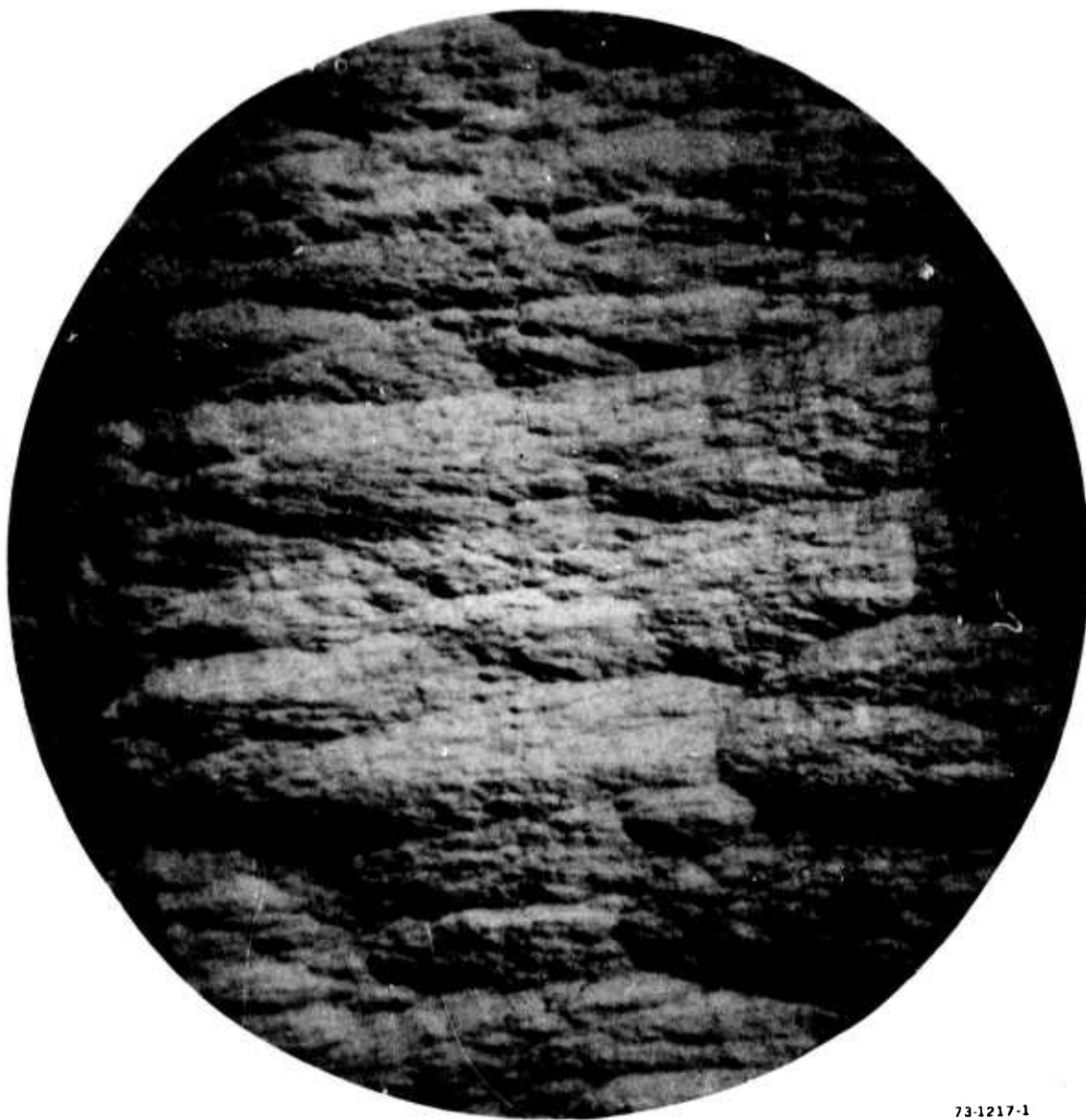


Figure 5. Coating Microstructure of 7.0-inch Throat Insert No. 6300-39.
Entrance End View, X60.



73-1217-2

Figure 6. Coating Microstructure of 7.0-inch Throat Insert No. 6300-9
Exit End View, X60.



73-1217-1

**Figure 7. Coating Microstructure of 7.0-inch Throat Insert
No. 6300-32. Entrance End View, 135X.**

Table II. 7.0-Inch Nozzle Throat Insert Deposition Conditions.

Run Ident No.	Log Book No.	Annulus N ₂ (SCFH)	Process N ₂ (SCFH)	CH ₄ (SCFH)	Volume Percent CH ₄	Deposition Temperature (°F)	Dep. Time (hr)	Remarks
6000-1	299-37	24	256	15	5.1	4060	4.00	Tubular deposition run conducted to determine coating thickness profile.
6300-1	299-42	24	256	15	5.1	4200	4.00	Initial 7.0-inch nozzle throat insert deposition run.
6300-2	299-44	24	256	15	5.1	4200	4.00	Substrate moved up in chamber to increase coating thickness at entrance end.
6302-3	299-45	24	256	15	5.1	4000	6.00	Contoured mandrel used to increase proportional coating thickness at ends.
6300-4	299-46	30	320	18	4.9	4000	4.50	Deposition time reduced to reduce coating thickness. Gas flow rates increased to eliminate sooting.
6300-5	299-48	30	320	18	4.9	3950	4.50	New injector tip utilized in attempt to eliminate growth on injector tip.
6300-6	299-49	24	256	15	5.1	3950	4.63	Lower gas flow rates tried to determine if they can be utilized with new injector tip design.
6300-7	299-73	24	256	15	5.1	3950	5.00	New, longer substrate used for first time. Mandrel design modified to obtain greater proportional coating thickness at exit end.
6300-8	299-74	24	256	15	5.1	3950	4.00	Injector moved 1/2 inch down in chamber to increase deposition rate at throat. Mandrel shortened 1/2 inch.
6300-9	299-75	24	256	15	5.1	3950	5.00	New deposition chamber design utilized to permit greater injector stand-off in attempt to improve coating thickness distribution.

Table II. (continued).

Run Ident No.	Log Book No.	Annulus N ₂ (SCFH)	Process N ₂ (SCFH)	CH ₄ (SCFH)	Volume Percent CH ₄	Deposition Temperature (°F)	Dep. Time (hr)	Remarks
6300-10	009-1	24	256	15	5.1	3950	7.80	Injector moved 1/8 inch closer to substrate to increase deposition rate at exit end.
6300-11	009-2	24	256	15	5.1	3950	8.25	Mandrel shortened 1/2 inch and injector moved down 1/2 inch to increase deposition rate at throat and exit.
6300-12	009-3	24	256	15	5.1	3950	8.00	None
6302-13	009-4	24	256	15	5.1	3950	8.00	Injector orifices found to be partially blocked after deposition. May have contributed to roughness.
6300-14	009-5	24	256	15	5.1	3950	8.00	Injector orifices cleaned thoroughly before deposition.
6300-15	009-6	24	256	15	5.1	3950	5.75	None
6300-16	009-7	30	320	18	4.9	3950	5.00	Gas flow rates increased to improve coating surface condition.
6200-17	009-8	24	256	15	5.1	3950	7.00	Mandrel configuration modified in attempt to improve coating surface condition. Returned to old gas flow rates.
6300-18 (SN-1)	009-9	24	256	15	5.1	3950	5.83	None
6300-19	009-10	24	256	15	5.1	3950	6.73	Mandrel shortened 1/4 inch at tip, to increase deposition rate at downstream end of substrate.
6300-20	009-11	24	256	15	5.1	3950	6.75	Mandrel shortened additional 1/4 inch and injector lowered 1/4 inch to increase deposition rate at downstream end of substrate.
6300-21	009-13	30	320	15	4.1	3950	4.00	Returned to earlier deposition chamber configuration in attempt to achieve improved coating surface condition.

Table II. (continued).

Run Ident No.	Log Book No.	Annulus N ₂ (SCFH)	Process N ₂ (SCFH)	CH ₄ (SCFH)	Volume Percent CH ₄	Deposition Temperature (°F)	Dep. Time (hr)	Remarks
6300-22	009-14	30	200	10	4.2	4100	5.00	Reduced total gas flow rates and increased deposition; temperature to determine effect on coating.
6300-23	009-15	30	200	10	4.2	4100	6.00	Shortened and rounded mandrel to improve gas flow characteristics and increase deposition rate at downstream end of substrate.
6300-24	009-16	30	220	16	6.0	4100	6.00	Lowered mandrel and increased CH ₄ concentration to increase deposition rate at downstream end of substrate.
6300-25	009-17	30	320	15	4.1	4100	5.50	Increased process N ₂ to reduce sooting in gas phase. Removed mandrel to determine effect on coating.
6300-26	009-18	30	320	10	2.8	4100	5.50	Reduced CH ₄ concentration to reduce sooting in gas phase.
6300-27	009-19	30	320	10	2.8	4100	5.00	Installed second row of holes in injector tip to direct gas to aft end of substrate.
6300-28	009-20	30	320	10	2.8	4100	5.83	Mandrel reinstalled to increase deposition rate.
6300-29	009-21	30	320	10	2.8	4100	5.50	Substrate lowered 1/2 inch and injector 1/4 inch to increase deposition rate at substrate ends.
6300-30	009-22	30	320	15	4.1	4100	6.50	Returned to deposition chamber configuration of 6300-17. Mandrel base bound to canister base causing mandrel to rotate with substrate.
6300-31	009-23	85	320	15	3.6	4100	6.50	Returned to deposition chamber configuration similar to 6300-9 and 6300-10. Mandrel mounted on posts to increase gas exhaust area.
6300-32	009-24	100	480	15	2.5	4100	6.00	Process N ₂ rate increased to reduce sooting in gas phase.

Table II. (continued).

Run Ident No.	Log Book No.	Annulus N ₂ (SCFH)	Process N ₂ (SCFH)	CH ₄ (SCFH)	Volume Percent CH ₄	Deposition Temperature (°F)	Dep. Time (hr)	Remarks
6300-33	009-26	100	480	15	2.5	4100	6.00	None
6300-34 (SN-3)	009-29	100	480	15	2.5	4100	6.00	None
6300-35	009-35	100	480	15	2.5	4100	5.00	None
6300-36	009-37	100	480	15	2.5	4000	6.25	Deposition temperature reduced in belief that optical pyrometer was in error. Was later found to be untrue.
6300-37	009-39	100	480	15	2.5	4100-4200	6.00	Deposition temperature increased, slowly and uniformly, to 4200° F at end of run to compensate for insulating effect of increasing coating thickness.
6300-38	009-40	100	480	15	2.5	4100-4200	5.60	None
6300-39	009-41	100	480	15	2.5	4100-4200	5.30	None
6300-40	009-44	100	480	15	2.5	4100-4200	5.30	None
6300-41	009-46	100	480	15	2.5	4100-4200	5.10	None
6300-42 (SN-4)	009-47	100	480	15	2.5	4100-4200	5.10	None
6300-43	009-48	100	480	15	2.5	4100-4200	4.70	None
6300-44	001-12	100	480	15	2.5	4100-4200	3.43	None
6300-45 (SN-5)	001-13	100	480	15	2.5	4100-4200	5.27	None

Table III. 7.0-Inch Nozzle Throat Insert Substrate and Coating Data.

Run Ident. No.	Log Book No.	Substrate		Coating Thickness (in)			Deposition Rate (mils/hr)			Appearance
		Material	Configuration	Entrance	Throat	Exit	Entrance	Throat	Exit	
6000-1	299-37	AGSR-CG	Tubular	0.055	0.042	0.019	13.8	10.5	4.8	Coating surface quality good
6300-1	299-42	AGSR-CG								Coating quality good. One nodule 1/4 inch from entrance end. 1/8-inch dia X 1/16 inch high
6300-2	299-44	AGSR-CG		0.028	0.066	0.025	7.0	16.5	6.5	Coating quality good. No microscopic examination
6302-3	299-45	AGSR-CG		0.079	0.090	0.056	13.2	15.0	9.3	Entrance: Many short fine discontinuous delaminations in coating very near interface. Exit: No cracks or delaminations: coating from throat to exit end rough and coarse in structure.
6300-4	299-46	AGSR-CG	1	0.067	0.072	0.054	14.9	16.0	12.0	Entrance: Many short fine discontinuous delaminations in coating near interface Same overall appearance as 299-45. Exit: No cracks or delaminations: coating from throat to exit end rough and coarse in structure. Large clinker grew on injector tip.
6300-5	299-48	AGSR-VCG Surface Precoated	1	0.076	0.072	0.042	16.9	16.0	9.3	Entrance: A line of discontinuous delaminations visible near interface extend for 360 degrees. Exit: No flaws.
6300-6	299-49	AGSR-VCG Surface Precoated	1A	0.067	0.068	0.041	14.5	14.7	8.9	Entrance: A few very fine short (2 to 6 growth cones long) delaminations visible near interface. Exit: No flaws. Coating surface smooth
6300-7	299-73	AGSR-VCG Surface Precoated	2	0.080	0.060	0.046	16.0	12.0	9.2	Entrance: Coating texture is very rough with broad growth cones. A few short delaminations, extending through 6 to 10 growth cones and one delamination approximately 1 1/2-inch long, are visible. Exit area: No cracks or delaminations.
6300-8	299-74	AGSR-VCG Surface Precoated	2	0.033	0.072	0.034	8.2	18.0	8.5	Coating surface texture is rough throughout. Entrance and Exit: No cracks or delaminations.
6300-9	299-75	AGSR-VCG Surface Precoated	2	0.038	0.041	0.030	7.6	8.2	6.0	Entrance: No cracks or delaminations. Exit: Two very short fine delaminations. 10 to 20 growth cones long, near substrate interface.

Table III. (continued).

Run Ident. No.	Log Book No.	Substrate		Coating Thickness (in)			Deposition Rate (mils/hr)			Appearance
		Material	Configuration	Entrance	Throat	Exit	Entrance	Throat	Exit	
6300-10	009-1	AGSR-VCG Surface Precoated	2A	0.058	0.054	0.044	7.4	6.9	5.6	Entrance: Delaminated in three places near coating surface. Two are 20 degrees long and the third 5 degrees long. Removal of additional 1/4-inch of stock eliminated these delaminations. Exit: Delaminated for 360 degrees near the substrate interface.
6300-11	009-2	AGSR-VCG Surface Precoated	2B	0.057	0.068	0.052	6.9	8.2	6.3	Entrance: Fine discontinuous delamination begins at the UTC 45-degrees mark and extends around to within 45 degrees of the UTC zero degree mark. Exit: At 70-degrees point a fine discontinuous delamination begins and extends for 90 degrees. Remainder of coating is good. Coating rough and irregular.
6300-12	009-3	AGSR-VCG Surface Precoated	2B	0.044	0.093	0.049	5.5	11.6	6.1	Coating rough and irregular.
6300-13	009-4	AGSR-VCG Surface Precoated	2B	0.055	0.086	0.051	6.9	10.8	6.4	Entrance end: Three minute delaminations, 8 to 10 growth cones in length. Exit end: Several short fine delaminations near substrate interface.
6300-14	009-5	AGSR-VCG Surface Precoated	2B	0.050	0.077	0.051	6.2	9.6	6.4	Coating surface still somewhat rough. Three small growths visible in throat area seem to originate near coating surface. No cracks or delaminations visible at either end.
6300-15	009-6	Recoated 6300-12	—	0.037	0.050	0.034	6.4	8.7	5.9	Coating surface fair. Slightly better than previous run.
6300-16	009-7	AGSR-VCG Surface Precoated	2C	0.031	0.054	0.038	6.2	10.8	7.6	Coating surface fair.
6300-17	009-8	AGSR-VCG Surface Precoated	2C	0.071	0.071	0.050	10.1	10.1	7.1	Coating surface is rough in texture from entrance end to throat. Coating at entrance end contains an occasional delamination, 3 to 5 cones long near interface. Coating at exit end contains a series of short, fine discontinuous delaminations near middle of coating thickness.
6300-18 (SN-1)	009-9	AGSR-VCG Surface Precoated	2C	0.059	0.052	0.033	10.1	8.9	5.7	No cracks or delaminations. Surface texture coarse from entrance end to throat.

Table III. (continued).

Run Ident. No.	Log Book No.	Substrate		Coating Thickness (in)			Deposition Rate (mils/hr)			Appearance
		Material	Configuration	Entrance	Throat	Exit	Entrance	Throat	Exit	
6300-19 (SN-2)	009-10	AGSR-VCG Annealed. Surface Precoated	2C	0.062	0.055	0.041	9.2	8.2	6.1	No cracks or delaminations. Surface texture coarse from entrance end to throat
6300-20	009-11	AGSR-VCG Annealed. Surface Precoated	2C	0.067	0.059	0.038	9.9	8.7	5.6	Entrance end: No cracks or delaminations. Surface texture is rough. Exit end: Two mills of surface coating spalled; remaining coating shows no flaws.
6300-21	009-13	AGSR-VCG Surface Precoated	2C	0.070	0.045	0.036	17.5	11.2	9.0	Coating from entrance end to throat rough.
6300-22	009-14	Recoated 6300-21	—	0.061	0.038	0.033	12.2	7.6	6.6	Coating from entrance end to throat rough.
6300-23	009-15	Recoated 6300-21	—	0.066	0.041	0.031	11.0	6.8	5.2	Coating quality at entrance end improved. However, it is still somewhat rough.
6300-24	009-16	Recoated 6300-21	—	—	0.043	—	—	7.2	—	Mandrel and entrance end of nozzle covered with sooty growths. Exit end of coating irregular and also contains several sooty growths.
6300-25	009-17	Recoated 6300-21	—	—	—	—	—	—	—	Substrate completely covered with cliniker-like deposits.
6300-26	009-18	AGSR-VCG	2C	0.057	—	—	10.4	—	—	No coating from throat to exit end.
6300-27	009-19	Recoated 6300-26	—	0.023	0.037	0.017	4.6	7.4	3.4	Coating fairly clean. A few large nodules (1/16-inch diameter) at entrance end.
6300-28	009-20	Recoated 6300-26	—	0.029	0.048	0.034	5.0	8.2	5.8	Coating of fair quality. A few large nodules at entrance end.
6300-29	009-21	AGSR-VCG Surface Precoated	2C	0.040	0.048	0.034	7.3	8.7	6.2	Coating rough with several large nodules at entrance end.
6300-30	009-22	AGSR-VCG	2C	—	—	—	—	—	—	Coating very rough and irregular. No meaningful measurements could be taken.
6300-31	009-23	Surface Precoated AGSR-VCG Surface Precoated	2C	0.052	0.058	0.044	8.0	8.9	6.8	Coating from entrance end to throat contains many flower-like carbon growths.
6300-32	009-24	AGSR-VCG Surface Precoated	2C	0.058	0.060	0.048	9.7	10.0	8.0	Coating and substrate cracked radially in two places during machining. Coating surface much smoother than in previous runs.
6300-33	009-26	AGSR-VCG Annealed Surface Precoated	2C	0.052	0.060	0.045	8.7	10.0	7.5	No cracks or delaminations. Coating quality appears to be good.

Table III. (continued).

Run Ident. No.	Log Book No.	Substrate		Coating Thickness (in)			Deposition Rate (mils/hr)			Appearance
		Material	Configuration	Entrance	Throat	Exit	Entrance	Throat	Exit	
6300-34 (SN-3)	009-29	AGSR-VCG Annealed. Surface Precoated	2C	0.052	0.055	0.040	8.7	9.2	6.7	No cracks or delaminations.
6300-35	009-35	AGSR-VCG Annealed. Surface Precoated	2C	0.042	0.047	0.034	8.4	9.4	6.8	No apparent defects. Sent to TRW. Thin delaminations observed later.
6300-36	009-37	AGSR-VCG Annealed. Surface Precoated	2C	0.056	0.068	0.049	9.0	10.9	7.8	Coating somewhat rough and grayish in color. No significant delaminations visible.
6300-37	009-39	AGSR-VCG Annealed. Surface Precoated	2C	0.048	0.056	0.043	8.0	9.3	7.2	No examination of coating ends. Substrate and coating cracked axially. Coating surface quality is good.
6300-38	009-40	AGSR-VCG Annealed. Surface Precoated	2C	0.050	0.054	0.045	8.9	9.6	8.0	No defects as deposited. 90-degrees delamination observed subsequently.
6300-39	009-41	AGSR-VCG Annealed. Surface Precoated	2C	0.054	0.055	0.043	10.2	10.4	8.1	No defects.
6300-40	009-44	AGSR-VCG Annealed.	2D	0.047	0.057	0.044	8.9	10.8	8.3	Entrance end stuck to coating fixture and delaminated when separated.
6300-41	009-46	AGSR-VCG Annealed. Surface Precoated	2D	0.048	0.056	0.042	9.4	10.9	8.2	Coating and substrate split axially in two places 90-degrees apart.
63-0042 (SN-4)	009-47	AGSR-VCG Annealed. Surface Precoated	3	0.051	0.057	0.043	10.0	11.2	8.4	No significant flaws.
6300-43	009-48	AGSR-VCG Annealed. Surface Precoated	3	0.048	0.046	0.036	10.2	9.8	7.7	No significant flaws.
6300-44	002-12	AGSR-VCG Annealed. Surface Precoated	3	0.036	0.038	0.029	10.5	11.1	8.5	Entrance end: No cracks or delaminations. Exit end: Occasional short, very fine delaminations visible, in coating, near pores in substrate.
6300-45 (SN-5)	001-13	AGSR-VCG Annealed. Surface Precoated	3	0.054	0.057	0.047	10.2	10.8	8.9	Entrance end: No cracks or delaminations. Exit end: No cracks or delaminations.

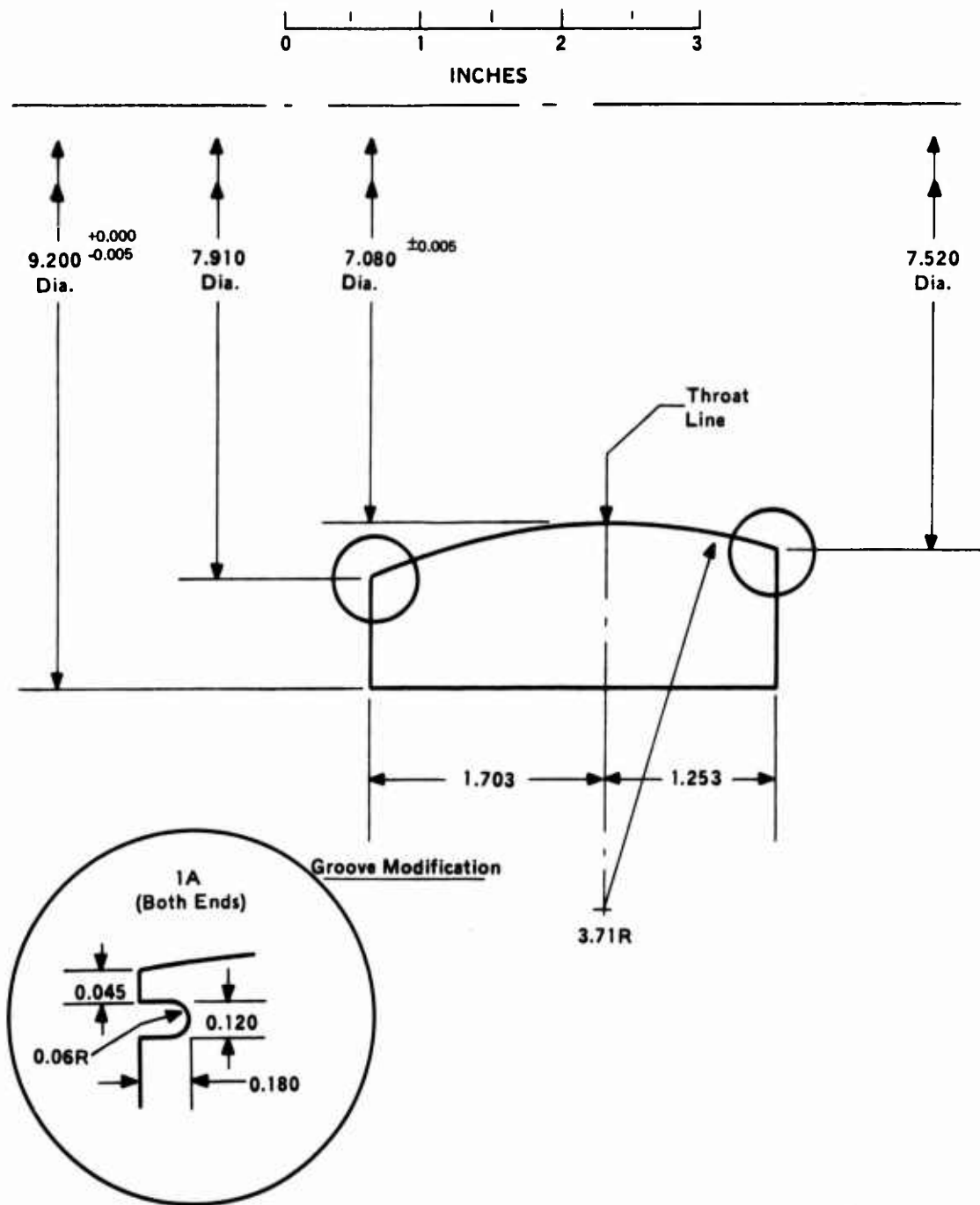


Figure 8. 7.0-inch Nozzle Throat Insert Substrate Configurations 1 and 1A.

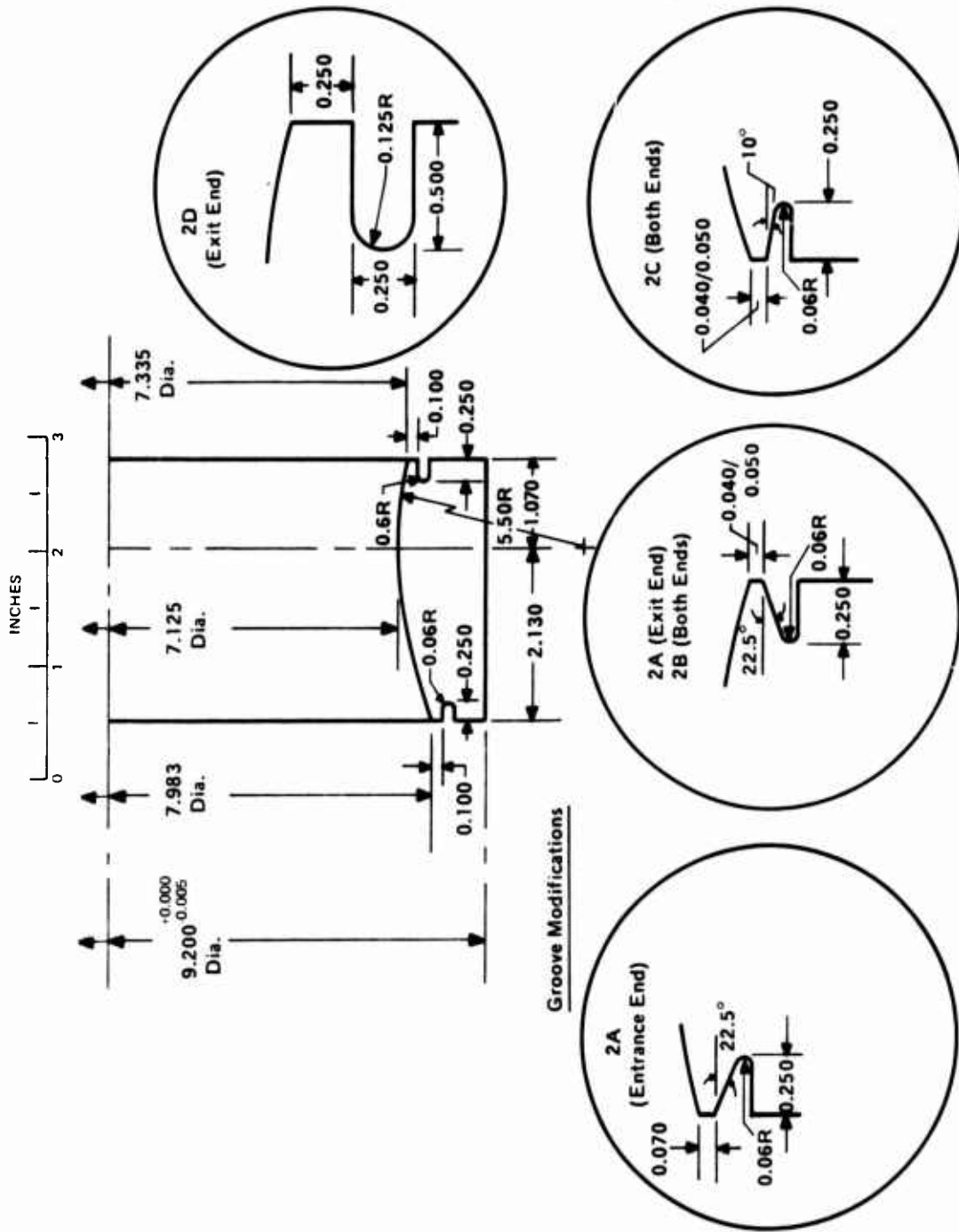


Figure 9. 7.0-inch Nozzle Throat Insert Substrate Configuration 2 (Including groove modifications).

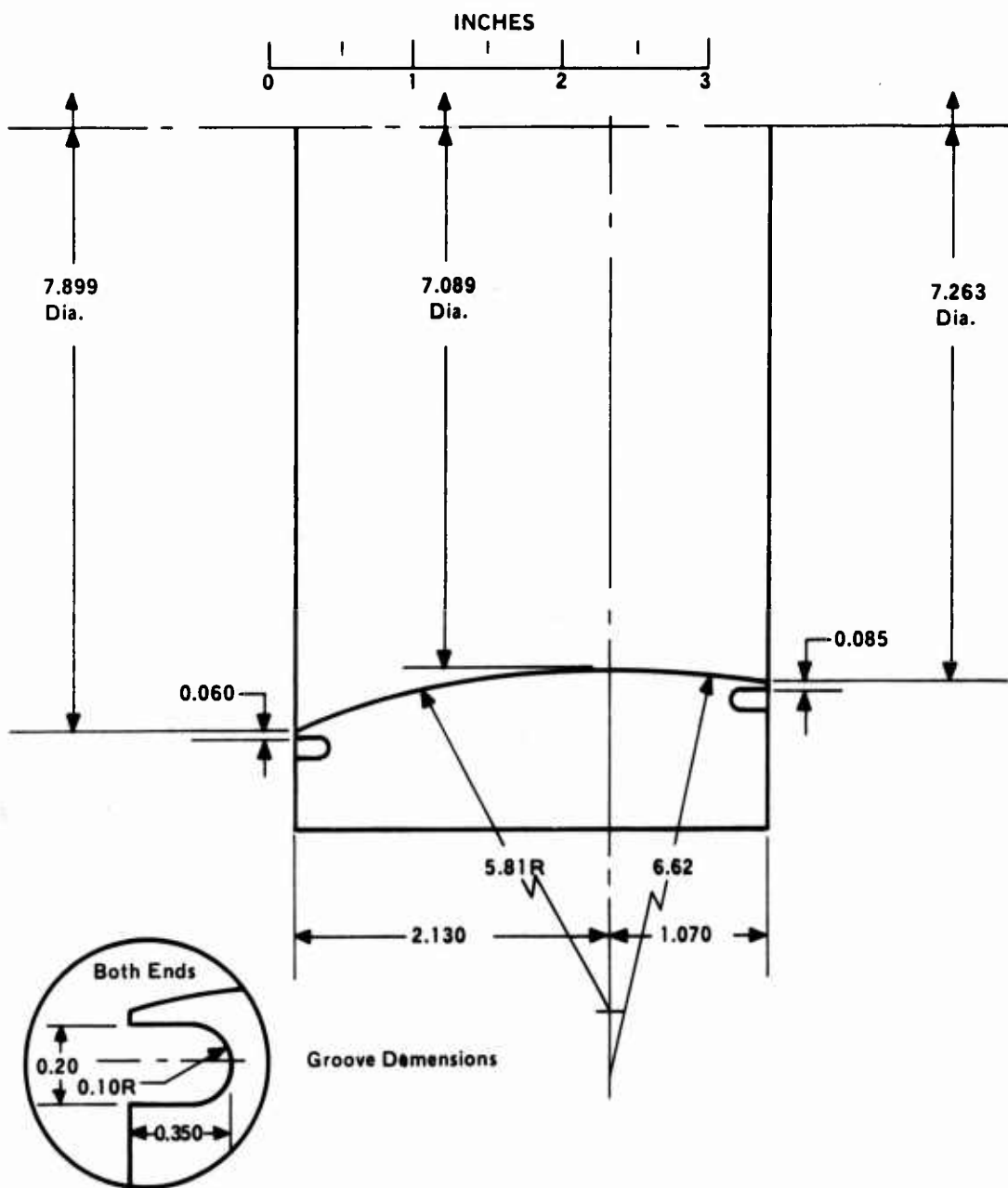


Figure 10. 7.0-inch Nozzle Throat Insert Substrate Configuration 3.

Table IV. 7.0-Inch Nozzle Throat Insert Substrate Dimensional Changes After Coating.

Run Ident No.	Log Book No.	Substrate Material	Percent Change in Substrate Dimensions After Coating			
			Entrance OD	Throat OD	Exit OD	Length
6300-38	009-40	AGSR-VCG (Annealed) ↓	0.36	0.20	0.24	-0.03
6300-39	009-41		0.40	0.16	0.21	0.03
6300-40	009-44		0.15	0.12	0.16	—
6300-42 (SN-4)	009-47		0.46	0.23	0.25	—
6300-43	009-48		0.41	0.26	0.26	—
6300-44	001-12		0.22	0.17	0.18	-0.9
6300-45 (SN-5)	001-13		0.38	0.34	0.34	—

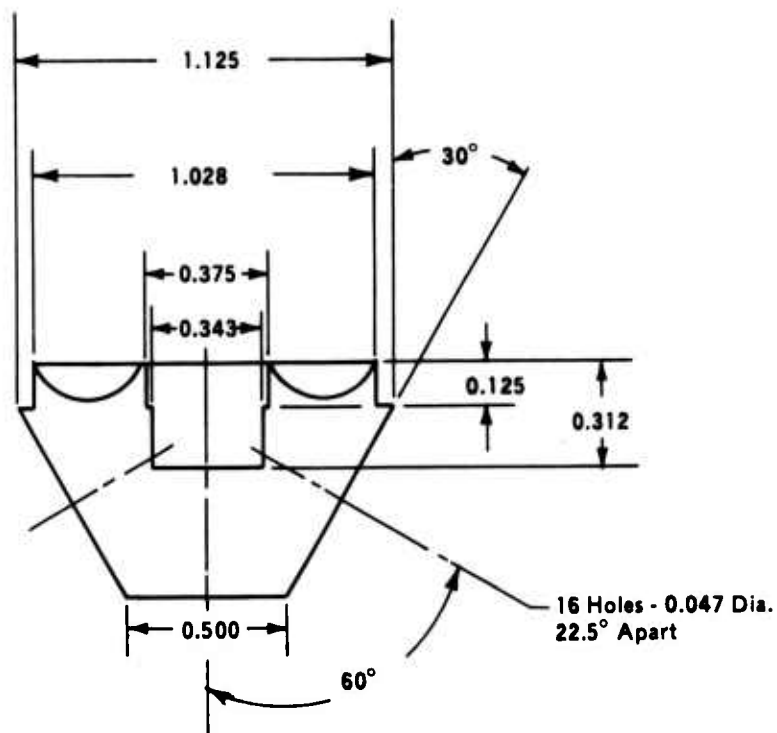
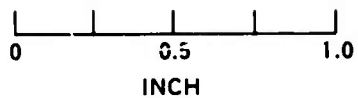


Figure 11. 7.0-inch Injector Tip Configuration 1.

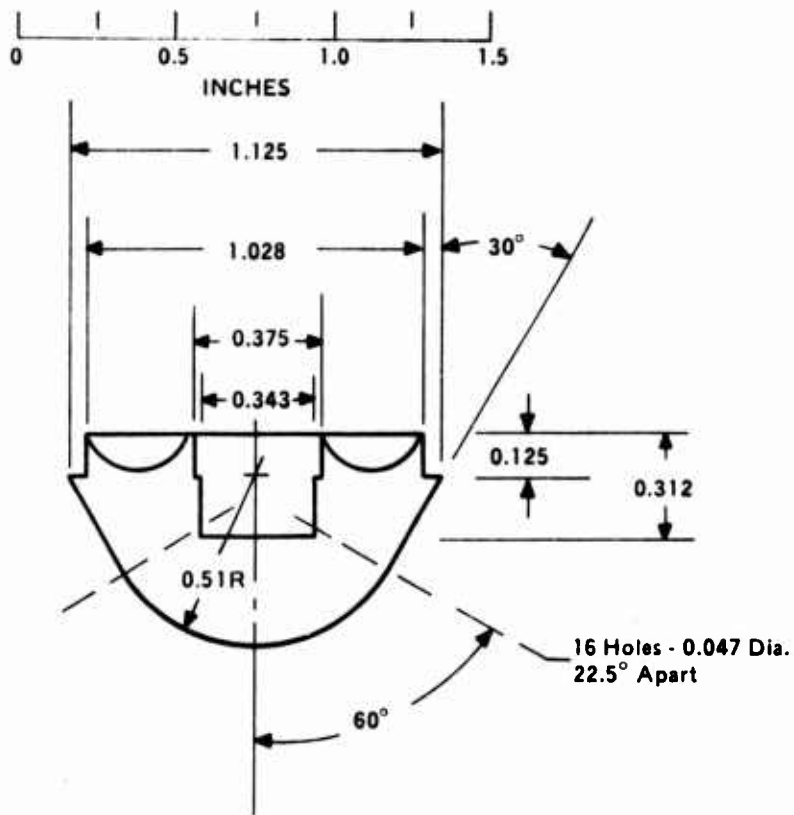


Figure 12. 7.0-inch Injector Tip Configuration 2.

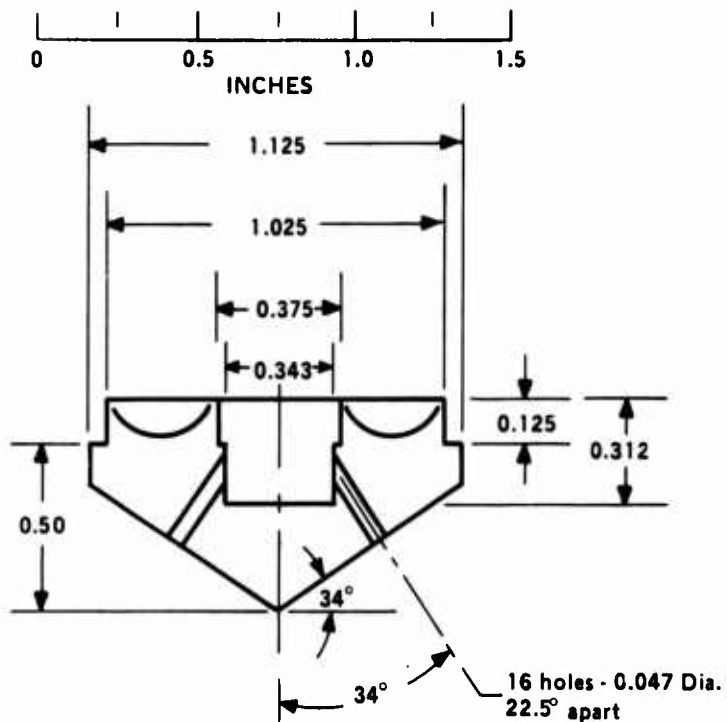


Figure 13. 7.0-inch Injector Tip Configuration 3.

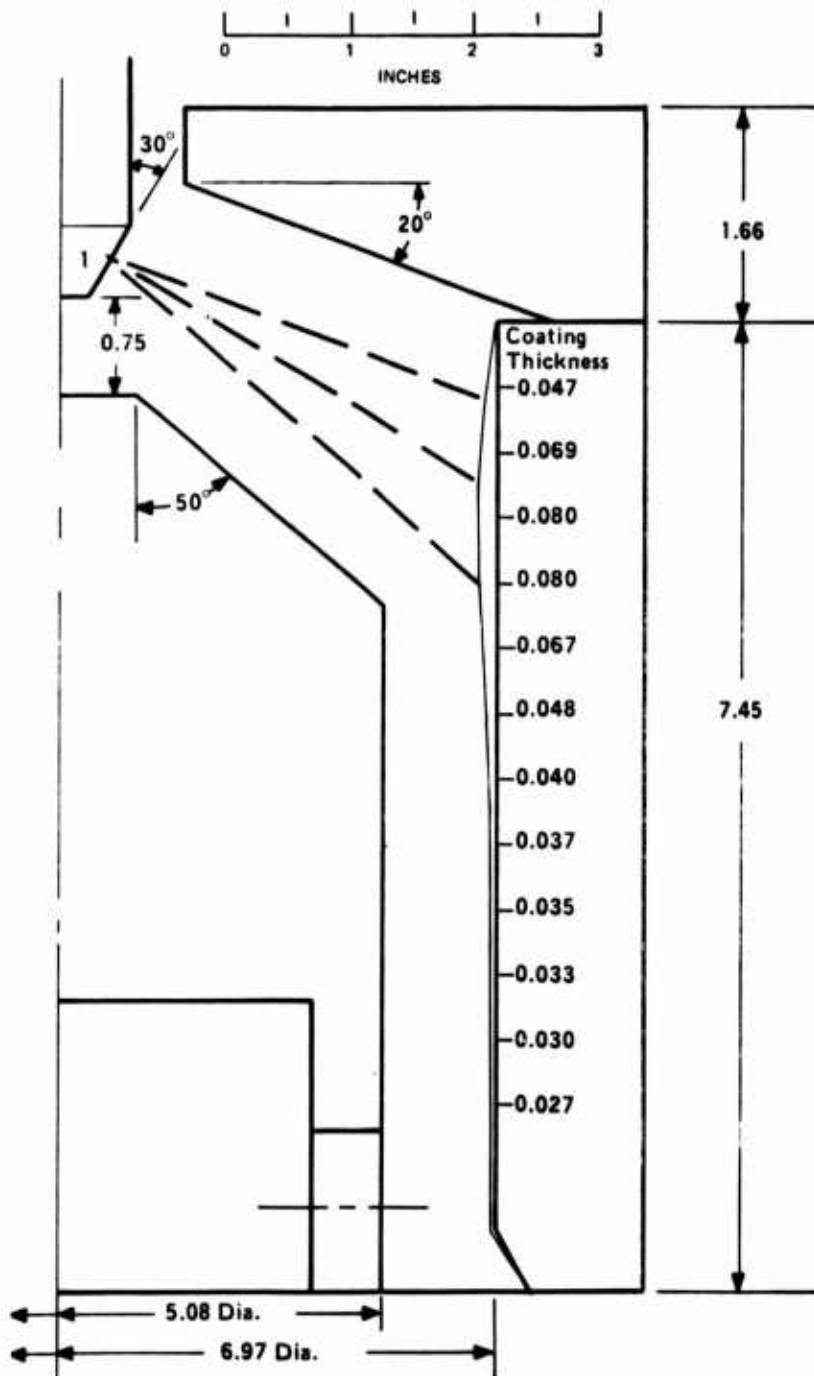


Figure 14. Deposition Chamber Geometry of Run No. 6000-1.

Run 6300-1, the first 7.0-inch nozzle throat insert deposition run, was conducted utilizing the deposition chamber geometry shown in Figure 15. The deposition gas flow rates were the same as those of the previous run. Post-deposition examination showed the coating surface finish to be acceptable with the exception of one small nodule near the entrance end. No cracks or delaminations were visible in either the coating or the substrate. The high deposition rate at the entrance end indicated that the substrate was positioned too low in the deposition chamber.

Run 6300-2 was conducted using the same procedure and gas flow rates as the previous deposition run. The mandrel was cleaned to the original diameter of 5.08 inches and positioned in the center of the nozzle I.D. as before to reduce the cross-sectional area within the deposition chamber. The deposition chamber geometry (Figure 16) was similar to that of the previous run. The substrate was moved up one inch to increase the deposition rate in the throat and downstream areas. Post-deposition examination showed the coating surface to be similar to that of the previous run. The deposition rate decreased by 49 percent at the entrance end, increased by 57 percent at the throat, and increased by 35 percent at the exit end. Because of the minimal thickness of the coating at the ends, no microscopic examination was conducted.

Run 6302-3 was conducted using the same gas flow rates as the previous run. To increase the deposition rate at the entrance end, relative to the throat, the substrate was moved down 1/2 inch in the deposition chamber. This substrate position was midway between that of 6300-1 and 6300-2. An attempt was made to increase the deposition rate at the exit end by tapering the mandrel diameter out from the throat area toward the exit end of the substrate. This resulted in a decrease of 52 percent in the annular cross-sectional area at the exit end. The deposition chamber geometry is shown in Figure 17. Post-deposition examination showed the coating surface to be rough from the throat area to the exit end indicating soot formation within the gas stream in this area. Evidence of this sooting could be seen on the mandrel where a V-shaped, clinkerlike deposit had formed. The coated substrate was trimmed, polished and examined microscopically at both ends. The coating contained many short, fine delaminations at the entrance end. No flaws were visible at the exit end. The deposition rate increased by 89 percent at the entrance end, decreased by 9 percent at the throat, and increased by 43 percent at the exit end.

Run 6300-4 was conducted using the same deposition chamber geometry (Figure 17) as the previous run. The process and annulus nitrogen flow rates were increased by 25 percent and the methane rate was increased by 20 percent. This effectively reduced the methane concentration by 4 percent. The increase in nitrogen rates and reduction of methane concentration were an attempt to reduce the amount of sooting in the gas phase and thereby improve the coating surface texture. Post-deposition examination showed the coating to be rough from the throat to the exit end, as in the previous run. A clinkerlike deposit had grown on the mandrel in the same manner as before. This problem was found to be related to misalignment of the injector gas exit ports. Although the increase in gas flow rates did not solve the coating roughness problem, it did increase the overall deposition rate and improve the uniformity of the axial coating thickness profile. The deposition rate increased by 13 percent at the entrance end, 7 percent at the throat, and 29 percent at the exit end.

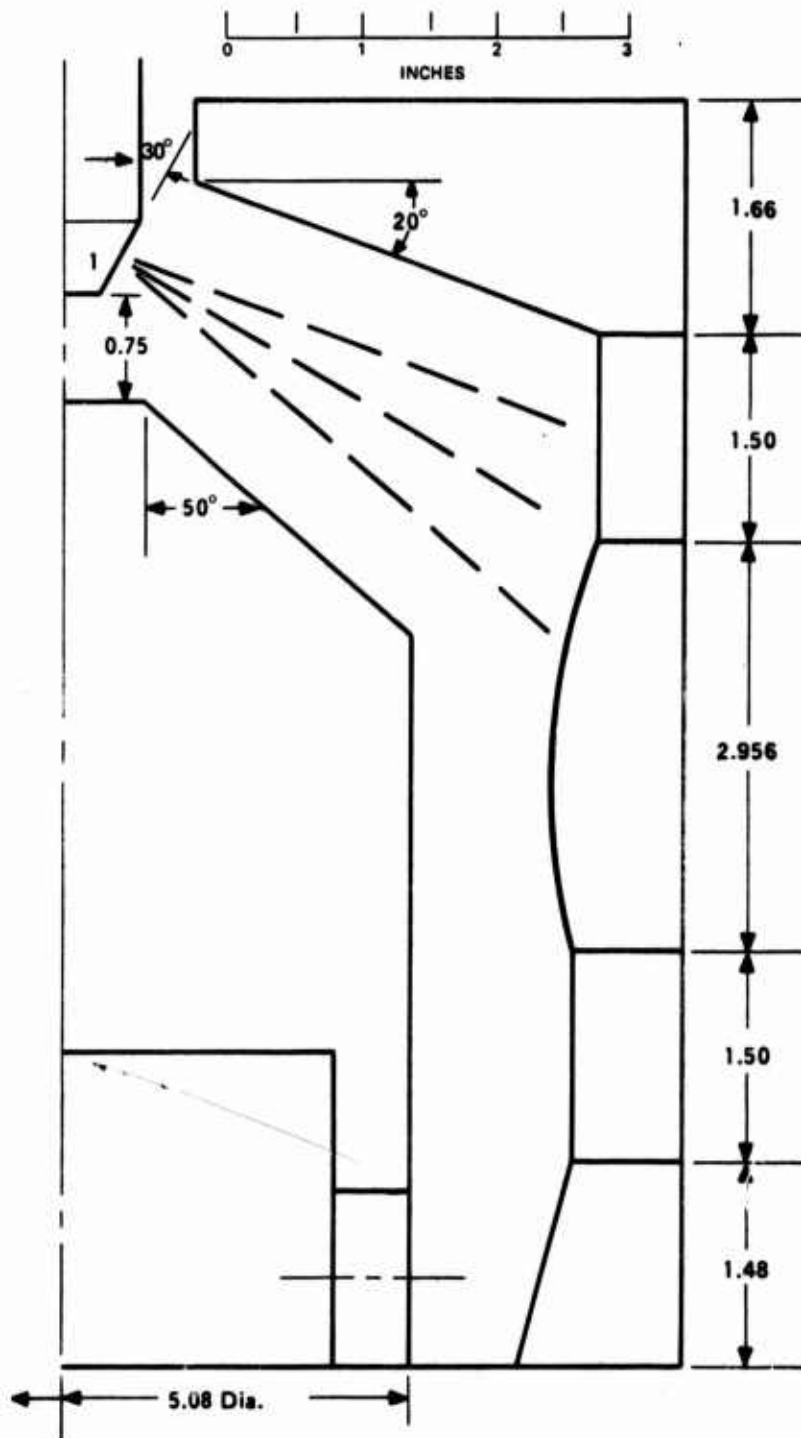


Figure 15. Deposition Chamber Geometry of Run No. 6300-1.

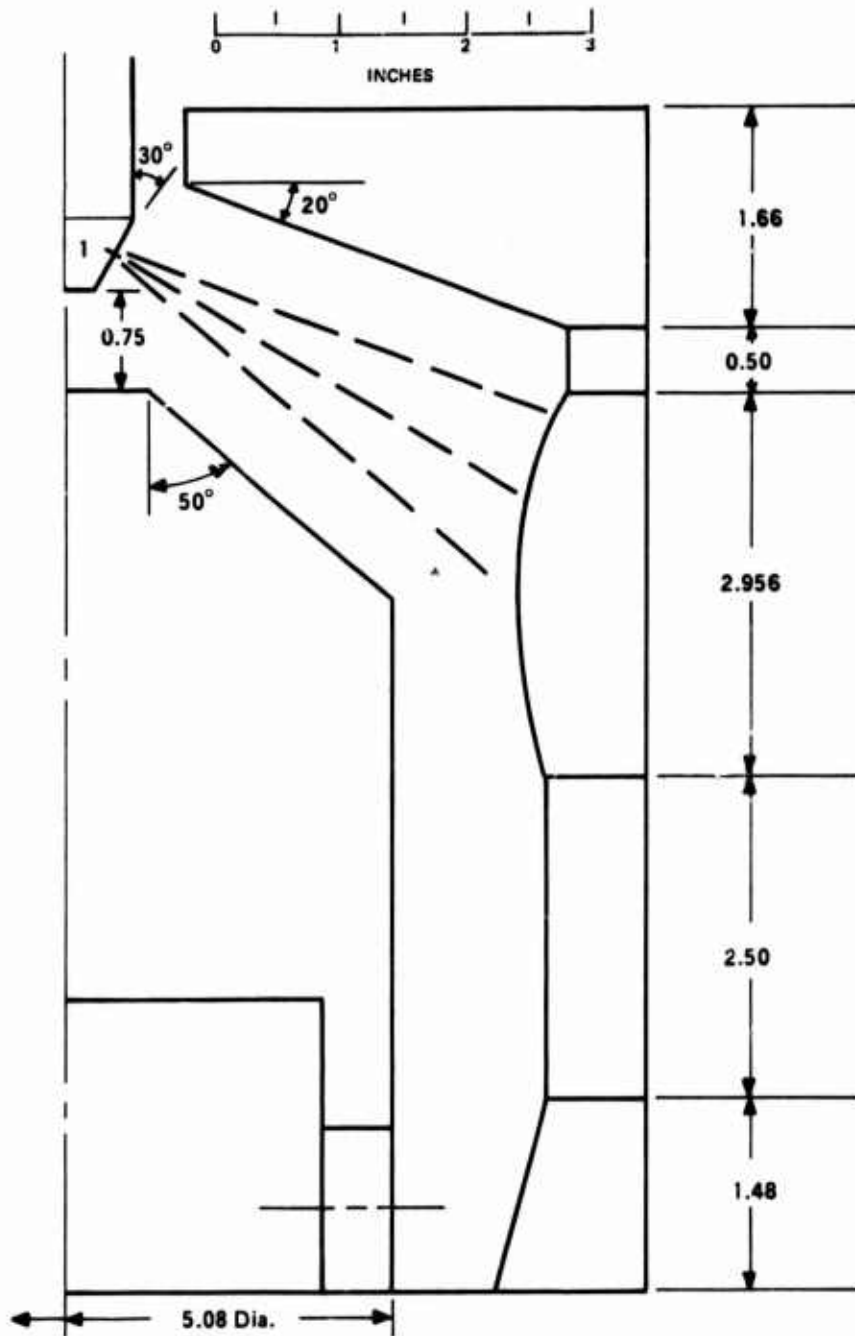


Figure 16. Deposition Chamber Geometry of Run No 6300-2.

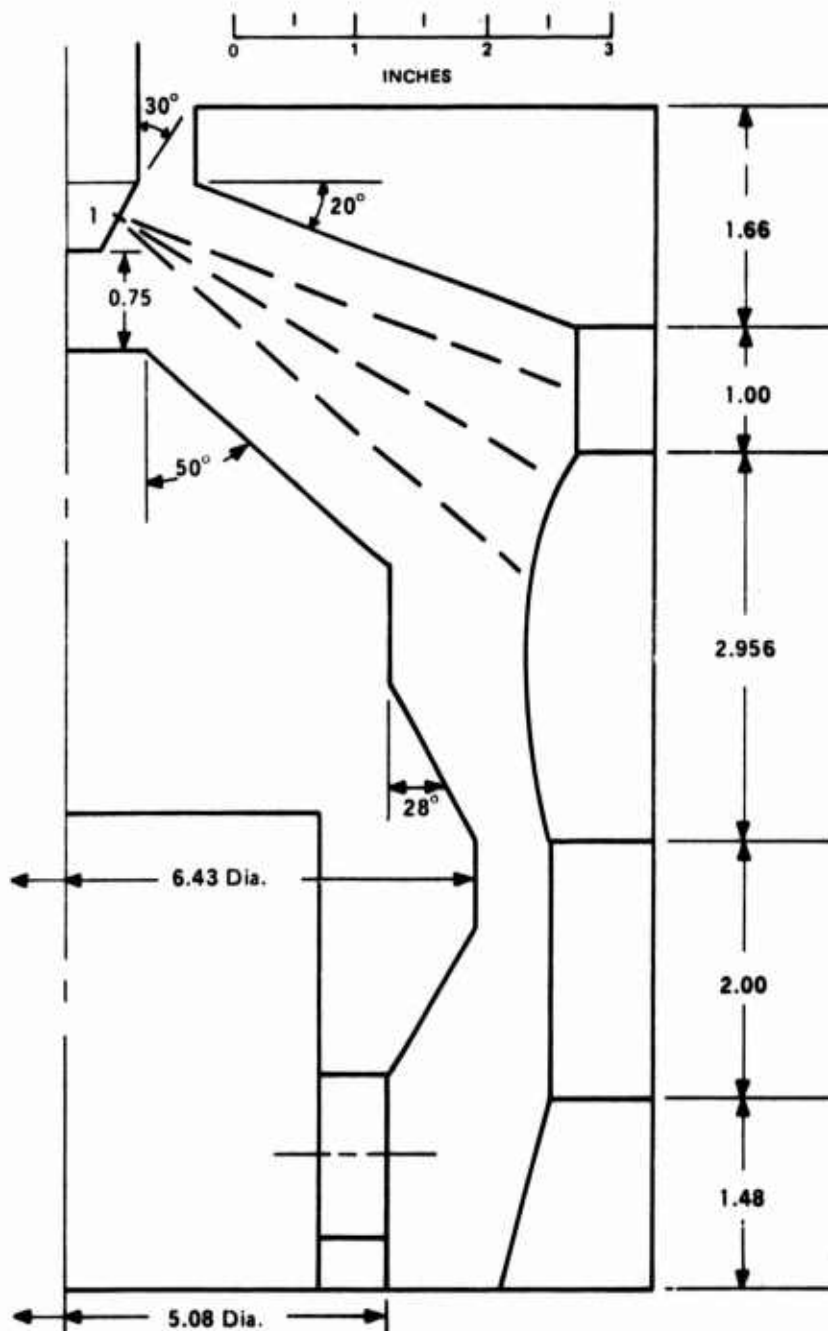


Figure 17. Deposition Chamber Geometry of Run No's 6302-3 and 6300-4.

Run 6300-5 was conducted using the same deposition gas flow rates as the previous run. A new injector tip (Configuration 2) was utilized to correct the coating roughness problem encountered in the previous runs. The deposition chamber geometry was similar to that of the previous run and is shown in Figure 18. Post-deposition examination showed the coating to be smooth and free of surface defects. No evidence of sooting could be seen on either the substrate or the mandrel. Microscopic examination of the polished coating ends revealed delaminations within the coating at the entrance end. These delaminations were the result of high stress levels at the coating end and were, in this case, directly related to the greater coating thickness of the entrance end. The increased deposition rate at the entrance end appears to be related to the impingement pattern of the gas cone on the substrate with the new injector tip configuration. As can be seen in Figure 18, the gas cone strikes the substrate approximately 1/4 inch higher than in the previous run. Because of this, the deposition rate increased by 13 percent at the entrance end and decreased by 22 percent at the exit end. The rate at the throat did not change.

Run 6300-6 was conducted utilizing the gas flow rates of the first four 7.0-inch runs to determine if the new injector tip design would function properly at the reduced rates. This run would, therefore, be comparable to Run 6302-3. The deposition chamber geometry was the same as that of the previous run (Figure 18). Post-deposition examination of the polished coating ends revealed a few very short, fine delaminations at the entrance end. These were minor in nature, and none were more than a few growth cones in length. Stress relief grooves were machined into the ends of this substrate before deposition. This represented the first use of these grooves in the large nozzle sizes, and it appears that they are effective in reducing coating end stresses as has been demonstrated in the past with smaller nozzle shapes. The reduction in gas flow rates yielded the expected reduction in deposition rate. Compared to 6302-3, the coating deposition rate at the entrance end increased somewhat and that at the exit decreased slightly. The rate at the throat showed very little change. These effects were consistent with the gas impingement pattern of the new injector tip on the forward end of the substrate.

Run 6300-7 was the first conducted using substrate Configuration 2. The deposition chamber geometry, shown in Figure 19, was modified to accommodate the longer substrate, but was in general similar to that of 6300-6. Deposition gas flow rates were the same as those of 6300-6. Post-deposition examination showed the coating to be disproportionately thick at the entrance end. The throat thickness was satisfactory, and the exit thickness was acceptable, although it was somewhat thinner than desired. The coating texture was rough throughout, especially at the entrance end. Microscopic examination disclosed no serious cracks or delaminations in either coating or substrate.

Run 6300-8 was conducted with the injector 1/2 inch lower in the deposition chamber. The mandrel was shortened by 1/2 inch at the tip with an appropriate change in angle. The deposition chamber geometry is shown in Figure 20. These changes were made to increase the proportional deposition rate from the throat to the exit end. Deposition gas flow rates were the same as those of the previous run. Post-deposition examination showed the deposition rate at the throat to be more than twice that at either end. This resulted in an unacceptable coating thickness profile. The coating surface texture was also rough as in the previous run.

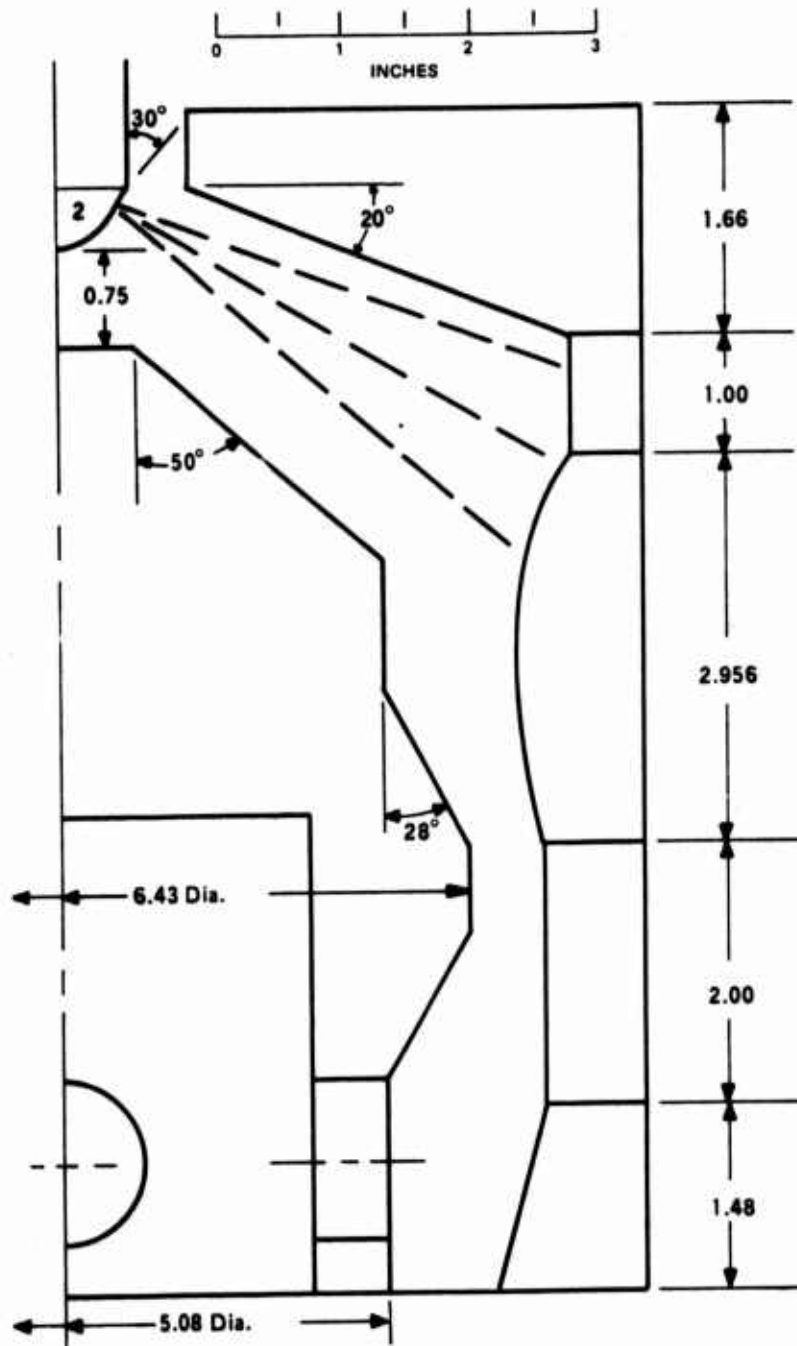


Figure 18. Deposition Chamber Geometry of Run No's 6300-5 and 6300-6.

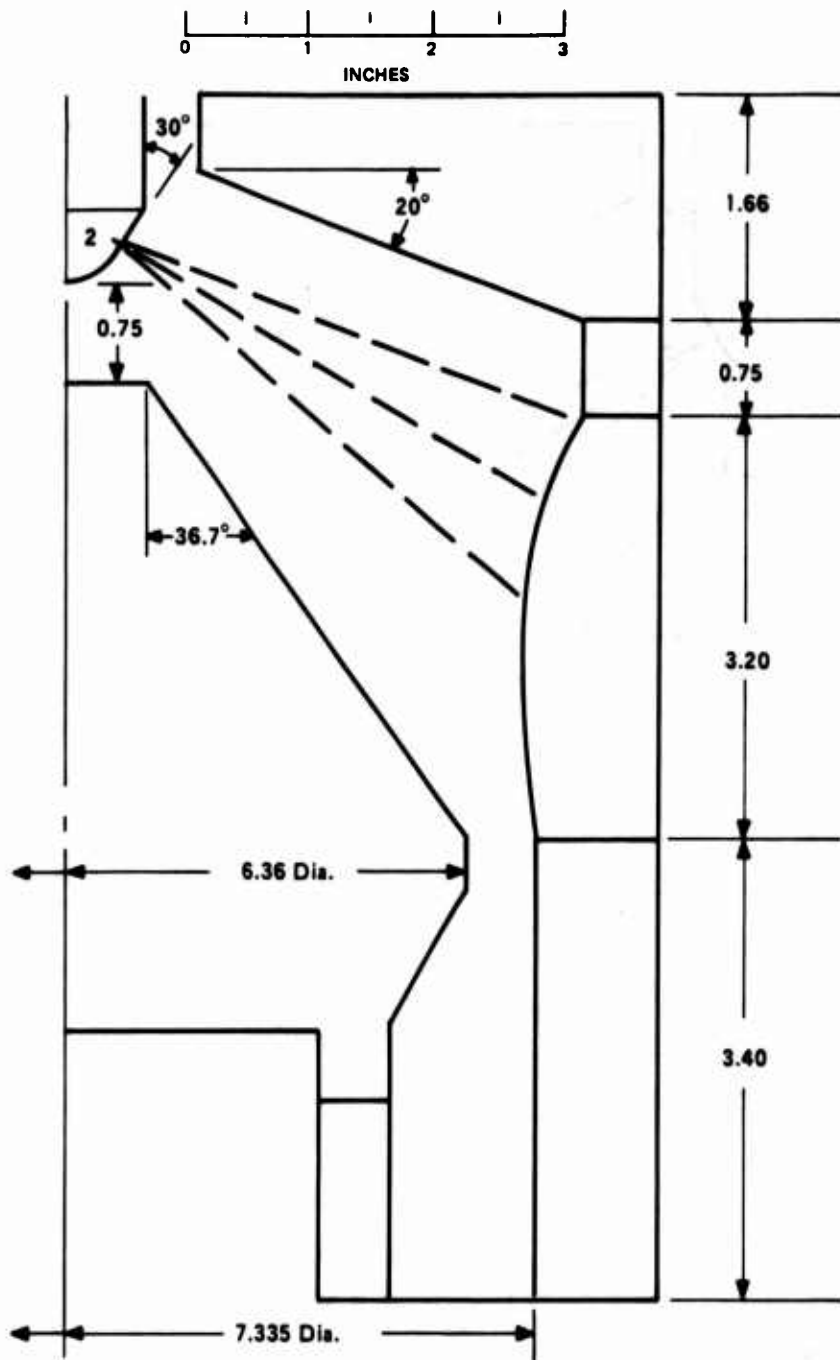


Figure 19. Deposition Chamber Geometry of Run No. 6300-7.

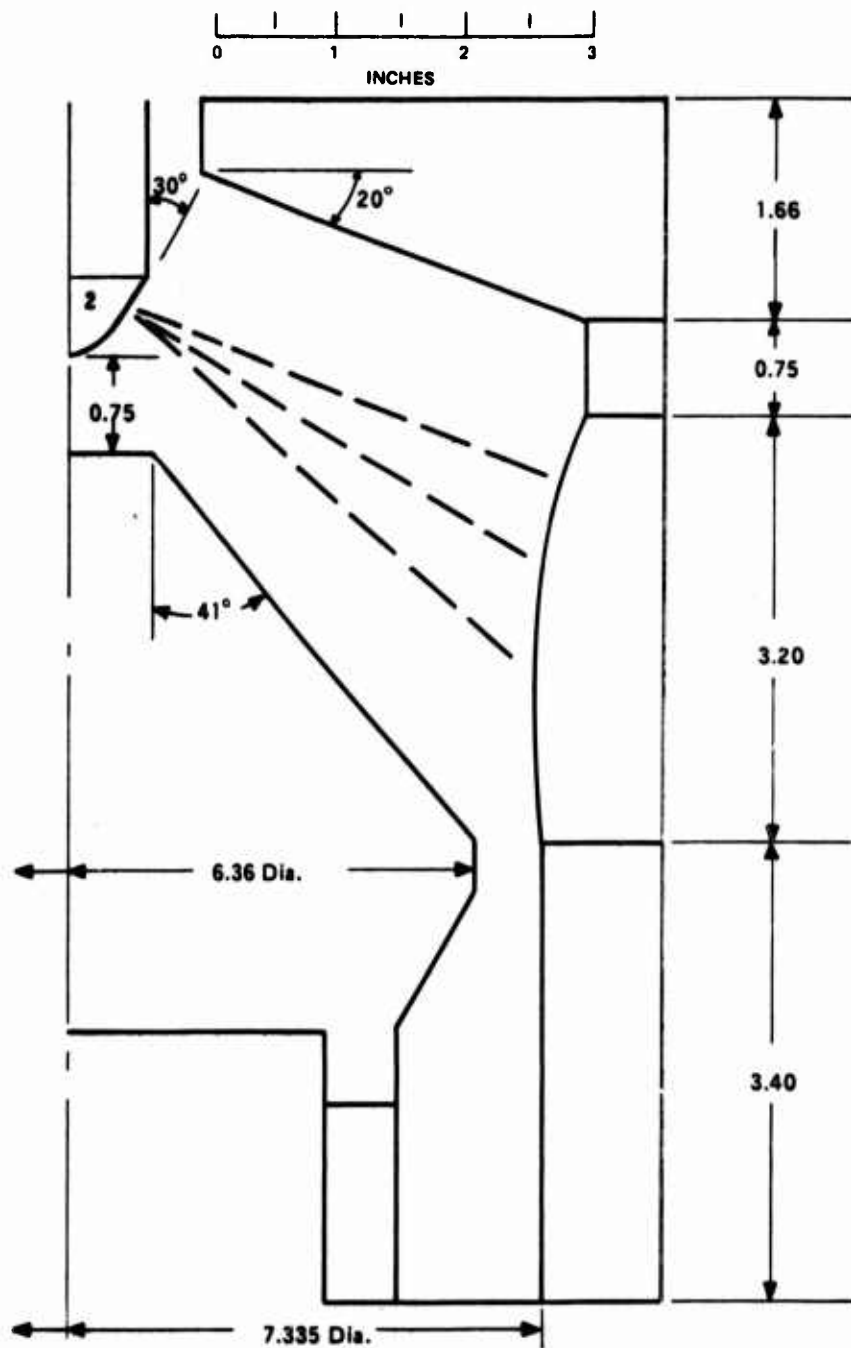


Figure 20. Deposition Chamber Geometry of Run No. 6300-8.

Run 6300-9 was conducted utilizing a modified deposition chamber geometry, as shown in Figure 21. This geometry permitted a greater injector standoff distance so the deposition gas cone could expand and cover the substrate surface. A new injector tip (Configuration 3) was utilized to accommodate this increased standoff. Deposition gas flow rates were the same as those of the previous run. Post-deposition examination showed the overall coating thickness to be less than acceptable for firing. The coating quality and thickness distribution were superior to that achieved using the old injector design. No cracks or delaminations were present in the coating at the entrance end. The coating at the exit end exhibited two very fine delaminations ten to twenty growth cones in length. These were relatively insignificant and the coating would have been considered acceptable for motor firing were it thick enough.

Run 6300-10 was conducted utilizing the same deposition chamber geometry (Figure 21) and gas flow rates as the previous run. The deposition time was increased to obtain an average coating thickness of 60 mils in the forward section of the substrate. The injector was moved down 1/8 inch to increase the proportional deposition rate at the exit end. Post-deposition examination showed the coating to have bridged the release gap between the entrance approach section and the entrance end of the substrate, bonding the two parts together. The entrance section was CS graphite and of higher thermal expansion than AGSR. This induced excessive stresses in the coating on the entrance piece and it delaminated. Because the coating had bridged the two parts, the delamination propagated into the coating on the substrate. The removal of an additional 0.250 inch of material from the nozzle entrance end was required to remove the effects of this delamination. The coating at the exit end also contained a delamination near the substrate interface extending for 360 degrees. There was no bridging of the coating indicating that this delamination was the result of excessive residual stress at the exit end. The deposition rate was highest at the entrance end of the substrate and decreased toward the downstream end.

Runs 6300-11 through 6300-15 were all conducted using the deposition chamber geometry shown in Figure 22. The deposition gas flow rates were the same as those of the previous run. Post-deposition examination of the five parts showed the coatings to be so rough in surface texture as to be unacceptable.

Run 6300-16 was conducted utilizing the deposition chamber configuration of the previous five runs (Figure 22). The annulus and process nitrogen rates were increased by 25 percent and the methane rate was increased by 20 percent in an attempt to reduce sooting in the gas phase and improve the coating surface texture. Post-deposition examination showed some improvement in the coating surface texture. The deposition rate at the entrance end was too low and, therefore, the coating was disproportionately thin in this area.

Runs 6300-17 through 6300-19 were all conducted using the deposition chamber geometry shown in Figure 23. Deposition gas flow rates were the same as those of the runs just prior to 6300-16. The coating achieved in 6300-17 contained a series of short, fine delaminations at the exit end. The coating from 6300-18 was somewhat thinner, and contained no cracks or delaminations. This part was selected for use in the first 7.0-inch test firing of the program, SN-1. The third part, 6300-19, was similar to 6300-18 and was selected for Test Firing SN-2. The coatings on both of these parts were somewhat rough from the entrance end to the throat plane and were not of the quality achieved later in the program. This probably accounts for their exceptionally poor performance during firing. See Volume I.

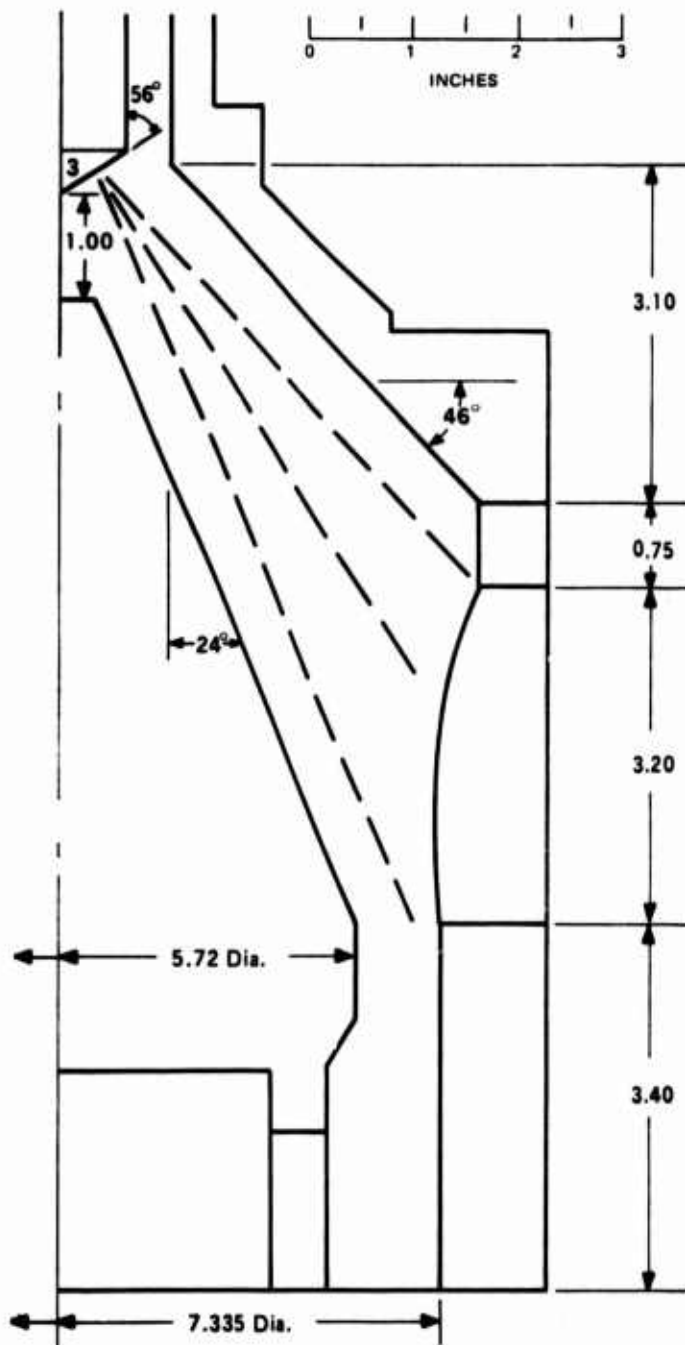


Figure 21. Deposition Chamber Geometry of Run No's 6300-9 and 6300-10.

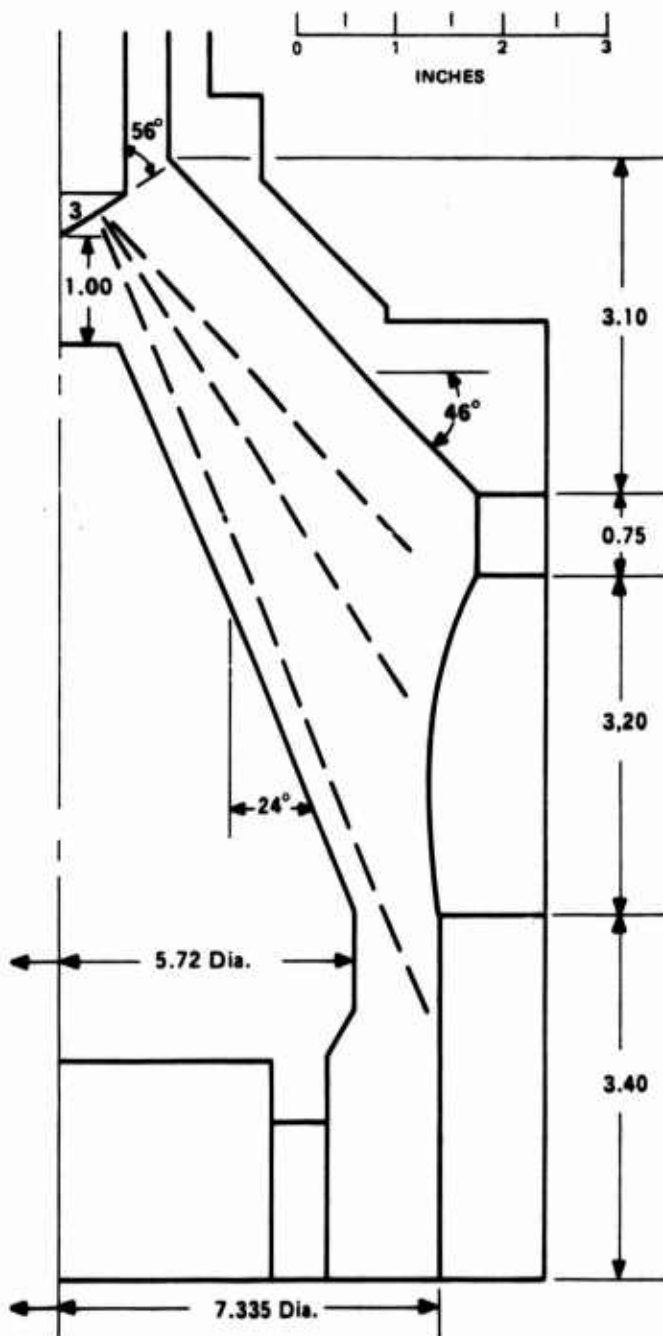


Figure 22. Deposition Chamber Geometry of Run No's. 6390-11 thru 6300-16.

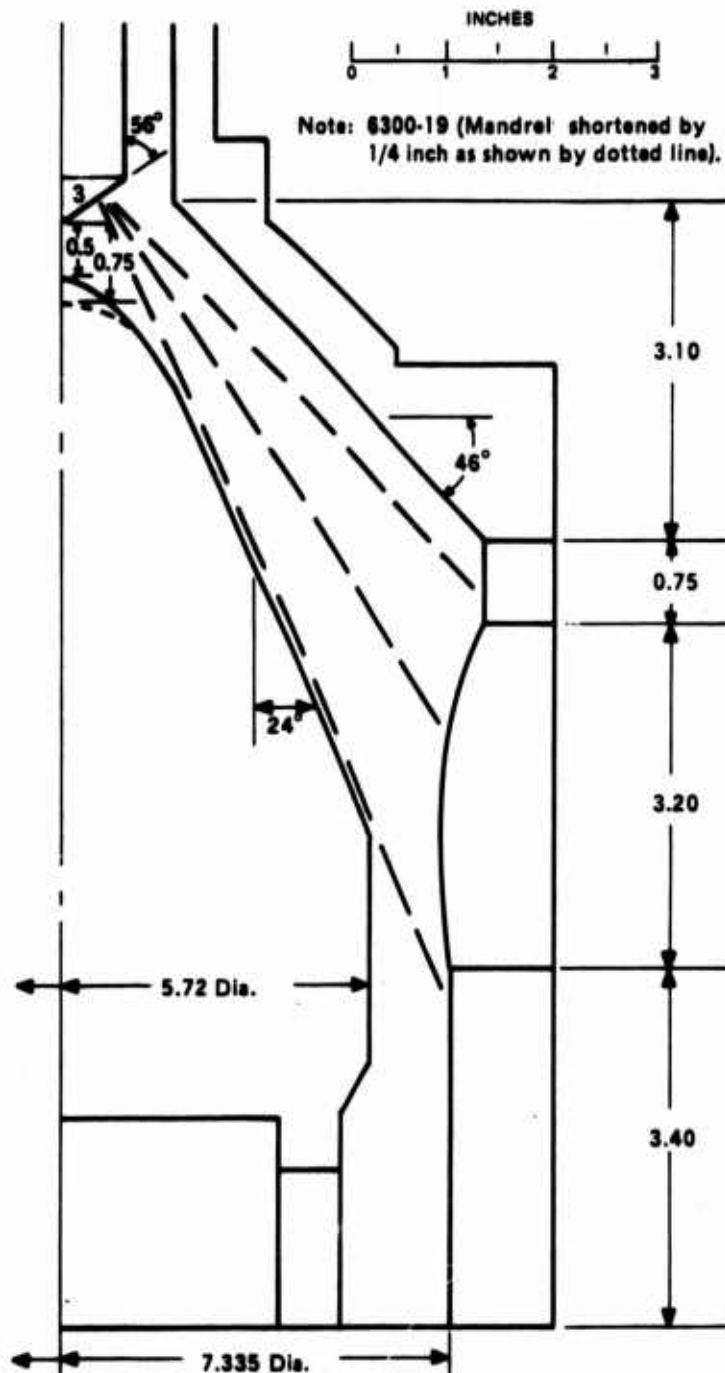


Figure 23. Deposition Chamber Geometry of Run No's. 6300-17 thru 6300-19 and Run No. 6300-30.

Run 6300-20 was conducted using the deposition chamber geometry shown in Figure 24. The injector was moved 1/4 inch closer to the substrate than in the previous run, and the mandrel was shortened by 1/2 inch in an attempt to increase the deposition rate at the exit end. All other conditions were the same as those of Run 6300-19. Post-deposition examination showed the injector movement to have had little effect on the coating thickness profile. The coating surface from the entrance end to the throat was rough, as in the previous runs. At the exit end, a 2-mil-thick layer of the coating surface separated after the trimming operation. A buildup of soot and clinkers formed on one area of the mandrel. As the substrate rotated past this area, a change in the deposition flow pattern resulted that was reflected as a spiraling band within the coating. This band represented an area of extensive sooting within the coating and was probably related to the spallation at the coating surface. The polished coating ends showed no cracks or delaminations.

Runs 6300-21 through 6300-24 represented a return to a geometry similar to that utilized for the first eight 7.0-inch nozzle insert deposition runs. The gas exhaust area was increased by setting the mandrel body on four 1/2-inch-diameter posts to prevent clogging. The deposition chamber geometries for these four runs are shown in Figures 25 through 28. None of the coatings fabricated during these four runs were acceptable.

Runs 6300-25 and 6300-26 were conducted with the mandrel removed and at an increased process nitrogen flow rate in an attempt to eliminate the sooting problem encountered in the previous four runs. The deposition chamber geometries are shown in Figures 29 and 30. Neither of these runs produced an acceptable coating.

Run 6300-27 was conducted in a manner similar to the previous run. The deposition chamber geometry is shown in Figure 31. The Configuration 2 injector tip was modified to Configuration 4 by drilling a second series of orifices below the first at a 45-degree angle. This angle of inclination is such that when the axis of the first series of orifices intersects the substrate above the throat line, the axis of the second series intersects the substrate between the throat and the exit end. Post-deposition examination showed the coating surface texture to be improved over that of the previous several runs. The deposition rate at the ends was too low in comparison with that of the throat.

Run 6300-28 was conducted with the mandrel reinstalled and utilized the modified injector tip. The deposition chamber geometry is shown in Figure 32. Post-deposition examination showed the coating surface texture to be of fair quality. The disparity between the end coating thicknesses and the throat showed little improvement over that of the previous run.

Run 6300-29 was conducted in the same manner as the previous run with the substrate positioned 1/2 inch lower in the deposition chamber to increase the deposition rate at the entrance end. The deposition chamber geometry is shown in Figure 33. Post-deposition examination showed the changes in deposition chamber geometry to have had the desired effect on the coating deposition rate profile. However, the coating was rough in texture and contained several large nodules at the exit end.

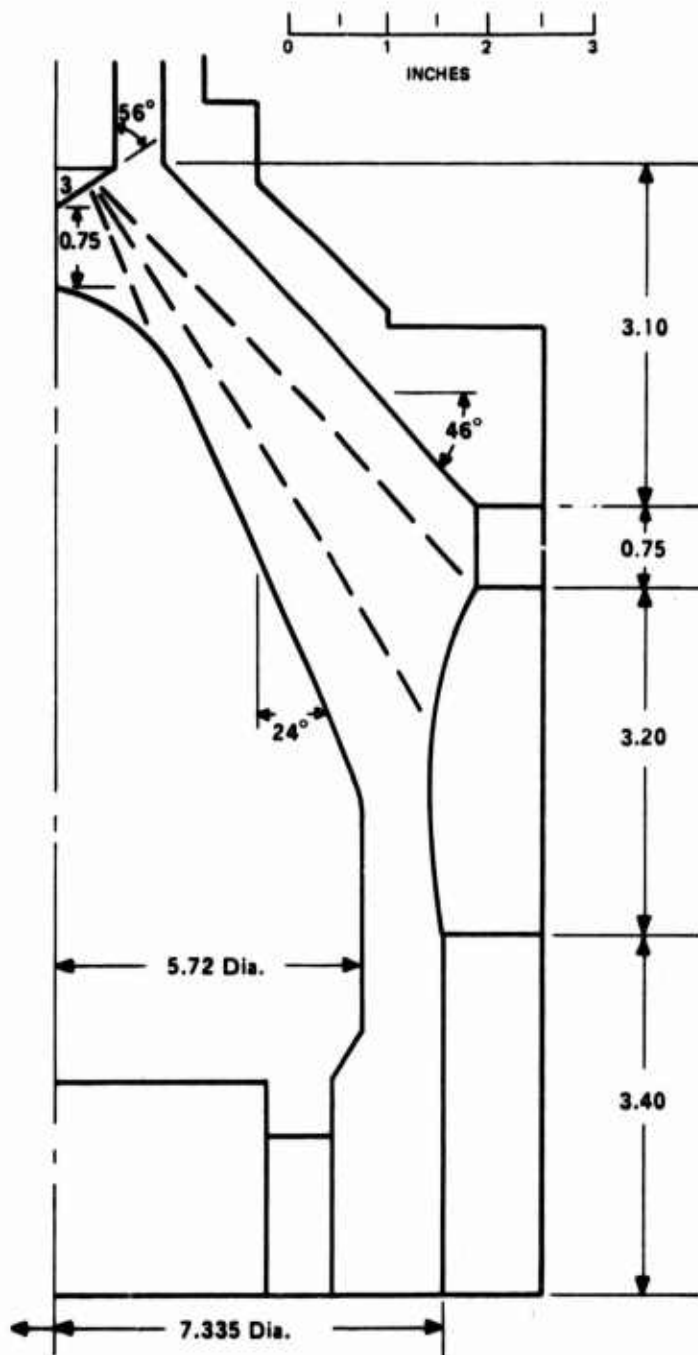


Figure 24. Deposition Chamber Geometry of Run No. 6300-20.

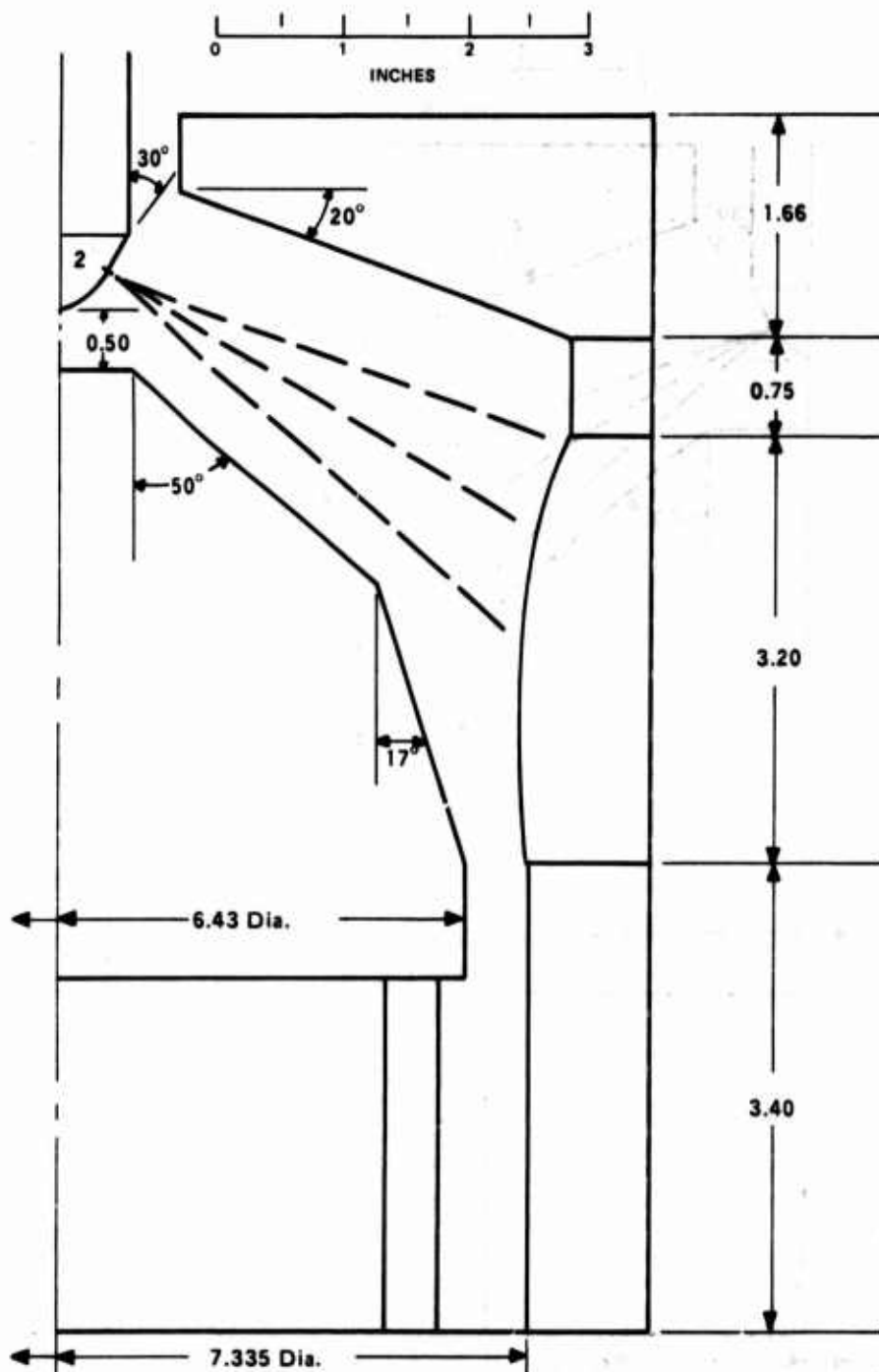


Figure 25. Deposition Chamber Geometry of Run No. 6300-21.

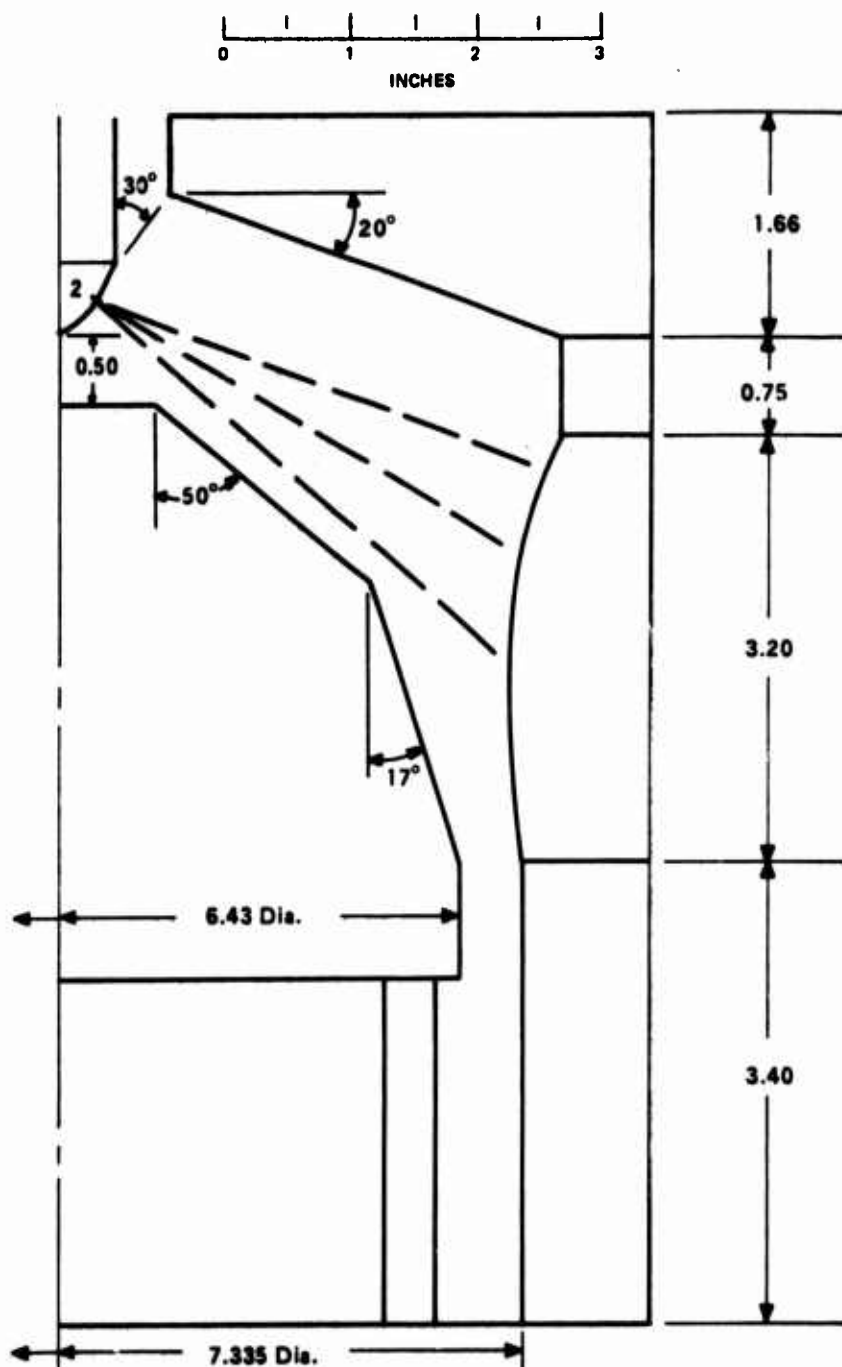


Figure 26. Deposition Chamber Geometry of Run No. 6300-22.

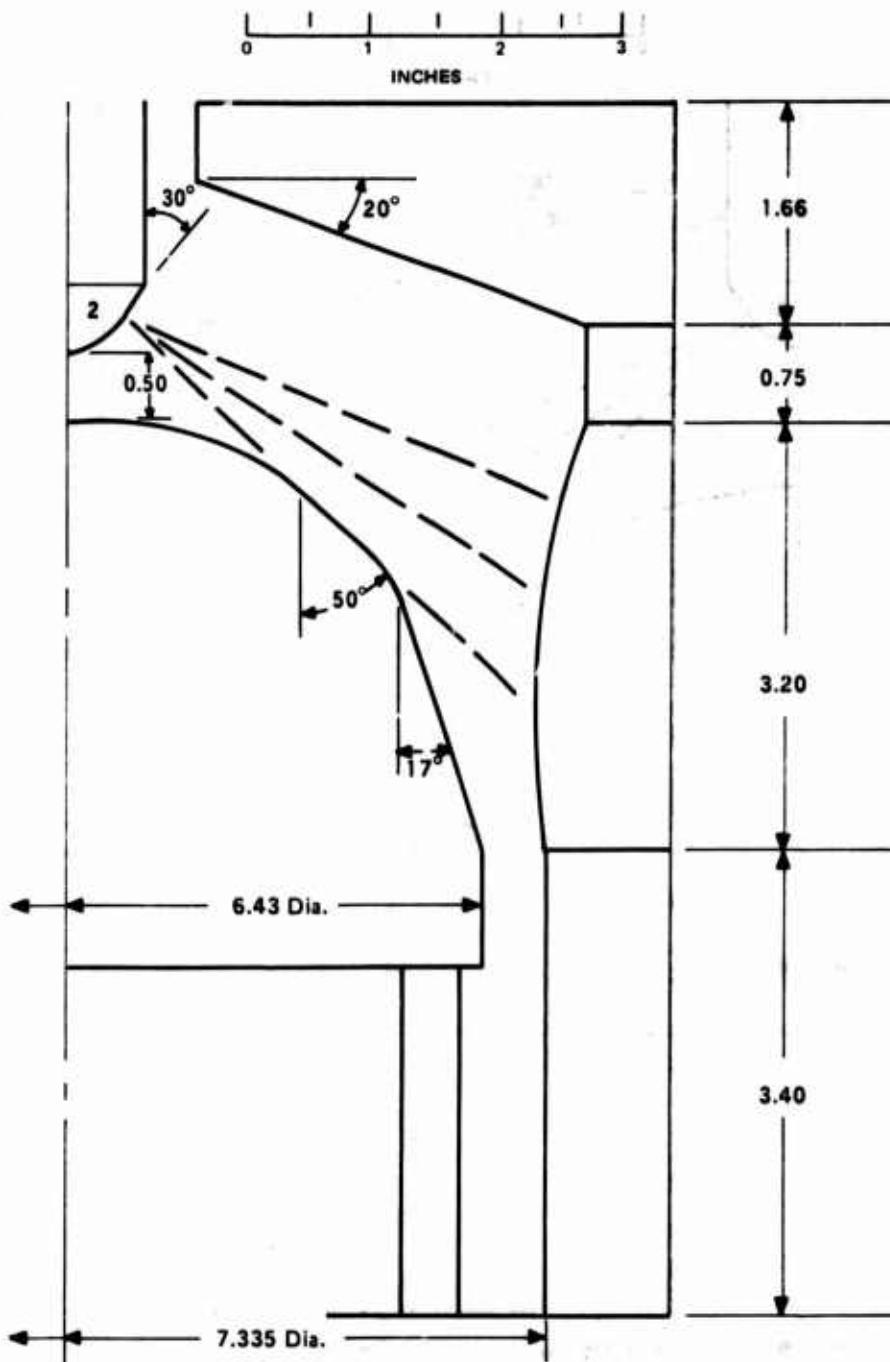


Figure 27. Deposition Chamber Geometry of Run No. 6300-23.

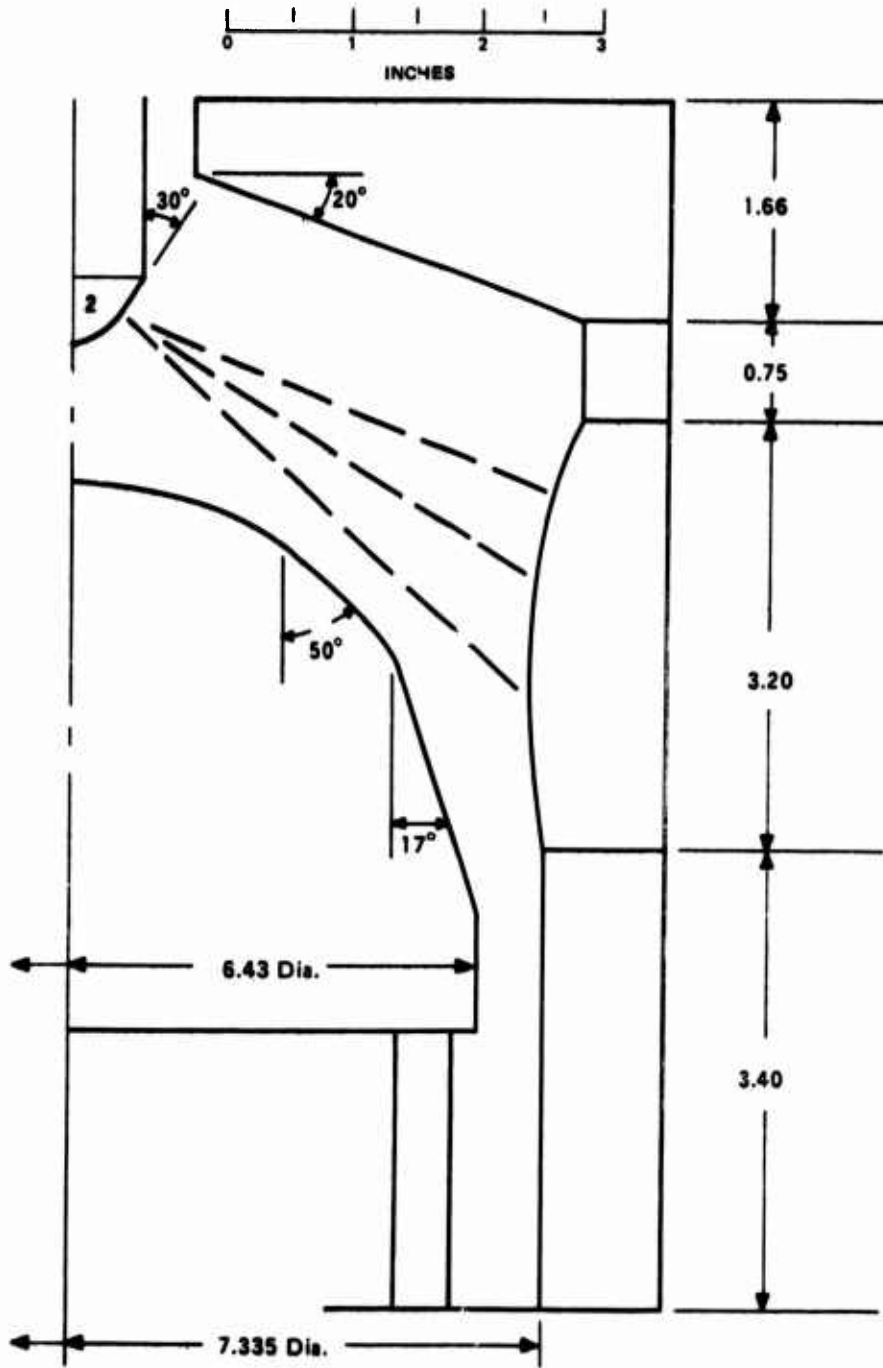


Figure 28. Deposition Chamber Geometry of Run No. 6300-24.

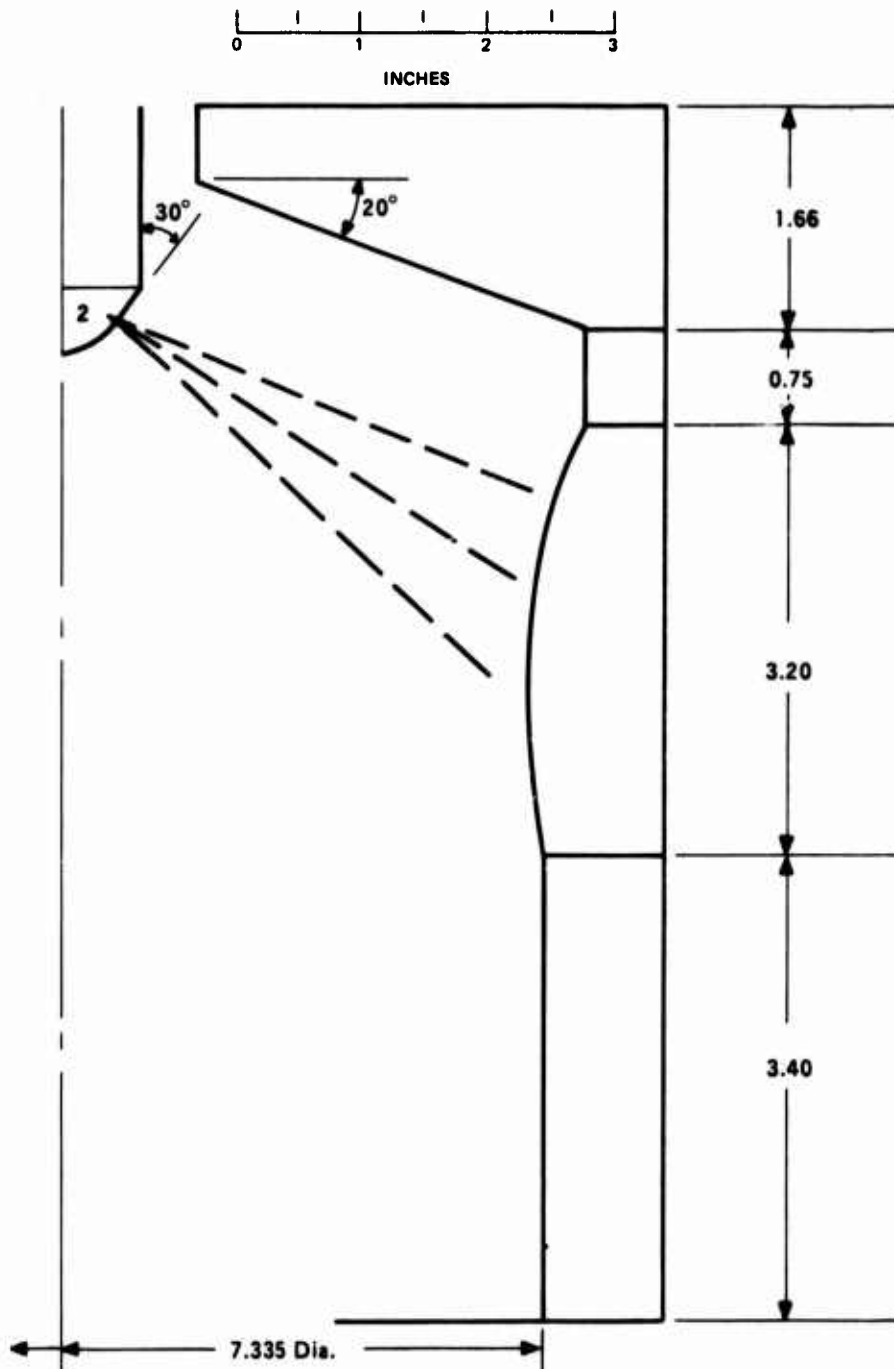


Figure 29. Deposition Chamber Geometry of Run No. 6300-25.

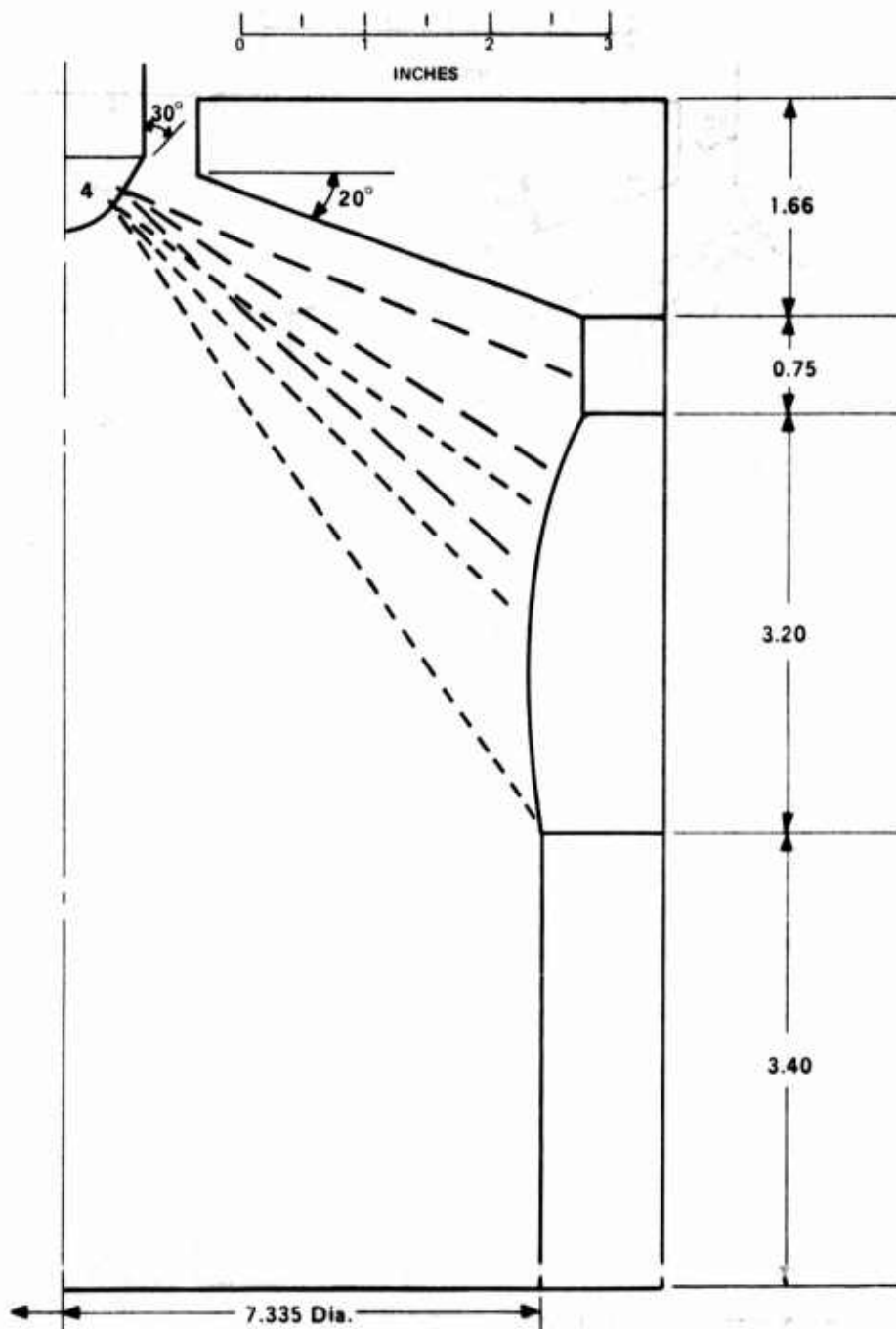


Figure 31. Deposition Chamber Geometry of Run No. 6300-27.

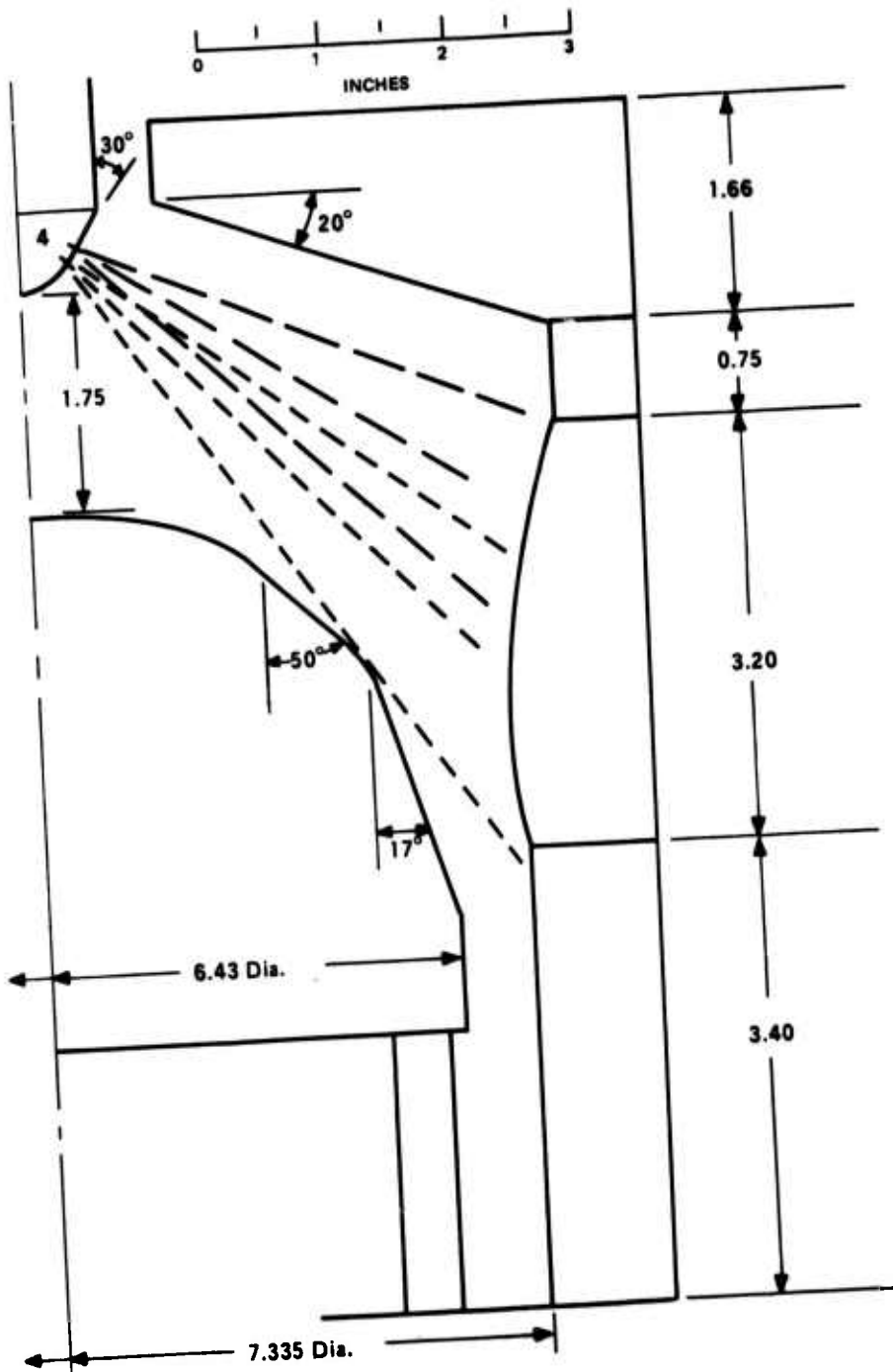


Figure 32. Deposition Chamber Geometry of Run No. 6300-28.

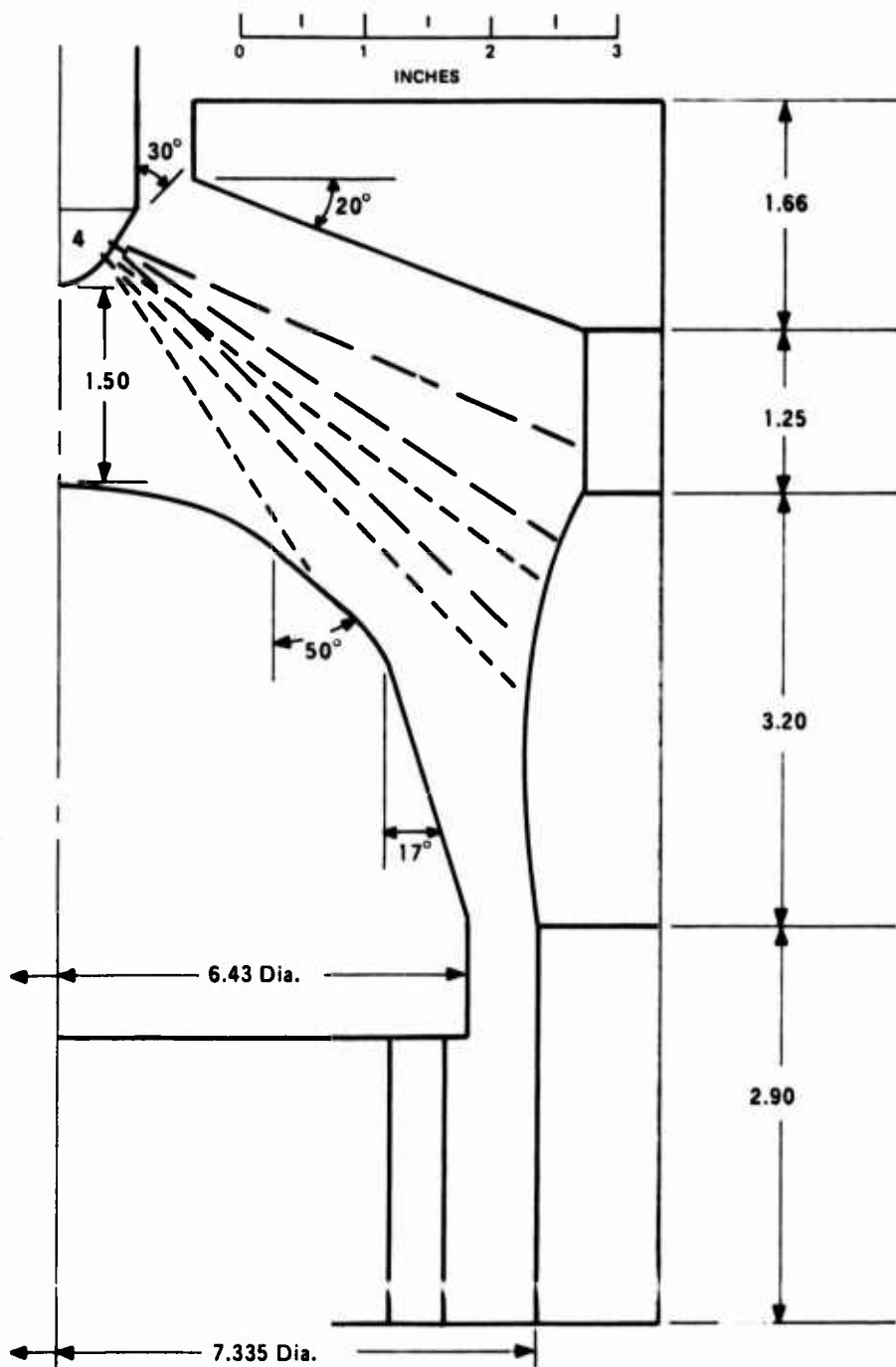


Figure 33. Deposition Chamber Geometry of Run No. 6300-29.

At this time, the short deposition chamber geometry was abandoned permanently.

Run 6300-30 was conducted utilizing the same deposition chamber geometry as 6300-17 (Figure 23), including the injector tip. The high nitrogen flow rates were maintained to help eliminate sooting in the gas phase. The methane rate was increased to increase the deposition rate. Post-deposition examination showed three of the six mandrel exhaust ports to be completely clogged by hard, sooty deposits, and the other three were almost clogged. The mandrel, which is supposed to remain stationary, had rotated with the nozzle substrate and was covered with hard, sooty deposits. The corresponding nozzle area was covered by a thick, rough PG deposit.

Run 6300-31 was conducted utilizing the deposition chamber geometry shown in Figure 34. The mandrel body was mounted on six 1/2-inch-diameter posts to increase the gas exhaust area and eliminate clogging. The mandrel was also pinned to the furnace base so it could not rotate. Post-deposition examination showed the coating to be covered with flowerlike carbon deposits in the entrance area. A continuous midplane delamination was visible within the coating which resulted from a brief interruption in gas flow during deposition. The mandrel gas exhaust area remained virtually unrestricted. The deposition rate profile was acceptable.

Runs 6300-32 through 6300-45 were all conducted using the deposition chamber geometry shown in Figure 35. At this time, the final deposition gas flow rates were established and were unchanged throughout the remaining 7.0-inch nozzle throat insert fabrication runs. At Run 6300-37, the deposition temperature was increased 100°F during deposition to compensate for the insulating effect of the increasing coating thickness (see Section V). All of the coatings fabricated during this series were smooth in surface texture with the exception of 6300-36, which was deposited at a deposition temperature of 4000°F. This indicates that a deposition surface temperature of 3800°F is minimal, and for this reason an indicated canister backside temperature of 4100-4200°F was utilized for the remaining nine runs. Examination of the polished coating ends showed a fine, continuously renucleated microstructure. Occasional intraconical delaminations were present in areas adjacent to large pores in the substrate. Two of the inserts cracked axially after deposition, indicating that even unbroken parts contained stresses approaching that of failure. Three of the nozzle throat inserts produced, 6300-34, 6300-42 and 6300-45, were utilized for Test Firings SN-3, SN-4 and SN-5, respectively.

2. 10.6-INCH NOZZLE THROAT INSERTS

Three 10.6-inch throat diameter nozzle insert deposition runs were conducted.

Deposition conditions are shown in Table V. Coating and substrate data are shown in Table VI.

The same injector tip design was utilized for all three runs and was the same as that used during the initial 7.0-inch deposition runs. (See Figure 11.)

One substrate design was used and this is shown in Figure 36.

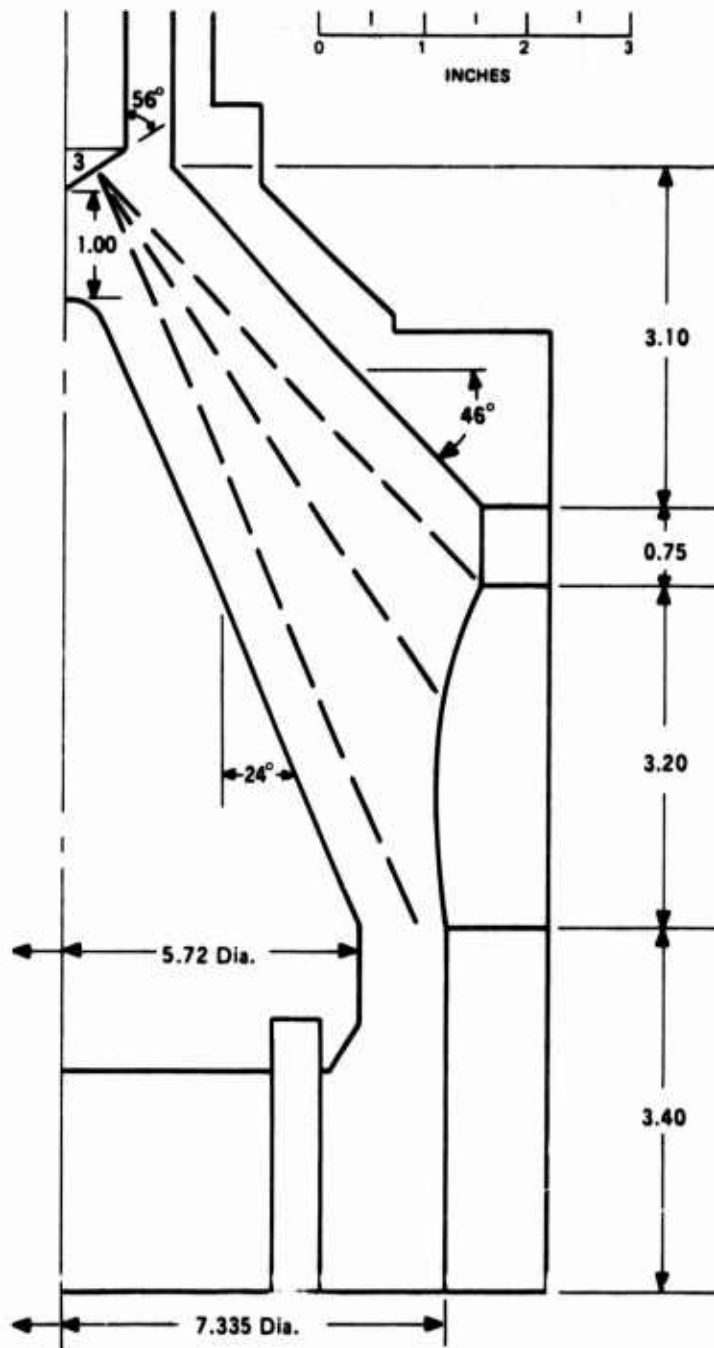


Figure 34. Deposition Chamber Geometry of Run No. 6300-31.

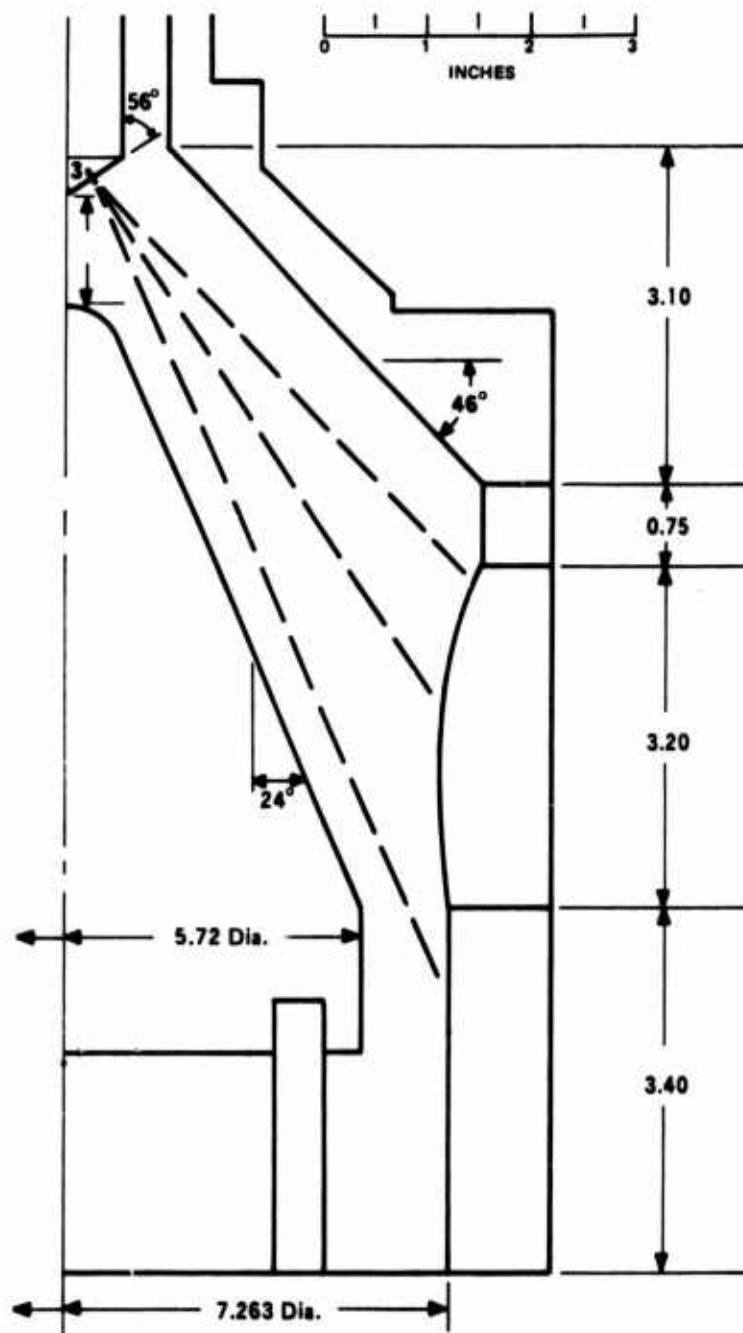


Figure 35. Deposition Chamber Geometry of Run No's. 6300-32 thru 6300-45.

Table V. 10.6-inch Nozzle Throat Insert Deposition Conditions.

Run Ident No.	Log Book No.	Annulus N ₂ (SCFH)	Process N ₂ (SCFH)	CH ₄ (SCFH)	Volume Percent CH ₄	Dep. Temp. (°F)	Dep. Time (hr)	Remarks
7300-1	299-52	30	320	18	5.1	3950	5.00	None
7300-2	299-53	80	448	24	4.5	3950	5.00	Nitrogen rates increased and CH ₄ concentration decreased to reduce sooting.
7300-3	299-56	80	448	24	4.5	3950	5.00	Rotator failed during deposition.

Table VI. 10.6-inch Nozzle Throat Insert Substrate and Coating Data.

Run Ident. No.	Log Book No.	Substrate		Coating Thickness (in)			Deposition Rate (mils/hr)			Appearance
		Material	Configuration	Entrance	Throat	Exit	Entrance	Throat	Exit	
7300-1	299-52	AGSR-VCG (surface treated)	1	0.040	0.039	0.008	8.0	7.8	1.6	Coating from entrance end to throat contains several flower-like carbon growths. No microscopic examination.
7300-2	299-53	Reused above part	1	0.012	0.051	0.024	2.4	10.2	4.8	Coating surface clean and smooth. A narrow annular ring of carbon growths grew at entrance end. No microscopic examination.
7300-3	299-56	AGSR-VCG (surface treated)	1	0.040	0.054	0.027 (Avg.)	8.0	10.8	5.4	Surface condition good. No cracks or delaminations visible at coating ends. Coating thickness varies from 0.015 to 0.039 at exit end.

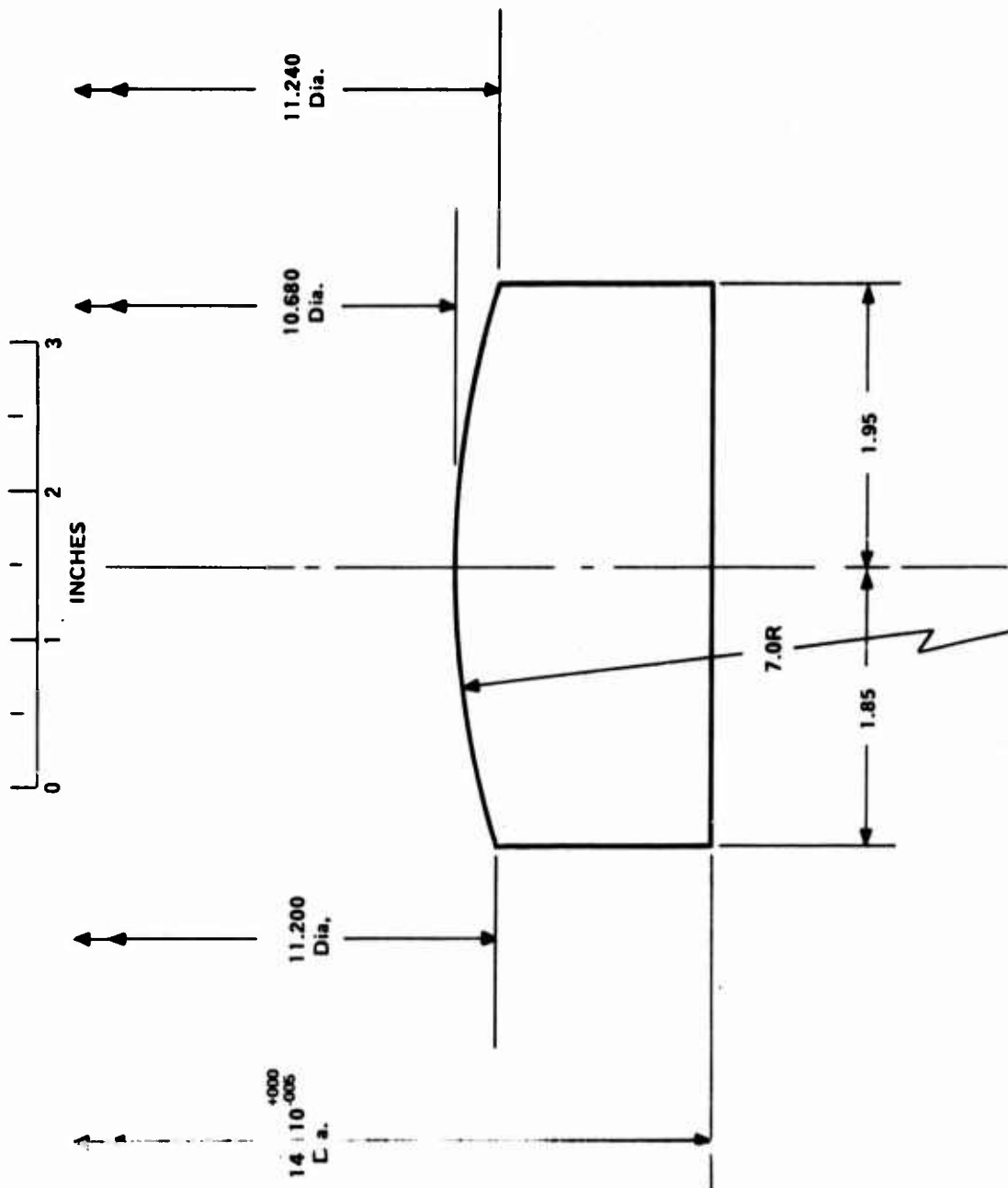


Figure 36. 10.6-inch Nozzle Throat Insert Substrate Configuration.

Run 7300-1, the first of the 10.6-inch series, was conducted utilizing the deposition-chamber geometry shown in Figure 37. Deposition conditions were selected from contemporary 7.0-inch deposition runs. Post-deposition examination showed considerable amounts of soot and flowerlike carbon growths to have accumulated on the inner surface of the deposition chamber. The coating surface was sprinkled with flowerlike carbon growths. Except for these growths, the coating was of acceptable quality.

Run 7300-2 was conducted at a nitrogen flow rate 59 percent higher than that of the previous run. The methane rate was increased by only 33 percent which decreased the concentration by 12 percent. These changes were made to reduce the amount of sooting in the gas phase and, therefore, eliminate the deposits of soot and flowerlike carbon growths which occurred in the previous run. The substrate was moved up 0.6 inch in the deposition chamber and the injector was moved down 0.25 inch to increase the deposition rate at the exit end. The deposition chamber geometry is shown in Figure 38. Post-deposition examination showed the coating surface quality to be good. The only defect was a narrow annular ring of carbon growths which had accumulated at the entrance end. This ring shadowed the coating surface and caused a substantial reduction in the coating thickness at the entrance end.

Run 7300-3 was the last 10.6-inch deposition run conducted and utilized the deposition chamber geometry shown in Figure 39. A new, larger diameter mandrel was used to increase the coating deposition rate. Deposition process conditions were the same as those of the previous run. The deposition chamber rotator mechanism failed during deposition and, consequently, no rotation occurred throughout the latter half of the cycle. Post-deposition examination showed no flaws in the coating surface or the polished coating ends. There was no evidence of the annular ring of growths which had formed in the previous run. The lack of rotation resulted in an unequal coating thickness at the exit end. This part split axially during shipment to the Atlantic Research Pine Ridge Facility about two weeks after deposition. The exact cause of this failure is unknown, but it is quite likely that the part was mishandled during shipment.

3. 13.0-INCH NOZZLE THROAT INSERTS

Twelve 13.0-inch-throat diameter nozzle insert fabrication runs were conducted.

Deposition conditions are shown in Table VII. Coating and substrate data are shown in Table VIII.

The injector tip configuration utilized for these runs was the same as that used in several of the 7.0-inch deposition runs. (See Figure 12.)

All substrates were of the configuration shown in Figure 40.

Run 8300-1, the first of the 13.0-inch series, was conducted utilizing gas flow rates established during the 10.6-inch series. The deposition chamber geometry is shown in Figure 41. After deposition, the area around the injector tip was filled with clinkerlike deposits. The nozzle substrate coating contained scattered flowerlike carbon growths from the entrance end to the throat. The area from the substrate throat to the gas exhaust ports was clogged with soot and clinkerlike deposits. The coating was cleaned and measured, but no microscopic examination was conducted.

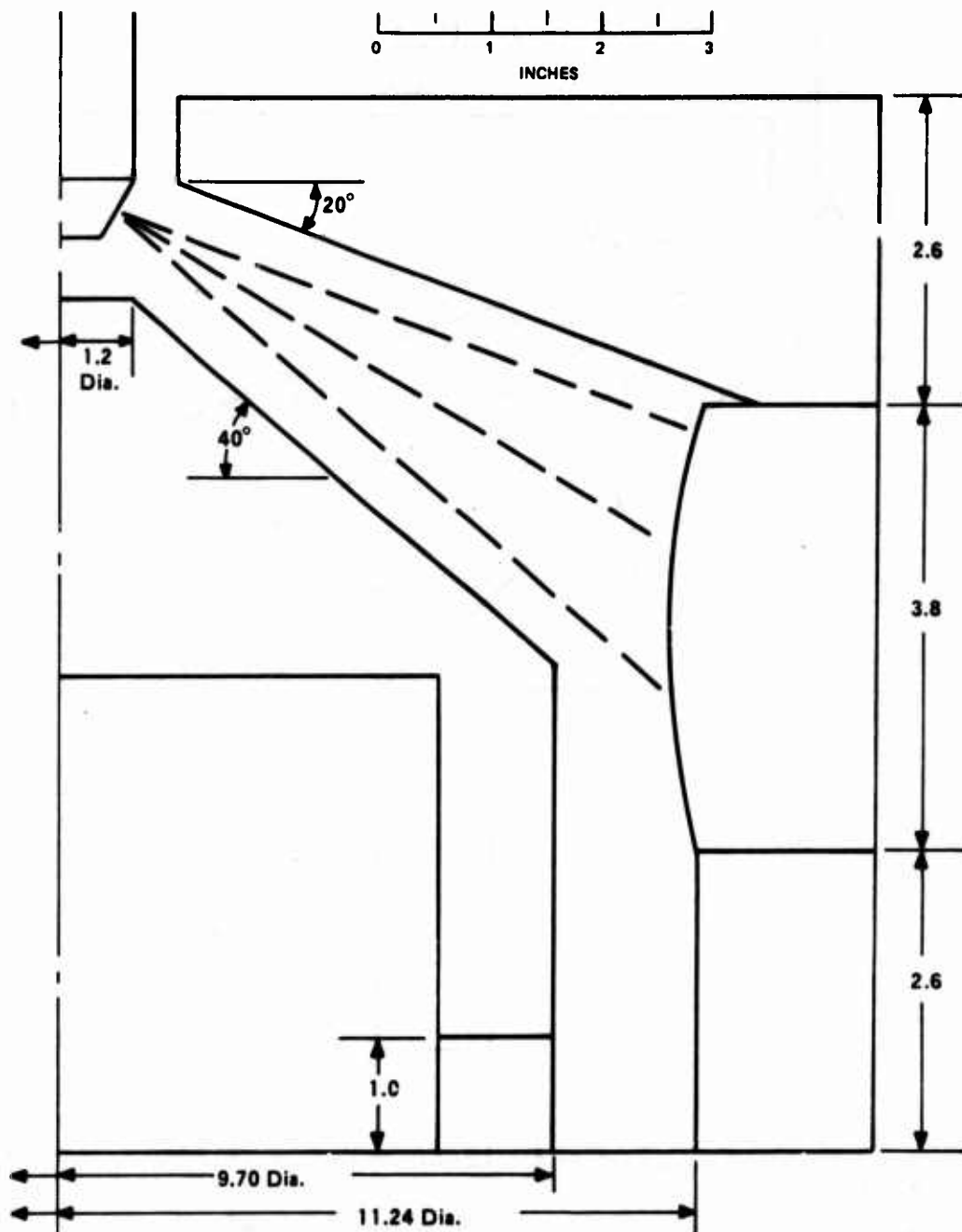


Figure 38. Deposition Chamber Geometry of Run No. 7300-2.

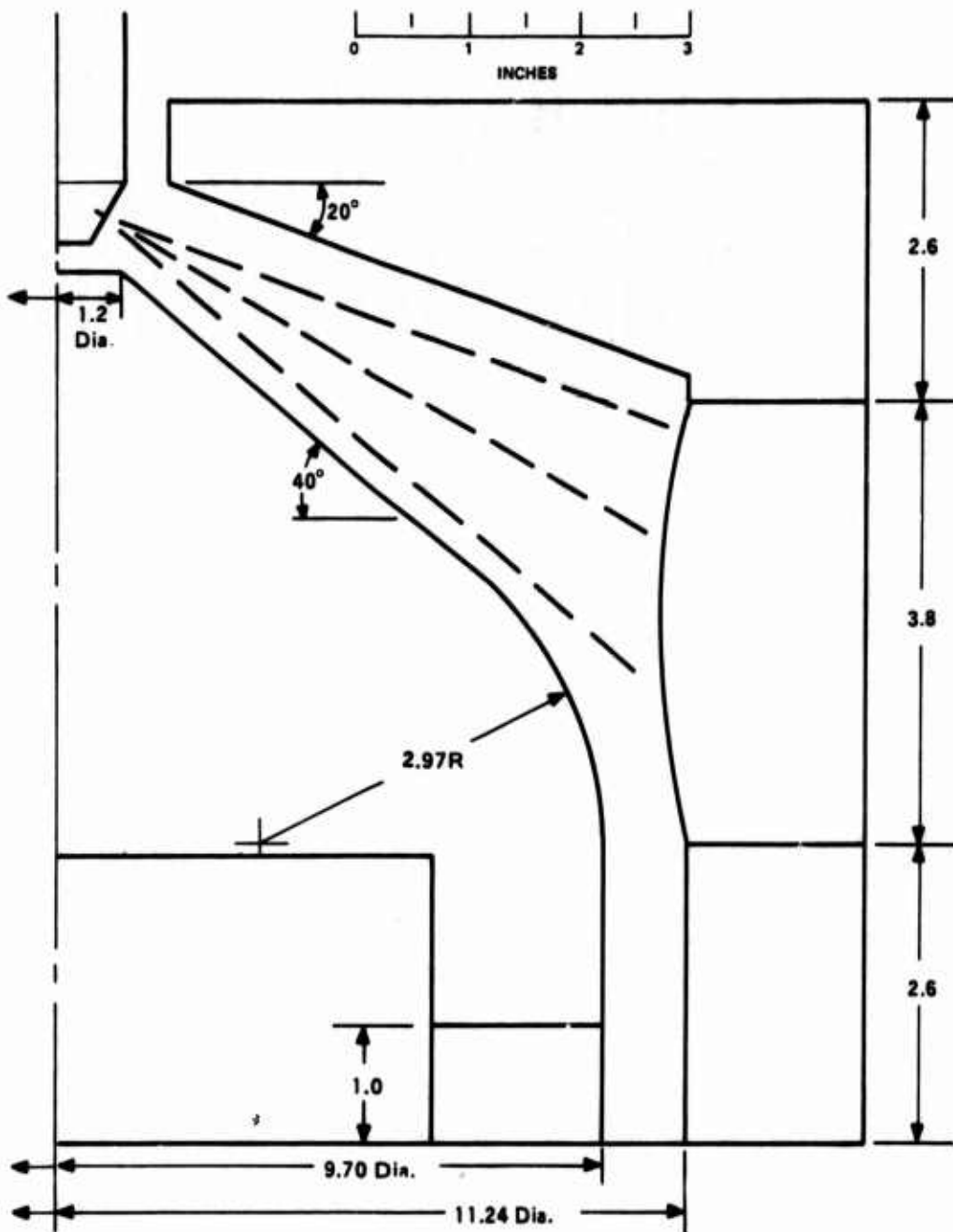


Figure 39. Deposition Chamber Geometry of Run No. 7300-3.

Table VII. 13.0-inch Nozzle Throat Insert Deposition Conditions.

Run Ident No.	Log Book No.	Annulus N ₂ (SCFH)	Process N ₂ (SCFH)	CH ₄ (SCFH)	Volume Percent CH ₄	Dep. Temp. (°F)	Dep. Time (hr)	Remarks
8300-1	299-60	80	448	24	4.5	3950	4.00	Pilot 13 in. deposition. Injector rests on tip of mandrel
8300-2	299-61	96	538	24	3.8	3950	5.00	N ₂ rate increased to reduce sooting within gas stream.
8300-3	299-62	96	538	28	4.4	3950	5.57	CH ₄ concentration increased to increase deposition rate
8300-4	299-63	88	673	35	4.5	3950	5.00	Total gas flow rate increased to reduce sooting within gas stream
8300-5	299-64	88	673	35	4.5	3950	4.00	Mandrel size reduced to prevent clogging of annular gas exhaust area
8300-6	299-65	88	673	35	4.5	3950	4.00	Mandrel size increased to increase deposition rate
8300-7	299-66	75	740	32	3.9	3950	4.75	Process N ₂ rate increased to reduce sooting within gas stream. At 2.83 hours gas exhaust tube collapsed causing a temporary increase in furnace gas pressure.
8300-8	299-67	75	740	32	3.9	3950	8.00	Repeat of above run with repaired gas exhaust tube.
8300-9	299-69	75	740	32	3.9	3950	4.83	Contoured entrance section utilized in deposition chamber to reduce turbulence and, thereby, eliminate sooting.
8300-10	299-70	75	740	32	3.9	3950	6.33	Mandrel removed to determine its affect on sooting in deposition chamber.
8300-11	299-71	75	740	32	3.9	3950	11.00	Injector lowered to increase deposition rate at downstream end of substrate. Gas exhaust tube plugged near end of run.
8300-12	299-72	75	740	32	3.9	3950	6.00	Gas exhaust tube removed to increase exhaust area. Hot gas leaked through brickwork and forced early termination of run.

Table VIII. 13.0-inch Nozzle Throat Insert Substrate and Coating Data.

Run Id. # No.	Log Book No.	Substrate		Coating Thickness (in)			Deposition Rate (mils/hr)			Appearance
		Material	Configuration	Entrance	Throat	Exit	Entrance	Throat	Exit	
83 3-1	295-60	AGSR-VCG (surface treated)	1	0.014	0.026	0.013	3.5	6.5	3.3	Injector area covered with clinkers. Entrance end to throat line sprinkled with hard flower-like carbon growths. Exit end coated with soft carbon deposits. Annular area at exit end filled with clinkers.
83 3-2	295-61	Reused above part	1	<0.001	0.26	<0.001	—	5.2	—	Similar to above. Entrance end to throat is clean. Exit end covered with soft carbon deposits.
83 3-3	295-62	Reused above part	1	<0.001	0.040	0.031	—	7.2	5.6	Entrance area to throat line sprinkled with hard flower-like carbon growths. Exit end cleaner than first two deposition runs but still has many sooty areas.
83 3-4	295-63	Reused above part	1	<0.001	0.51	<0.001	—	10.2	—	Entrance end to throat line covered with flower-like carbon growths. Exit end coated with soft carbon deposit.
83 3-5	295-64	Reused above part	1	NE ^a	0.026	0.025	—	6.5	6.3	Entrance end to throat line covered with flower-like carbon growths. Exit end good.
83 3-6	295-65	Reused above part	1	NE ^a	0.037	0.025	—	9.3	6.3	Entrance end to throat line covered with flower-like carbon growths. Exit end good.
83 3-7	295-66	Reused above part	1	NE ^a	0.034	0.020	—	7.2	4.2	Entrance and clean except for forward edge which contains a thin annular ring of hard deposits. Exit end good.
83 3-8	295-67	Reused above part	1	NE ^a	0.063	NE ^a	—	7.9	—	Coating from entrance end to throat contains several hard, flower-like carbon growths. Exit end clean except for extreme edge.
83 3-9	295-69	Reused above part	1	<0.001	0.045	0.010	—	9.3	2.1	Coating from entrance end to throat contains several hard, flower-like carbon growths. Exit end clean except for extreme edge.
83 3-10	295-70	Reused above part	1	0.020	0.032	0.007	3.2	5.1	1.1	Coating is clean except for entrance and exit ends around which a 0.1 to 0.2-in wide annular ring of growths accumulated.
83 3-11	295-71	AGSR-VCG (surface treated)	1	0.035	0.068	0.002	3.2	6.2	0.2	Entrance area: Coating tapers rapidly toward edge in a band 1/4 inch wide and extending for 360 degrees around perimeter. One flower-like carbon growth, 5/8-inch long X 1/2 inch wide X 1/4 inch high, halfway between end and throat. Exit Area: Coating tapers rapidly toward edge, in a band 1/2 inch wide and extending for 360 degrees around perimeter.
83 3-12	295-72	AGSR-VCG (surface treated)	1	NE	0.025	NE	—	4.2	—	Similar to above with many, small, newly formed carbon flowers throughout coating surface.

^aNot examined.

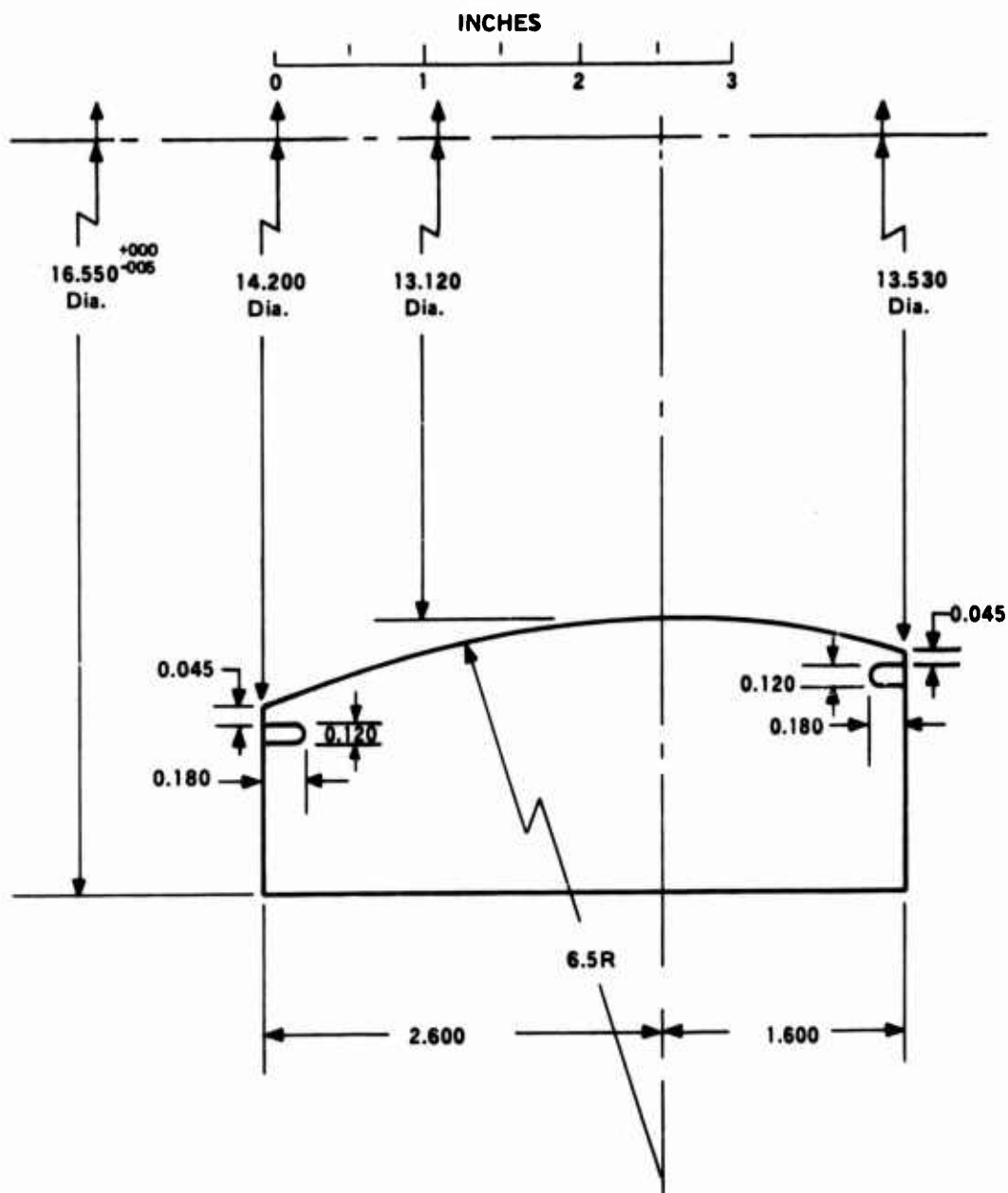


Figure 40. 13.0-inch Nozzle Throat Insert Substrate Configuration 1.

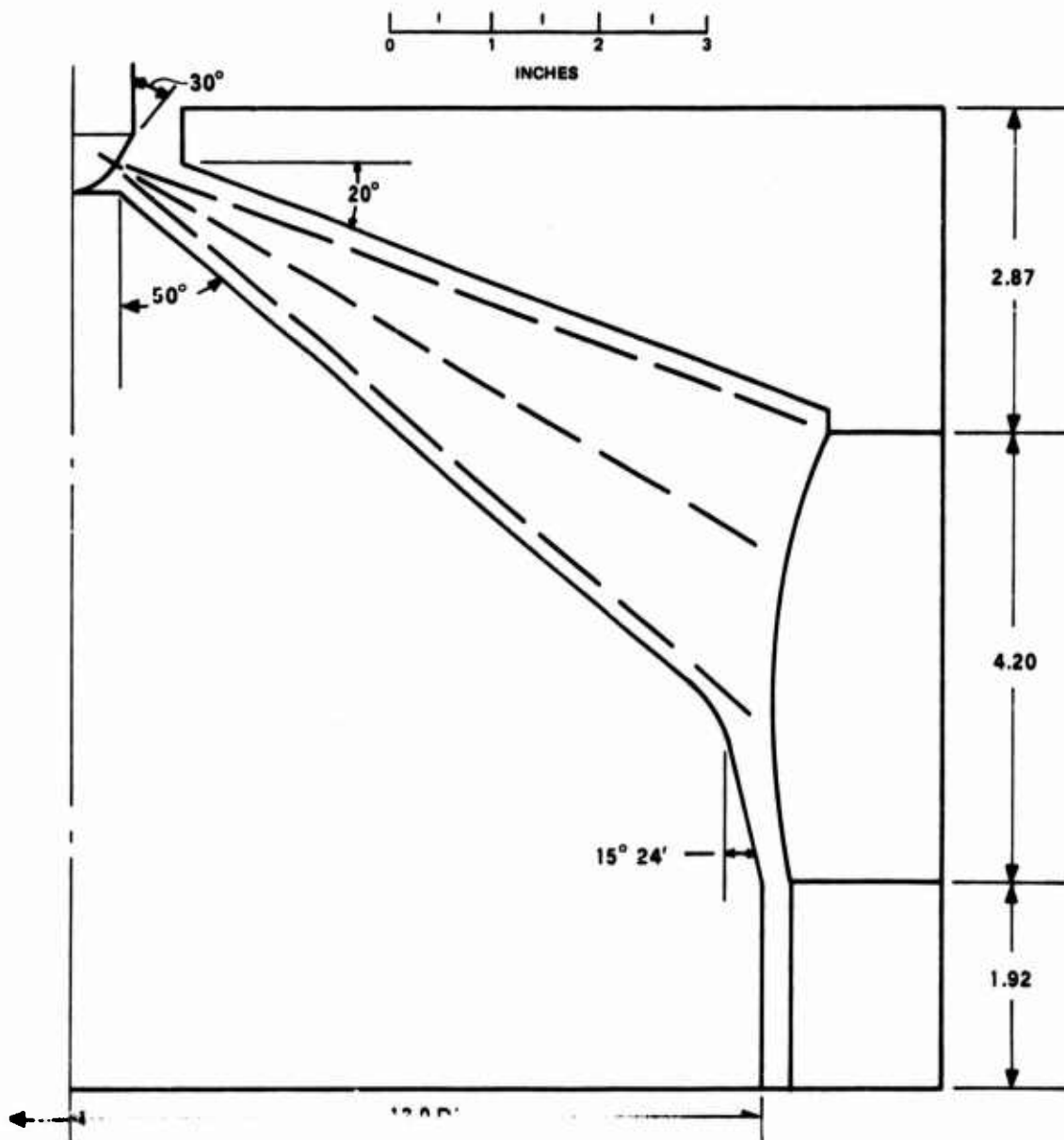


Figure 41. Deposition Chamber Geometry of Run No. 8300-1.

Run 8300-2 was conducted with a 20 percent increase in nitrogen flow rate. The methane flow rate was not changed. Two minor changes were made in the deposition chamber geometry (Figure 42). The mandrel was shortened by 1/4 inch at the tip and rounded. The lower mandrel radius was increased to facilitate gas flow through the throat and into the exhaust ports. After deposition, the gas inlet area was somewhat cleaner than the previous run. There were still, however, considerable amounts of sooty deposits in this area. The coated surface of the nozzle substrate was clean from the entrance end to the throat. The area from the substrate throat to the exit end was covered with hard, sooty deposits. Similar deposits had completely filled and blocked the gas exhaust section. The coating ends were too thin to be measured, so only the throat thickness was recorded. The deposition rate at the throat decreased by 20 percent, which corresponds closely with the 16 percent reduction in the methane concentration of the deposition gas.

Run 8300-3 was conducted using the same nitrogen flow rates as the previous run. The methane flow rate was increased by 17 percent to boost the deposition rate. The mandrel was shortened by 1/2 inch and the injector lowered 1/2 inch. The major diameter of the mandrel was tapered to increase the annular gas exhaust area in the lower area of the chamber. The deposition chamber geometry is shown in Figure 43. After 5 hours and 34 minutes of deposition, the exhaust area of the deposition chamber plugged, and the run was terminated. Post-deposition examination revealed the same type of sooty deposits in the gas inlet and exhaust areas as before. The nozzle coating showed scattered flowerlike carbon growths like those of the first 13.0-inch deposition run. The exit area of the substrate was cleaner than in the previous two runs, and a significant amount of coating was deposited in this area. The coating at the entrance end of the nozzle was too thin to be measured. An increase of 38 percent in the deposition rate occurred in the throat area which was much higher than the concentration increase of the methane indicating that the changes in deposition chamber geometry caused most of the increase.

Run 8300-4 was conducted at a 20 percent higher total deposition gas flow rate than the previous run. The methane concentration was essentially unchanged. No changes were made in the deposition chamber geometry (Figure 43). Post-deposition examination of the coated nozzle showed the surface at the entrance end to contain several hard flowerlike carbon growths. From the throat to the exit end, the coating surface was covered with sooty deposits that had built upward from the gas exhaust section. The annular gas exhaust section and the gas exhaust ports in the mandrel were plugged with hard carbon deposits. The deposition rate in the throat area increased by nearly 42 percent.

Run 8300-5 was conducted using the same gas flow rates as the previous run. The deposition chamber geometry (Figure 44) was modified by using the 10.6-inch nozzle mandrel instead of the mandrel originally designed for 13-inch deposition runs. This modification increased the annular gap of the exhaust section from 1/4 inch to nearly 2 inches. Post-deposition examination of the coating showed the entrance end to contain scattered flowerlike carbon growths. The coating from the throat to the exit end was clean and free of any irregularities. There was no indication of clogging in the exhaust section demonstrating the effectiveness of the increased annular gap in preventing sooting in this area. There were, however, extensive deposits within the mandrel gas exhaust ports which may have forced termination of the run had a longer deposition run been attempted. The deposition rate in the throat area decreased by 36 percent as a result of the increased cross-sectional area between the mandrel and the substrate.

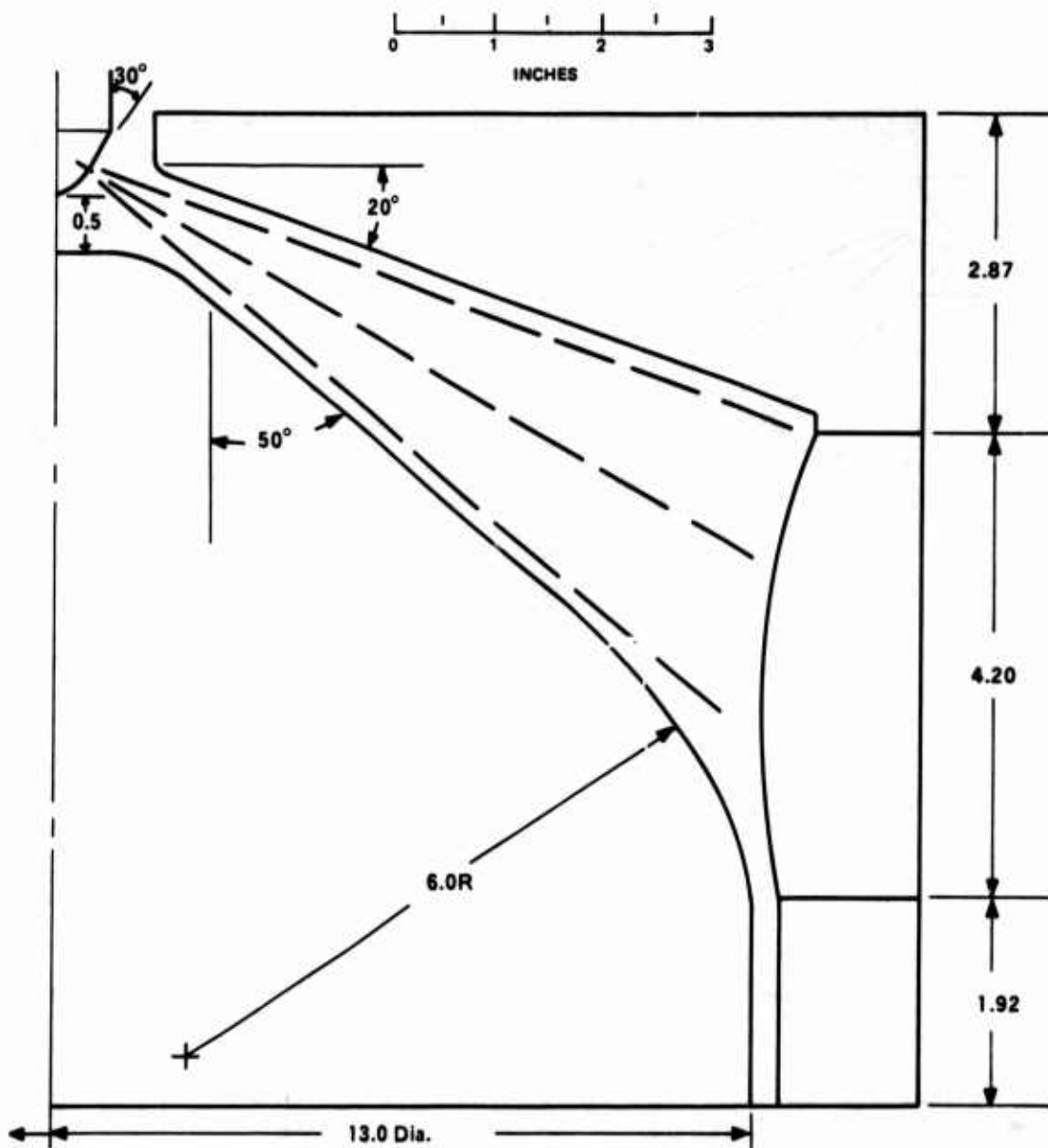


Figure 42. Deposition Chamber Geometry of Run No. 8300-2.

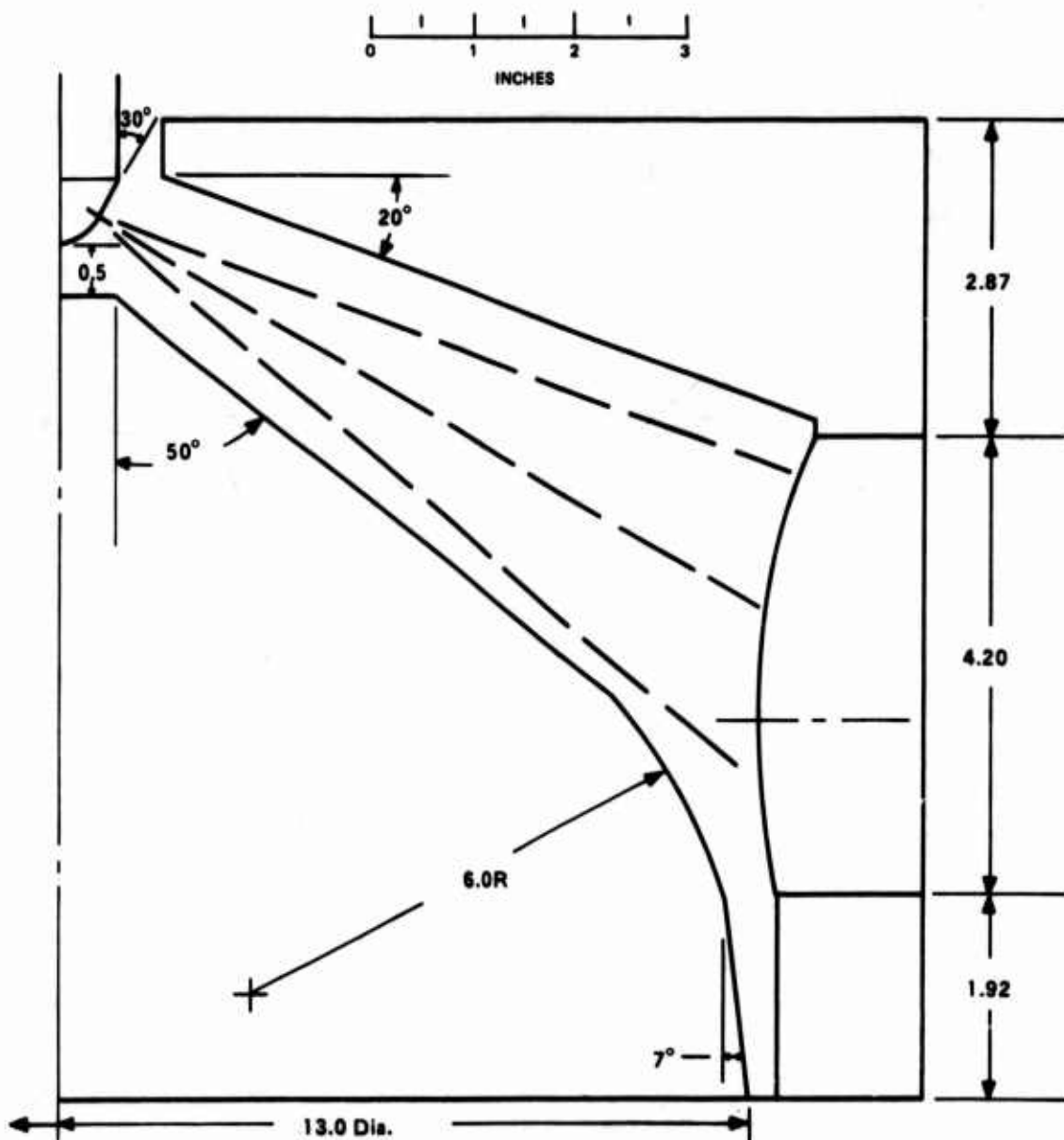


Figure 43. Deposition Chamber Geometry of Run No's. 8300-3 and 8300-4.

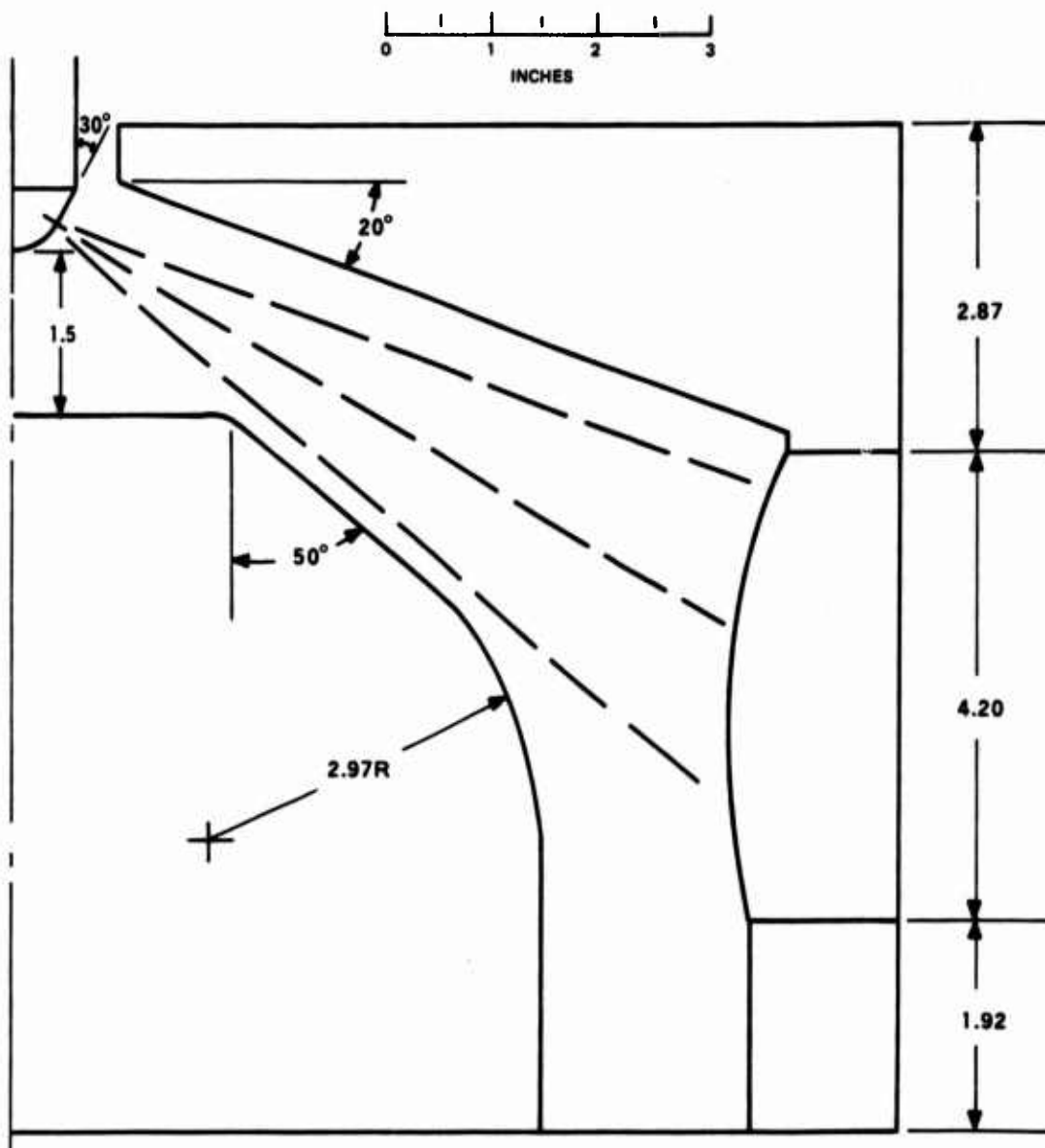


Figure 44. Deposition Chamber Geometry of Run No. 8300-5.

Run 8300-6 was conducted using the same process conditions as the previous run. The deposition chamber geometry (Figure 45) was changed by using a modified 13-inch mandrel with a reduced major diameter. This changed the annular gap of the exhaust section to one inch. The change was made to increase the PG deposition rate on the nozzle substrate while still maintaining enough gap in the exhaust section to prevent clogging. Post-deposition examination showed the coating at the entrance end to contain scattered flowerlike carbon growths as in past runs. No sooting was evident in the exhaust section except for the mandrel exhaust ports. The PG deposition rate had increased by 43 percent in the throat area but remained the same at the exit end.

Run 8300-7 was conducted using a 7 percent higher nitrogen rate and a 13 percent lower methane concentration. The methane concentration was reduced in an attempt to reduce the formation of the sooty, flowerlike growths which had been occurring at the entrance end. The deposition chamber geometry (Figure 45) was unchanged. Post-deposition examination showed the coating surface to be free of irregularities with the exception of the extreme entrance end. A narrow annular ring of deposits had formed in this area. These would normally be removed when the 100 mil trim was made. The exhaust section of the deposition chamber was free of soot with the exception of the mandrel exhaust ports which were nearly filled with soft deposits. The deposition rate decreased by 23 percent at the throat and 33 percent at the exit end.

Run 8300-8 was conducted using the same gas flow rates and deposition chamber geometry (Figure 45) as the previous run. The deposition time was extended to eight hours to obtain a 60-mil coating thickness. Post-deposition examination showed the entrance approach section of the deposition chamber and the entrance end of the substrate to be sprinkled with several hard, flowerlike carbon growths. The gas exhaust ports in the mandrel were plugged with hard, sooty deposits. No thickness measurements could be obtained at the nozzle coating ends because extensive, clinkerlike carbon growths had accumulated in these areas. The coating deposition rate in the throat area increased by slightly less than 10 percent.

Run 8300-9 was conducted using the same gas flow rates as the previous run. An aerodynamically contoured entrance approach section was utilized, and the mandrel exhaust ports were rounded to streamline the gas flow through the deposition chamber. The deposition chamber geometry is shown in Figure 46. Neither of the changes proved to be effective. After 4 hours and 50 minutes of deposition time, the mandrel exhaust ports clogged forcing termination of the run. Post-deposition examination showed the entrance approach area and the nozzle entrance end to be sprinkled with many hard, flowerlike growths. The deposition rate increased by 18 percent in the throat area. Very little measurable coating was obtained at the exit end.

Run 8300-10 was conducted using a deposition chamber geometry similar to that of the previous run except the mandrel was eliminated. The geometry is shown in Figure 47. The gas flow rates were the same as those of the previous run. Post-deposition examination showed the absence of the mandrel to have eliminated the flowerlike carbon growths in the upstream area of the deposition chamber. The nozzle coating was clean except for a narrow annular ring of growths at both the entrance and exit ends. The absence of a mandrel caused a drop of 45 percent in the deposition rate at the throat. The deposition rates at the ends were too low in proportion to that of the throat area. The gas exhaust area of the deposition chamber was clean, indicating that longer deposition times were possible.

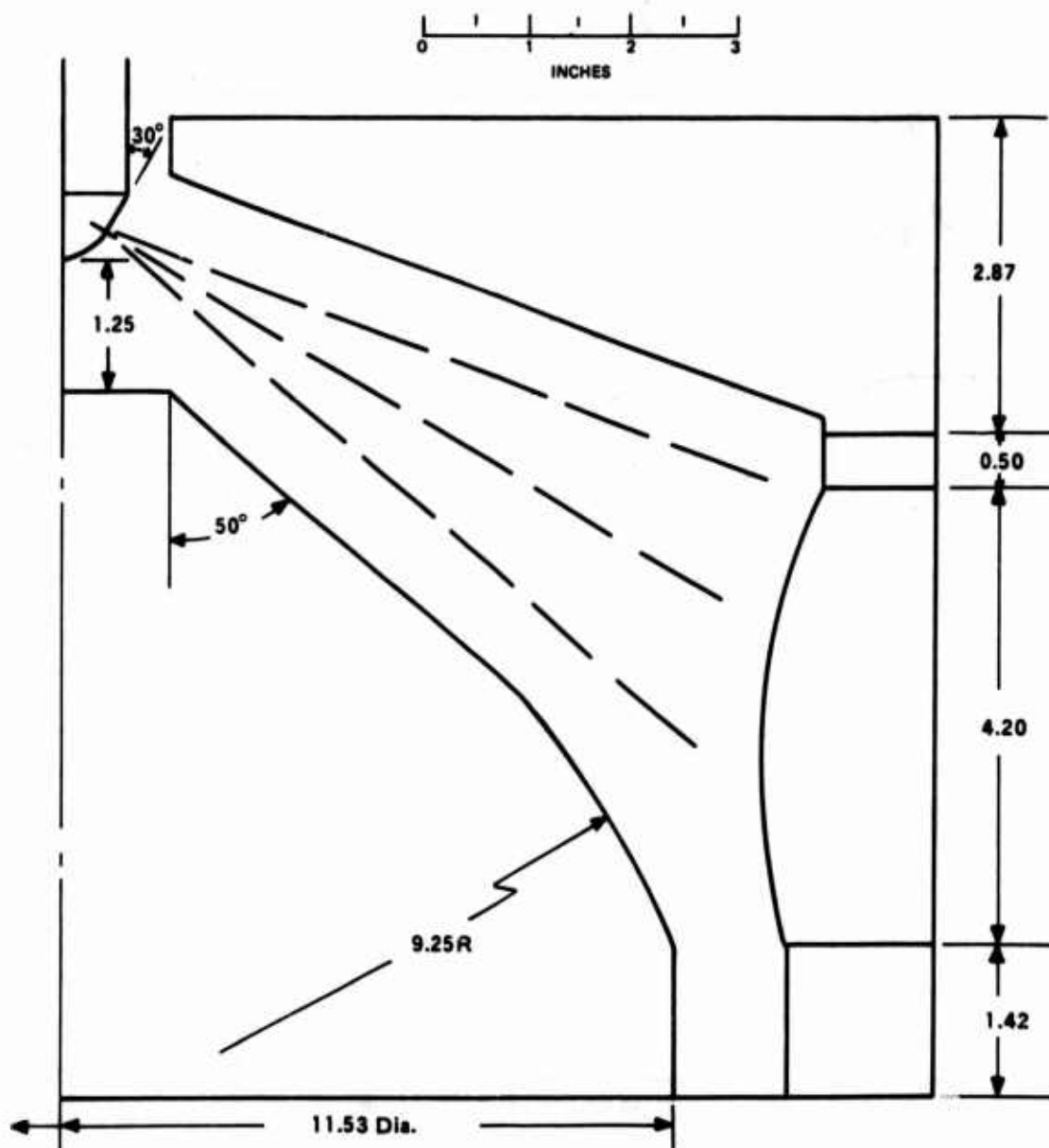


Figure 45. Deposition Chamber Geometry of Run No's. 8300-6, 8300-7 and 8300-8.

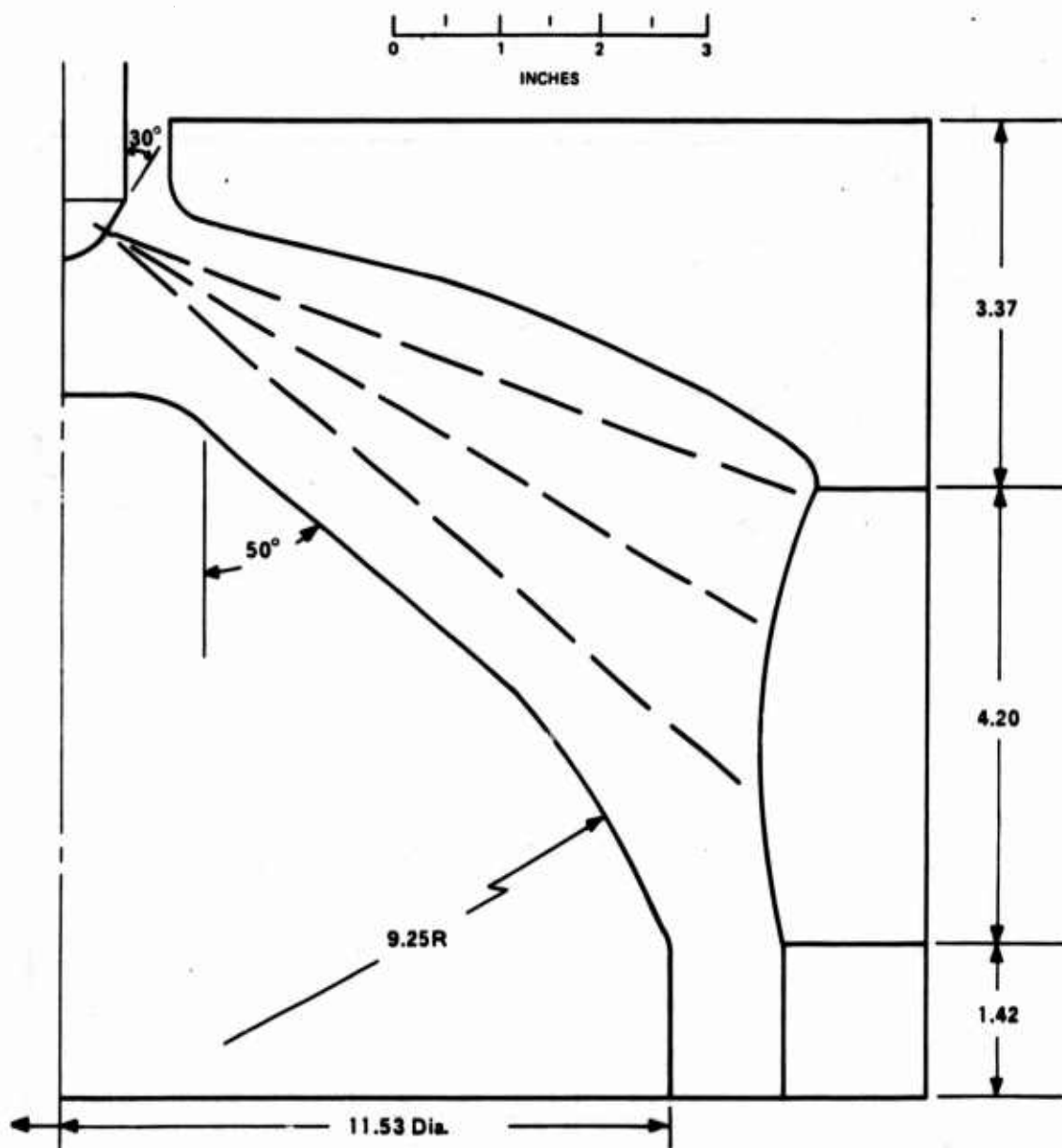


Figure 46. Deposition Chamber Geometry of Run No. 8300-9.

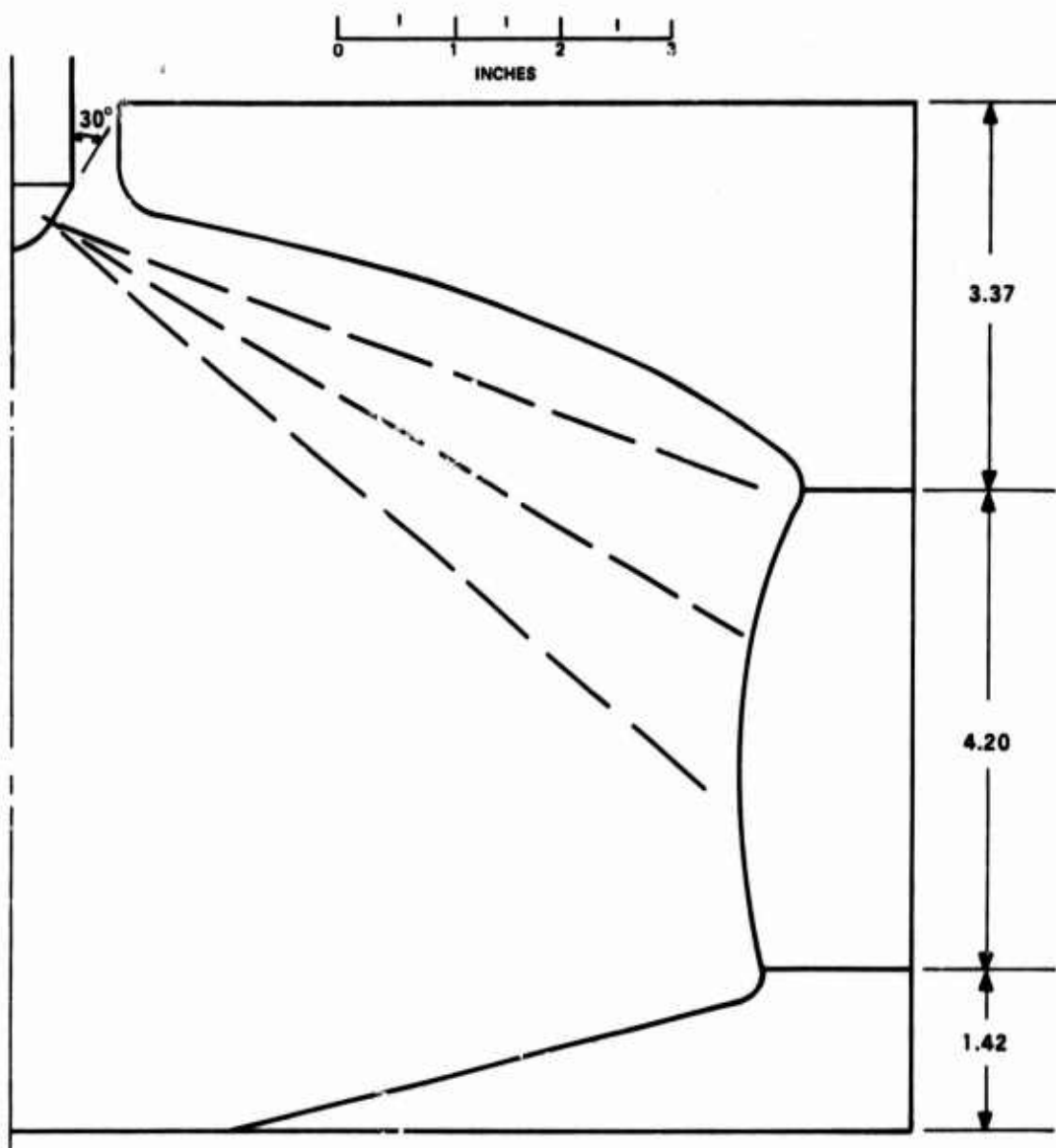


Figure 47. Deposition Chamber Geometry of Run No. 8300-10.

Run 8300-11 was conducted utilizing the same gas flow rates as the previous run. The injector was lowered 1/4 inch; otherwise, the deposition chamber geometry (see Figure 48) was the same as that of the previous run. The deposition time was increased to increase the coating thickness. Post-deposition examination showed a throat coating thickness of 68 mils, which was near the desired thickness. The deposition rate at the throat had increased by 22 percent. A 1/4-inch-wide annular ring of growths had formed around the entrance end of the nozzle. A similar band of growths, 1/2 inch wide, had also formed at the exit end. These rings masked the substrate at the ends, causing a substantial reduction of the coating thickness in these areas. Also contained within the coating was a single flowerlike growth halfway between the entrance end and the throat. The furnace gas exhaust tube liner had partially clogged during the run and this was thought to have caused soot to blow back into the deposition chamber. The liner was removed for the following run to prevent this problem.

Run 8300-12, the last of the 13.0-inch series, was conducted utilizing the same gas flow rates and deposition chamber geometry (Figure 48) as the previous run. It was to have been 11 hours in duration but was aborted after 6 hours because the brickwork in the furnace gas exhaust section overheated. Post-deposition examination showed the coating to be covered with small flowerlike carbon growths. These had just started to form and were probably related to the failure of the exhaust section of the furnace. Annular rings of carbon growths had started to form at the entrance and exit ends.

4. 12.45-INCH NOZZLE THROAT INSERTS

Fourteen 12.45-inch throat diameter nozzle insert fabrication runs were conducted. Because of the similarity of the two substrates, the 12.45-inch deposition runs should be considered a continuation of the 13.0-inch series.

A typical 12.45-inch throat insert is shown in Figure 49. Typical microstructures, observed at the coating ends, are shown in Figures 50 and 51.

Deposition conditions are shown in Table IX. Coating and substrate data are shown in Table X.

Before this series of runs was undertaken, the furnace susceptor length was increased from 10 to 15 inches. This permitted the deposition chamber geometry to be lengthened to obtain an increased injector standoff distance and reduced the angle of impingement of the deposition gas on the substrate surface. These modifications were necessitated by the increased substrate length and the high degree of wraparound at the substrate entrance end. The greater injector standoff allowed the gas cone to expand fully and completely enclose the substrate surface. The mandrel body was mounted on four 1/2-inch-diameter graphite pegs. This maximized the gas exhaust area and eliminated the clogging problem which occurred during the 13.0-inch deposition series.

The injector tip configuration for Runs 8300-13 through 8300-18 is shown in Figure 52. Figure 53 shows the configuration utilized for Runs 8300-19 through 8300-26.

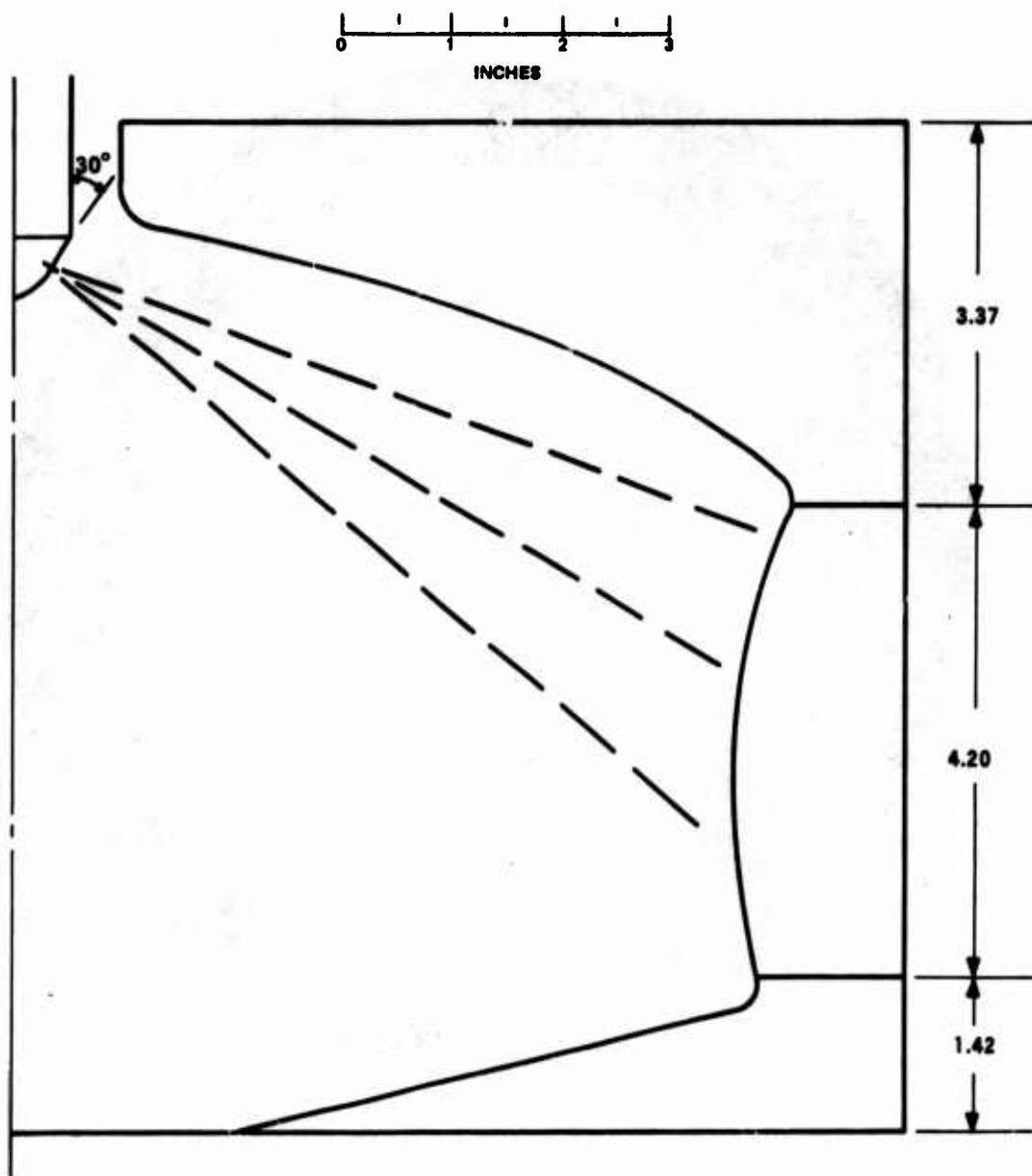


Figure 48. Deposition Chamber Geometry Run No's. 8300-11 and 8300-12.

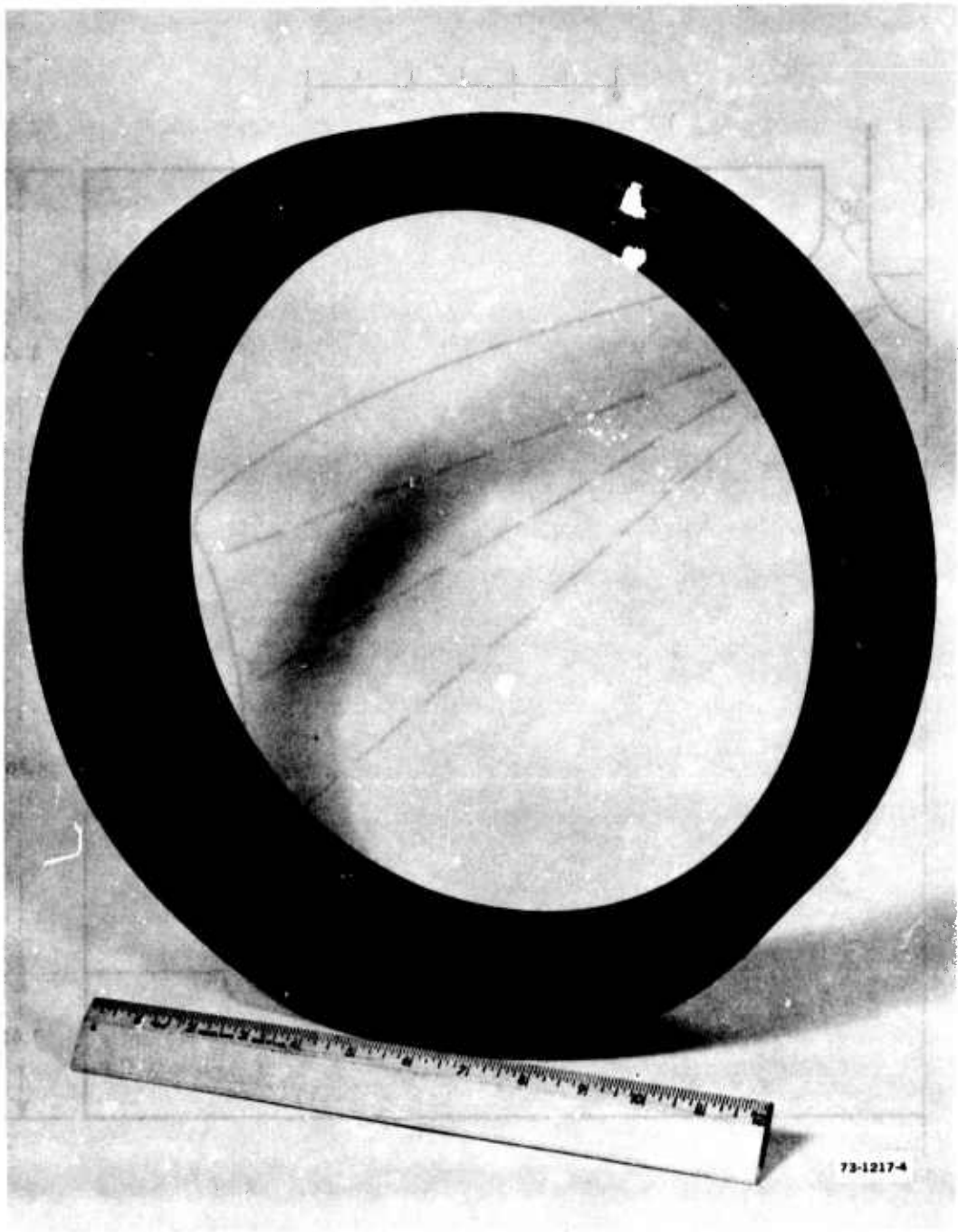


Figure 49. 12.45-inch Throat Insert No. 8300-24, Entrance End View.

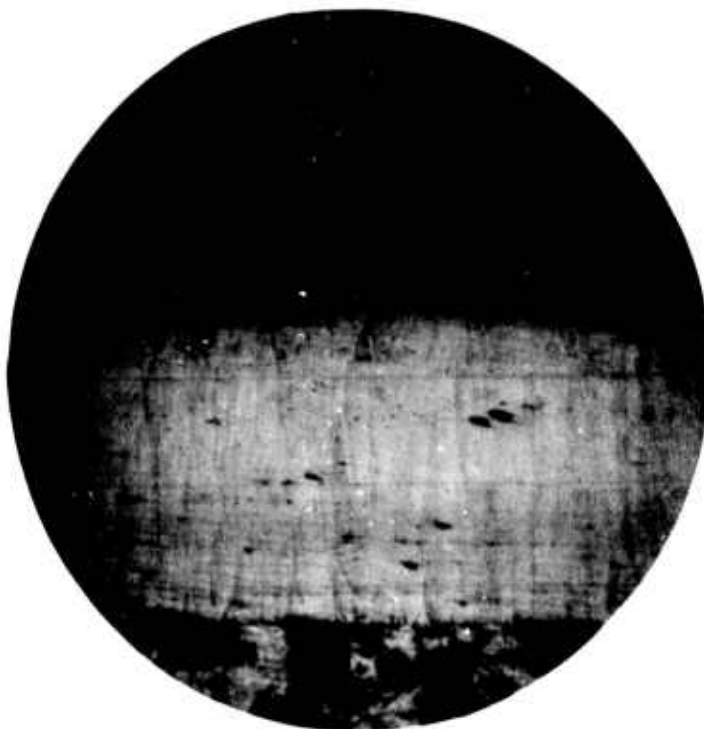


Figure 50. Coating Microstructure of 12.45-inch Insert No. 8300-21, Entrance End, 60X.

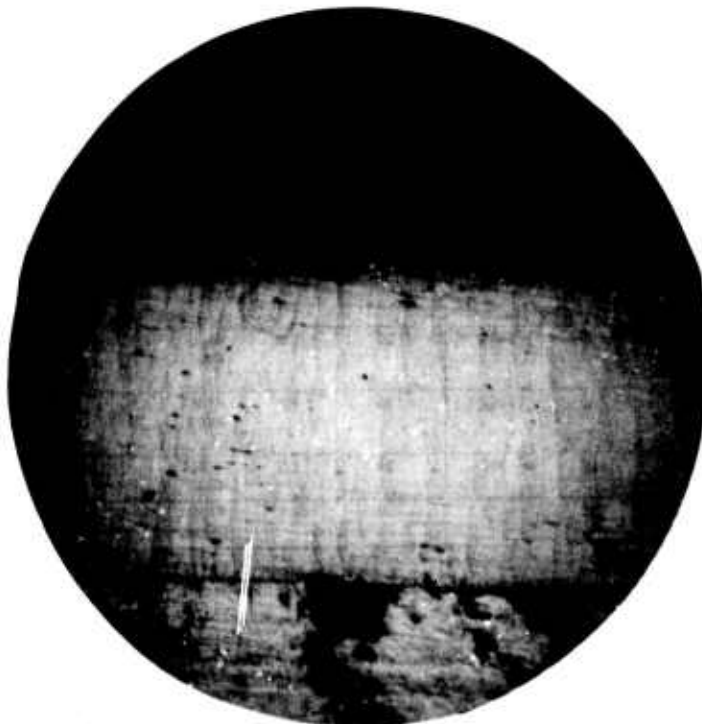


Figure 51. Coating Microstructure of 12.45-inch Insert No. 8300-21, Exit End, 60X

73-1217-3

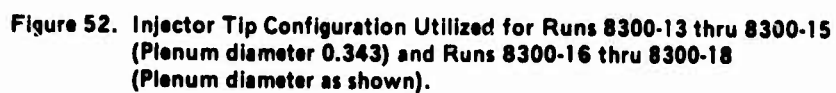
Table IX. 12.45-inch Nozzle Throat Insert Deposition Conditions.

Run Ident No.	Log Book No.	Annulus N ₂ (SCFH)	Process N ₂ (SCFH)	CH ₄ (SCFH)	Volume Percent CH ₄	Dep. Temp. (°F)	Dep. Time (hr)	Remarks
8300-13	009-27	100	960	30	2.8	3950	3.00	Pilot run utilizing 12.45-in. insert design. High N ₂ rate and low CH ₄ concentration utilized to minimize sooting in gas stream.
8300-14	009-28	100	960	30	2.8	3950	3.00	Large mandrel utilized to reduce annular area of deposition chamber. Mandrel set on four 1/2-inch diameter posts to increase gas exhaust area.
8300-15	009-30	100	960	30	2.8	3950	3.00	Utilized same configuration as 8300-13 with no mandrel
8300-16	009-31	100	1440	30	1.9	3950	3.00	Reinstalled mandrel from run 8300-13 to increase deposition rate. Increased N ₂ process rate to reduce sooting in gas stream.
8300-17	009-32	100	1200	30	2.3	3950	4.50	Reinstalled shortened mandrel from run 8300-14 to increase deposition rate. Process N ₂ rate reduced.
8300-18	009-33	100	1200	30	2.3	3950	8.00	Generator shut-off at 4.5 hours causing a temporary reduction of 900°F in the deposition temperature.
8300-19	009-34	100	1200	30	2.3	3950	8.00	Mandrel lowered 1/4 inch to increase deposition rate at downstream end of substrate. New injector tip with smaller orifices utilized.
8300-20	009-36	100	1452	30	1.9	3950	8.00	Increased process N ₂ rate to reduce sooting in gas stream.
8300-21	009-38	100	1452	30	1.9	4100-4350	8.50	Deposition temperature increased to increase coating density. Temperature also increased, during deposition to compensate for insulating effect of coating.
8300-22	009-42	100	1452	30	1.9	4100-4200	7.00	Mandrel raised in chamber in an attempt to increase the deposition rate at substrate exit end.
8300-23	009-45	100	1452	30	1.9	4100-4200	4.17	Mandrel appeared to be shading aft end of substrate so it was lowered.
8300-24	009-49	100	1452	30	1.9	4100-4200	8.50	Substrate raised 1/2-inch, in deposition chamber, to increase deposition rate at exit end.
8300-25	009-50	100	1452	39	2.5	4100-4200	7.10	CH ₄ rate increased to increase deposition rate.
8300-26	009-51	100	1452	39	2.5	4150 (Avg.)	4.00	Injector lowered 1/4 inch. Gas exhaust tube plugged at 4 hours.

Table X. 12.45-inch Nozzle Throat Insert Substrate and Coating Data.

Run Ident. No.	Log Book No.	Substrate		Coating Thickness (in)			Deposition Rate (mils/hr)			Appearance
		Material	Configuration	Entrance	Throat	Exit	Entrance	Throat	Exit	
300-13	009-27	AGSR-VCG (surface treated)	1	NE ^a	0.014	NE ^a	—	4.7	—	Entire deposition chamber inner surface covered by -linkers and flower-like carbon growths.
300-14	009-28	Reused above part	1	NE ^a	0.016	NE ^a	—	5.3	—	Entire mandrel surface covered with sooty deposits. Forward end of substrate covered with linkers. Exit end rough and irregular.
300-15	009-30	Reused above part	1	NE ^a	0.010	NE ^a	—	3.3	—	Coating covered with flower-like carbon growths.
300-16	009-31	Reused above part	1	0.015	0.014	0.015	5.0	4.7	5.0	Coating free of surface defects. End thicknesses are very difficult to determine and may be in error by 50 percent.
300-17	009-32	Reused above part.	1	0.033	0.032	0.029	7.3	7.1	6.4	Coating free of surface defects.
300-18	009-33	Reused above part	1	0.055	0.059	0.034	6.9	7.4	4.3	Coating surface free of defects. Coating delaminated where deposition temperature fell about midway through run.
300-19	009-34	AGSR-VCG (surface treated)	1	0.061	0.060	0.042	7.7	7.5	5.3	Coating gray in color and somewhat rough in surface texture. Entrance end delaminated severely during machining.
300-20	009-36	Reused 8300-18 substrate	1	0.057	0.050	0.039	7.1	6.3	4.9	Coating gray in color and slightly smoother than 009-34. No major defects. Some intraconical delaminations visible. Sent to TRW. Coating density somewhat less than 2.20 (2.15 - 2.20)
300-21	009-38	AGSR-VCG (surface treated)	1	0.060	0.061	0.040	7.1	7.2	4.7	Coating contains several nodules about 1/16 inch diameter between entrance end and throat. Coating black in color. No significant delaminations visible.
300-22	009-42	AGSR-VCG/ Annealed (surface treated)	1A	0.043	0.049	0.026	6.1	7.0	3.7	Coating surface appearance is good. Ends show no significant cracks or delaminations. A few large growth cones contain occasional intraconical delaminations. Sent to TRW.
8300-23	009-45	AGSR-VCG/ Annealed (surface treated)	1B	0.025	0.029	0.012	6.0	7.0	2.9	Coating surface appearance is very good. Coating ends similar in appearance to No. 009-42.
8300-24	009-49	AGSR-VCG/ Annealed (surface treated)	1C	0.058	0.055	0.054	6.8	6.5	6.4	No significant flaws.
8300-25	009-50	AGSR-VCG/ Annealed (surface treated)	1C	0.058	0.065	0.057	8.2	9.2	8.0	Two longitudinal cracks in coating inner surface extending from entrance to exit end. Ends of these cracks radiate into circumferential delaminations at both ends. Coating surface rough in texture and gray in color.
8300-26	009-51	AGSR-VCG/ Annealed (surface treated)	1C	0.023	0.033	0.033	5.8	8.3	8.3	No examination of coating ends. Coating surface rough in texture and gray in color.

^aNot Examined



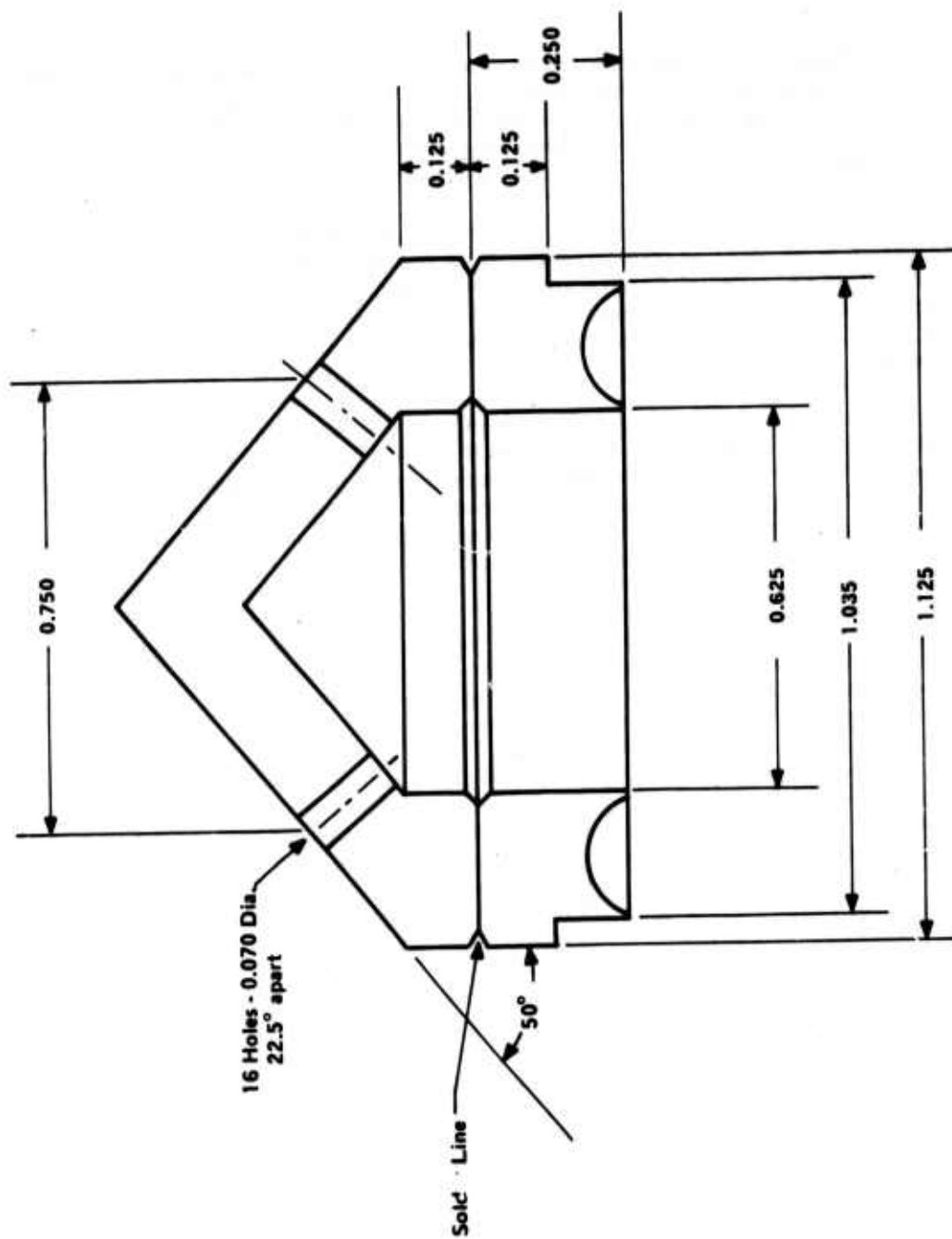


Figure 53. Injector Tip Configuration Utilized for Runs 8300-19 thru 8300-26.

The substrate inner contour was the same for all fourteen runs and is shown in Figure 54. Also shown are the various stress-relief groove modifications which were utilized. The substrate outside diameter was 16.550 inches for Runs 8300-13 through 8300-22. The substrate outside diameter was reduced to 15.550 inches for Runs 8300-23 through 8300-26 to allow the substrate to yield during cooldown and, therefore, relieve some of the stresses induced within the coating because of substrate/coating CTE mismatch.

Substrate dimensions were recorded before and after deposition for Runs 8300-22, 8300-23, 8300-25 and 8300-26 to determine how much deformation of the substrates occurred after cooldown. These data are summarized in Table XI. Although the data is fragmentary, there was in all cases a definite expansion of the substrate outside diameter after coating. The magnitude of these deformations is indicative of the severe stresses which exist in both coating and substrate after cooldown. The data from the length measurements is too fragmentary to be meaningful.

Run 8300-13, the first of the 12.45-inch series, was conducted utilizing a total gas flow rate 29 percent higher than that of the latter 13.0-inch deposition runs. The methane concentration was, however, reduced by 28 percent. The higher flow rates and lower methane concentration were an attempt to reduce sooting within the gas phase, which was the primary cause of the clinkerlike growths and other similar aberrations which occurred in the 13.0-inch series. The deposition chamber geometry is shown in Figure 55. Post-deposition examination showed the entire deposition chamber to be covered with flowerlike carbon growths. The coating at the nozzle ends was too thin to be measurable.

Run 8300-14 was conducted using the same gas flow rates as the previous run. A much larger mandrel was utilized to reduce the free-volume within the deposition chamber. The deposition chamber geometry is shown in Figure 56. Post-deposition examination showed the deposition chamber to be covered with flowerlike carbon growths. There was significantly more sooting than in the previous run.

Run 8300-15 was conducted using the same gas flow rates as the previous two 12.45-inch deposition runs. The deposition chamber geometry was the same as that of Run 8300-13 (see Figure 55), except the mandrel was removed. Post-deposition examination showed the entire inner surface of the deposition chamber to be covered with flowerlike carbon growths. An examination of the injector tip showed the gas flow rate through five adjacent ports to be considerably lower than that of the other eleven. This condition caused an area of gas recirculation within the deposition chamber and probably contributed to the excessive sooting encountered during this and the previous two 12.45-inch deposition runs.

Run 8300-16 was conducted utilizing a 50 percent higher process nitrogen flow rate than that of the previous run. The deposition chamber geometry was the same as that of Run 8300-13 (see Figure 55), during which the smaller of the two 12.45-inch mandrels was used. The injector tip plenum was enlarged to correct the problem of unequal flow rates which was discovered after the previous run. Post-deposition examination showed the deposition chamber to be completely free of the type of abnormal growths encountered in the three previous 12.45-inch runs. The nozzle coating was smooth, and the thickness distribution was acceptable. The deposition rate was lower than desired, and the objective of the next fabrication run was to increase this rate.

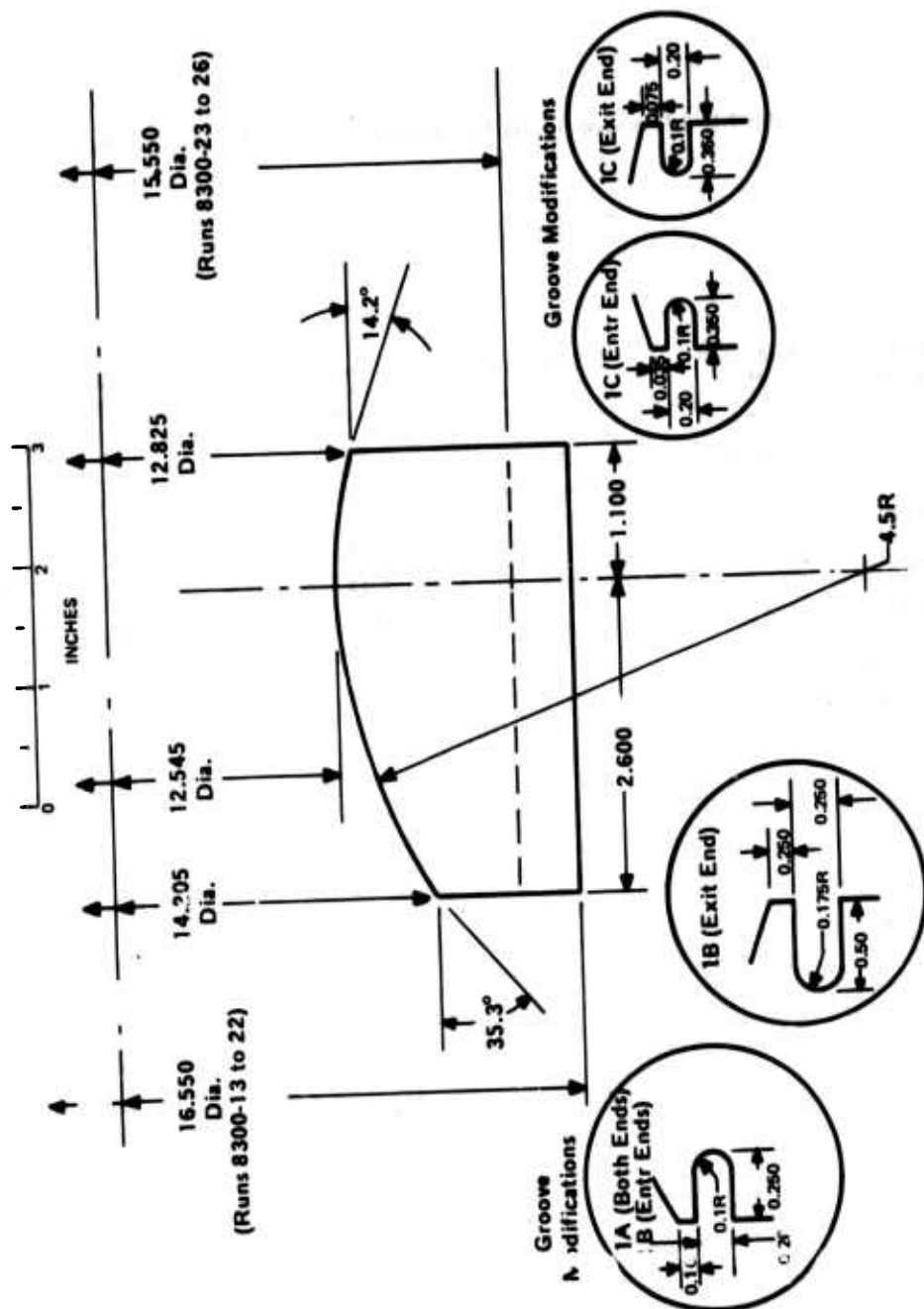



Figure 54. 12.45-inch Nozzle Throat Insert Substrate Configuration 1 (Including groove modifications).

Table XI. 12.45-inch Nozzle Throat Insert Substrate Dimensional Data.

<u>Run Ident No.</u>	<u>Log Book No.</u>	<u>Substrate Material</u>	<u>Entrance OD</u>	<u>Throat OD</u>	<u>Exit OD</u>	<u>Length</u>
8300-22	009-42	AGSR-VCG (Annealed) 	0.20	0.15	0.14	—
8300-23	009-45		0.19	0.11	0.10	—
8300-25	009-50		0.14	—	0.10	0
8300-26	009-51		0.14	—	0.10	0.08
Average			0.17	0.13	0.11	0.04

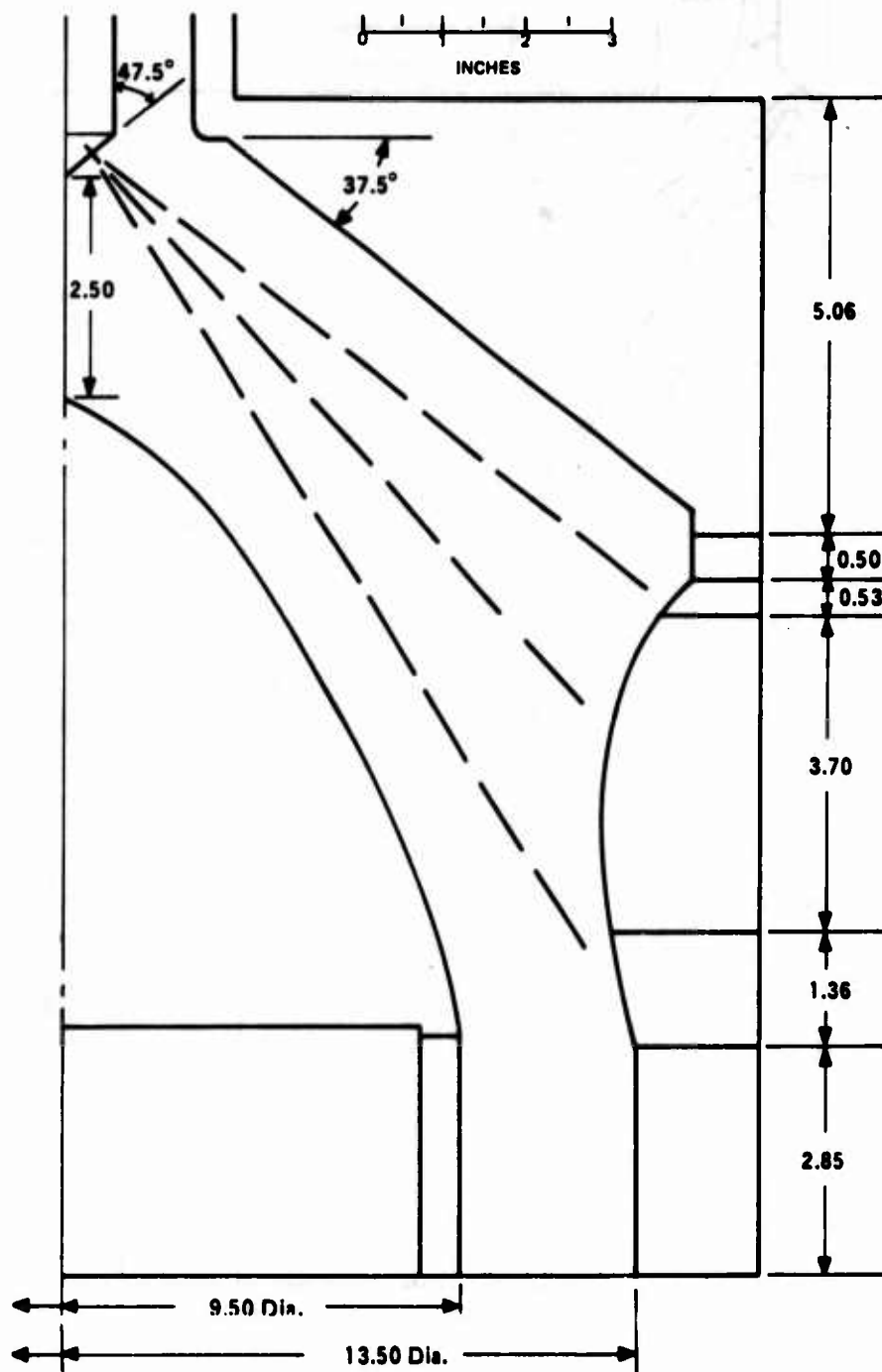


Figure 55. Deposition Chamber Geometry of Run No's. 8300-13, 8300-15 (Mandrel removed) and 8300-16.

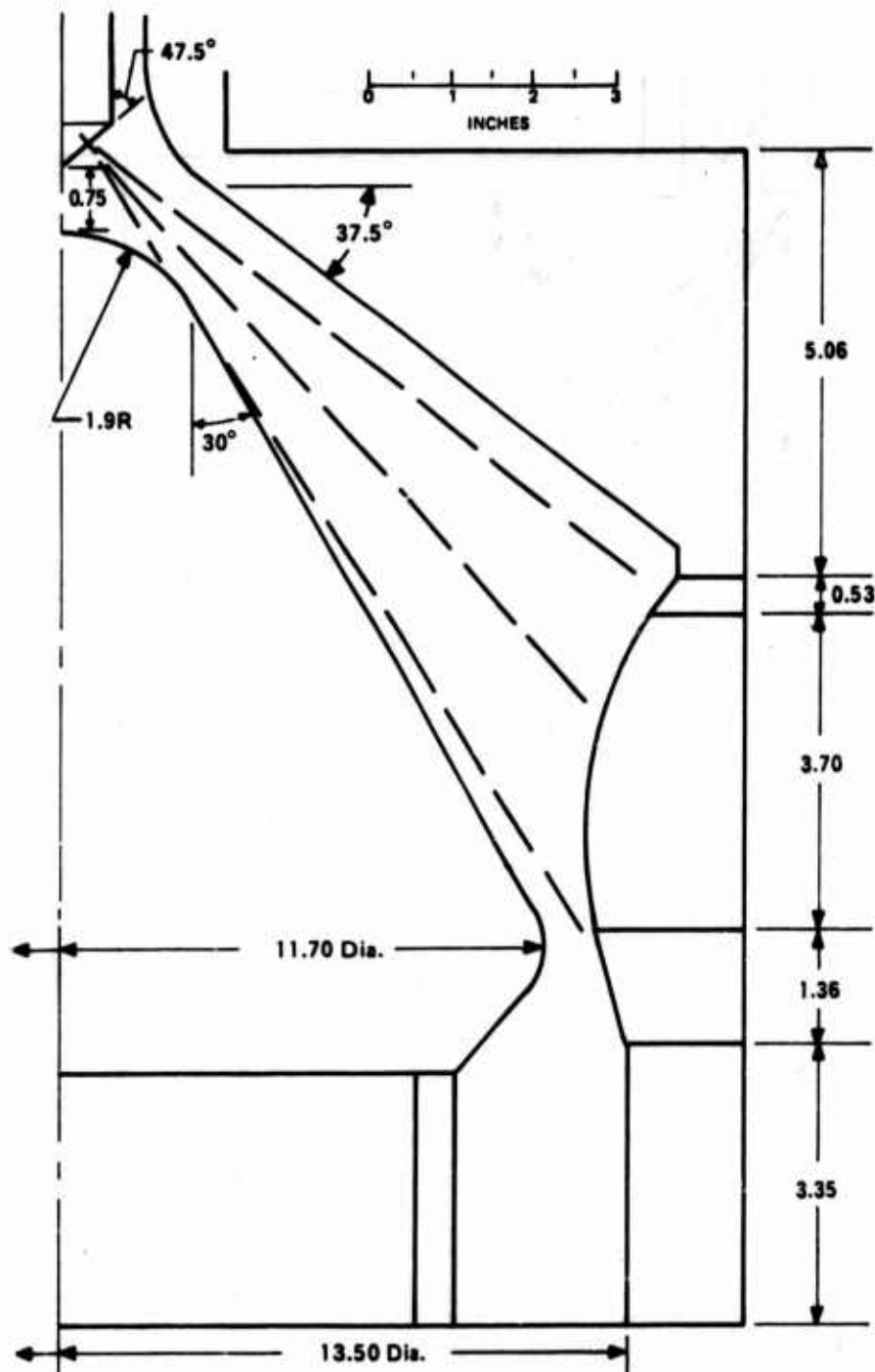


Figure 56. Deposition Chamber Geometry of Run No. 8300-14.

Run 8300-17 was conducted using a process nitrogen flow rate midway between that of Runs 8300-15 and 8300-16. The methane rate was unchanged, which effectively increased the concentration by 21 percent. The larger of the two 12.45-inch mandrels was shortened by 1.5 inches at the tip and installed to increase the deposition rate. The deposition chamber geometry is shown in Figure 57. Post-deposition examination showed the deposition chamber to be free of any abnormal deposits. The nozzle coating was smooth and free of surface defects and the gas exhaust area was clean. The deposition rate increased by 46 percent at the entrance end, 51 percent at the throat and 28 percent at the exit end.

Run 8300-18 was conducted utilizing the same gas flow rates and deposition chamber geometry (Figure 57) as the previous run with one slight modification; the injector was moved 0.25 inch closer to the nozzle substrate. After 4 1/2 hours of deposition, the power to the furnace was interrupted by a loss of water pressure in the motor generator. The deposition temperature dropped to 3050°F at this time, and approximately 1 1/2 hours were required for the furnace to regain the desired temperature. Post-deposition examination showed the deposition chamber to be free of any abnormal carbon growths, and the surface appearance of the nozzle coating was good. The drop in temperature caused a line of renucleation within the coating, and as a result the coating delaminated in this area. The coating deposition rate decreased by 5 percent at the entrance end and increased by 4 percent at the throat. The rate at the exit end decreased by 33 percent.

Run 8300-19 was conducted utilizing the same deposition gas flow rates as the previous two runs. The mandrel was lowered 1/4 inch to increase the deposition rate at the exit end. The deposition chamber geometry is shown in Figure 58. A new injector tip was fabricated (see Figure 53) with reduced orifice diameters to increase the pressure in the plenum and stabilize the flow rate through the individual gas ports. Post-deposition examination showed the coating to be gray in color and to have a somewhat rough surface texture; the microstructure showed large cone angles. The coating at the entrance end delaminated extensively during the trimming operation. The deposition rate increased by 12 percent at the entrance end, 1 percent at the throat and 23 percent at the exit end.

Run 8300-20 was conducted utilizing a process nitrogen rate slightly higher than 8300-16. This represented an increase of 21 percent over the process nitrogen rate of the previous run. Other process conditions were the same as those of the previous run. The mandrel was moved up 1/4 inch in the deposition chamber; otherwise, the geometry was like that of the previous run (see Figure 58). These changes were made in an attempt to improve the coating microstructure and surface condition which had deteriorated in the previous run. Post-deposition examination showed the coating surface to be similar to that of 8300-19. No significant defects were visible in the polished coating ends. The coating microstructure was somewhat improved over that of 8300-19 but was still not acceptable. The density of the coating was determined to be less than 2.20 g/cc, using the sink/float technique, indicating that the deposition temperature was too low. An overall decrease in deposition rate occurred because of the reduced methane concentration in the process gas.

Run 8300-21 was conducted at an increased deposition temperature. The temperature at the beginning of the cycle was 4100°F. The deposition temperature was to have been slowly increased 400°F during the run. However, full power was reached at six hours, at which time a 250°F temperature increase was achieved. From that time, the temperature readings declined slowly to 4200°F at which time deposition was terminated. The general increase in deposition temperature was utilized to increase the coating density and to improve the coating microstructure. The temperature increase during deposition was to maintain the surface temperature of the coating

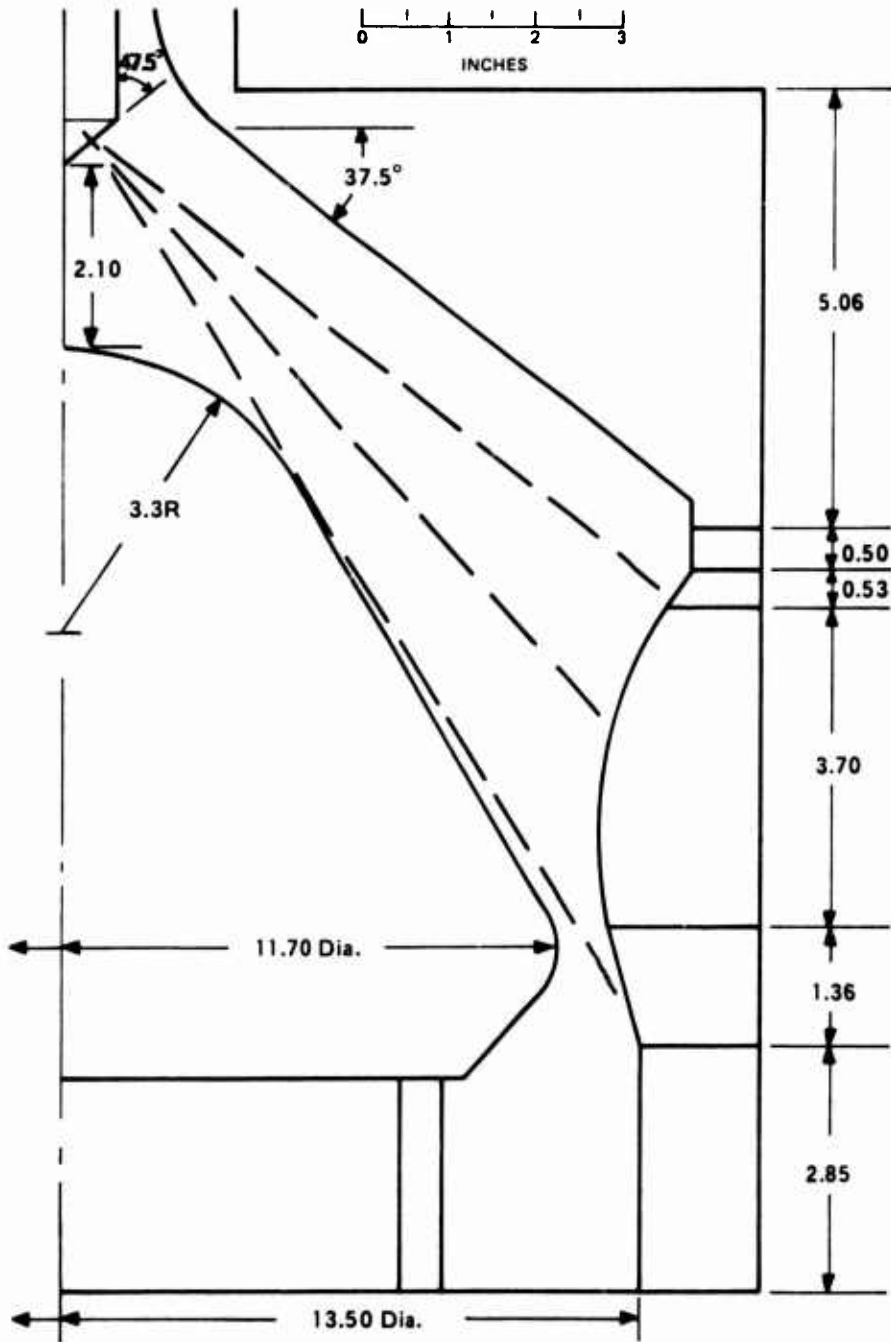


Figure 57. Deposition Chamber Geometry of Run No's. 8300-17 and 3300-18 (Injector lowered 1/4 inch).

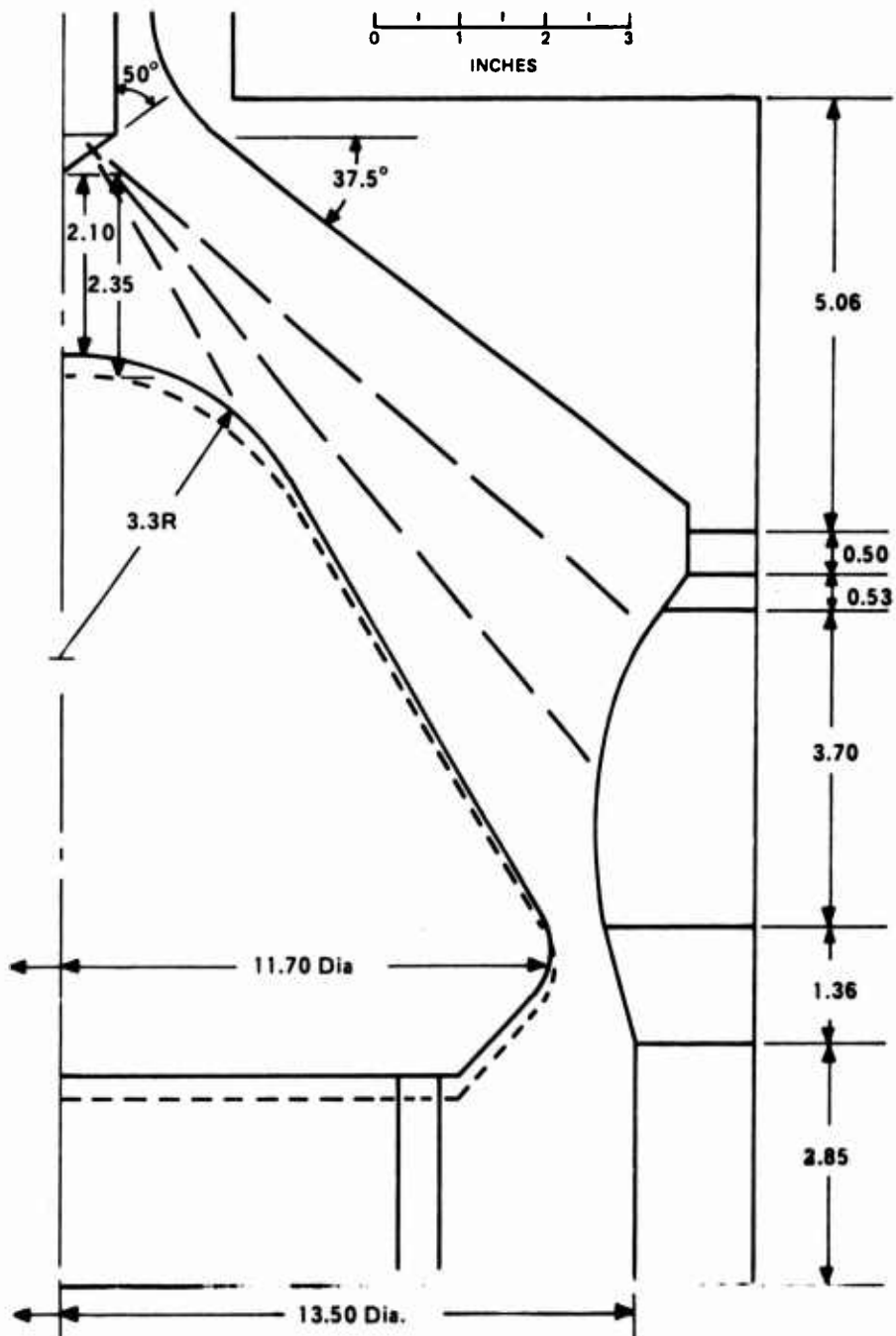


Figure 58. Deposition Chamber Geometry of Run No's 8300-19 (Mandrel position indicated by broken line), 8300-20 and 8300-21.

as the coating thickness increased. The deposition gas flow rates and the deposition chamber geometry (Figure 58) were the same as those of the previous run. Post-deposition examination showed the coating to be of acceptable quality with the exception of several large nodules at the entrance end. These nodules appeared to have started early in the cycle and were all about the same size. Microscopic examination of the coating ends showed no major cracks or delaminations. The coating deposition rate increased by 14 percent at the throat and decreased by 4 percent at the exit end. No change occurred at the entrance end.

Run 8300-22 was conducted utilizing the same deposition gas flow rates as the previous run. The mandrel body was raised 0.8 inch to fill some of the free-volume in the deposition chamber and increase the deposition rate of the coating. The deposition chamber geometry is shown in Figure 59. The deposition temperature was 4100°F at the beginning of the cycle and was increased, slowly and evenly, to 4200°F at termination. Post-deposition examination showed the coating surface texture to be very good. Microscopic examination of the polished coating ends showed no cracks or significant delaminations. There were a few large growth cones present which contained an occasional intraconical delamination. The coating thickness at the throat was less than the desired 60 mils. The deposition rate decreased by 14 percent at the entrance end, 3 percent at the throat and 21 percent at the exit end. Apparently the mandrel was deflecting the gas, from the substrate, causing an overall reduction in the deposition rate.

Run 8300-23 was conducted for 4 hours and 10 minutes. The planned time was 8 1/2 hours, but a malfunction of the methane regulator caused a severe drop in the flow rate and deposition had to be terminated prematurely. The deposition chamber geometry (Figure 60) was the same as that of the previous run except the mandrel body was lowered 3/8 inch. The deposition gas flow rates were the same as those of the previous run. Post-deposition examination showed the coating surface appearance to be very good. Microscopic examination of the polished coated ends indicated that the coating structure was the same as that of the previous 12.46-inch nozzle. The deposition rates at the entrance end and the throat were essentially unchanged. However, the rate at the exit end had declined by 22 percent and, consequently, the exit end coating was much thinner than desired.

Run 8300-24 was conducted using the same gas flow rates as the past several runs. The stress relief grooves in the substrate ends conformed to the dimensions established by the stress analysis groove optimization studies for the 7-inch size (see Volume II). The substrate was raised 0.5 inch in the deposition chamber to increase the coating deposition rate at the exit end. The deposition chamber geometry is shown in Figure 61. Post-deposition examination showed the coating surface quality to be very good. The coating thickness distribution was satisfactory with a variation of only 4 mils from entrance to exit end. Microscopic examination of the polished coating ends showed a good renucleated structure with only an occasional large growth cone containing intraconical delaminations. No significant cracks or delaminations were visible at either end.

Run 8300-25 was conducted at a 32 percent higher methane concentration than that of the previous run in an attempt to increase the coating deposition rate. The remaining deposition gas flow rates and the deposition chamber geometry (Figure 61) were the same as those of the previous run. During deposition the furnace rotator stopped twice. The second time the furnace power had to be interrupted long enough to replace the rotator motor;

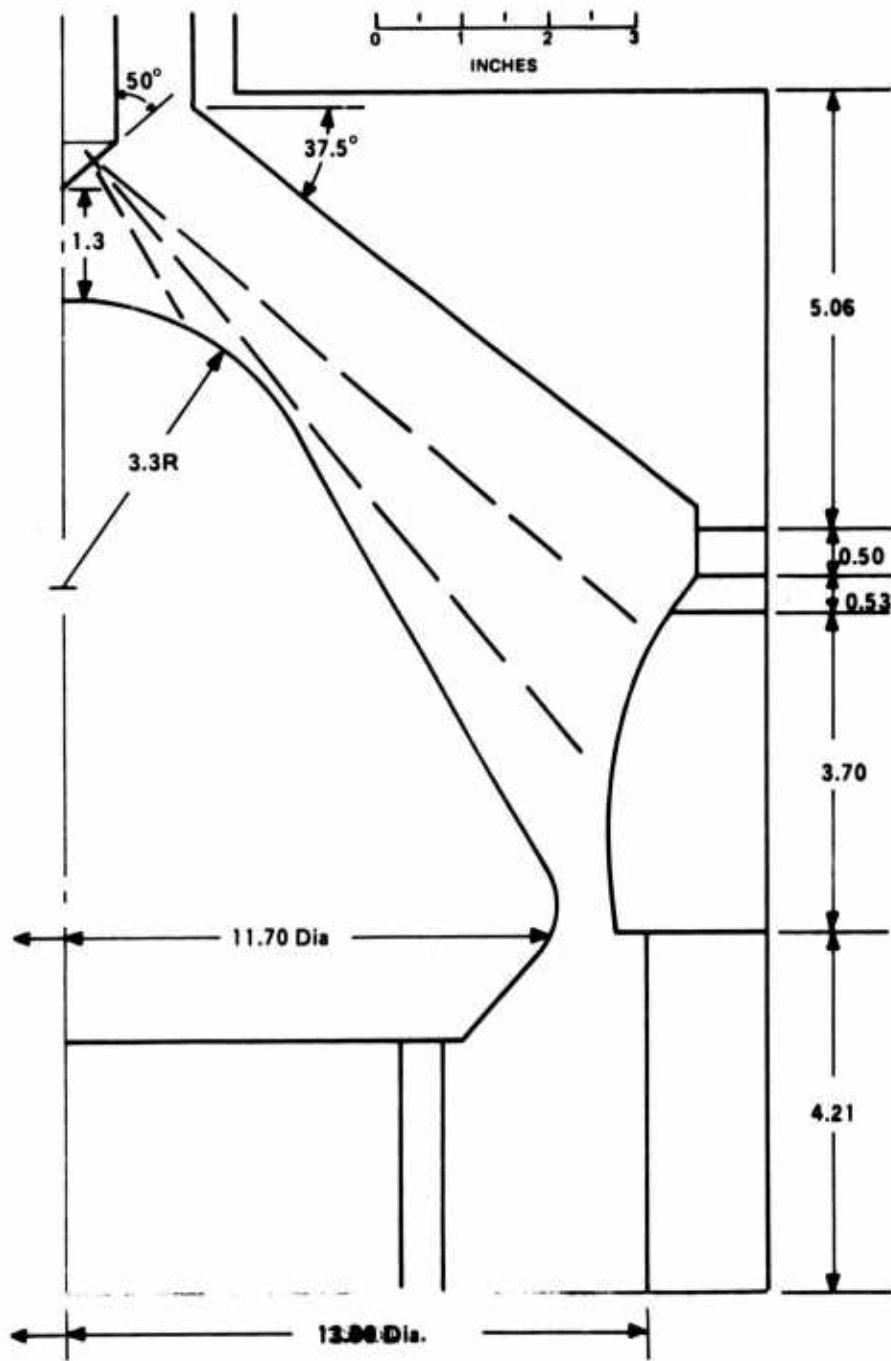


Figure 59. Deposition Chamber Geometry of Run No. 8300-22.

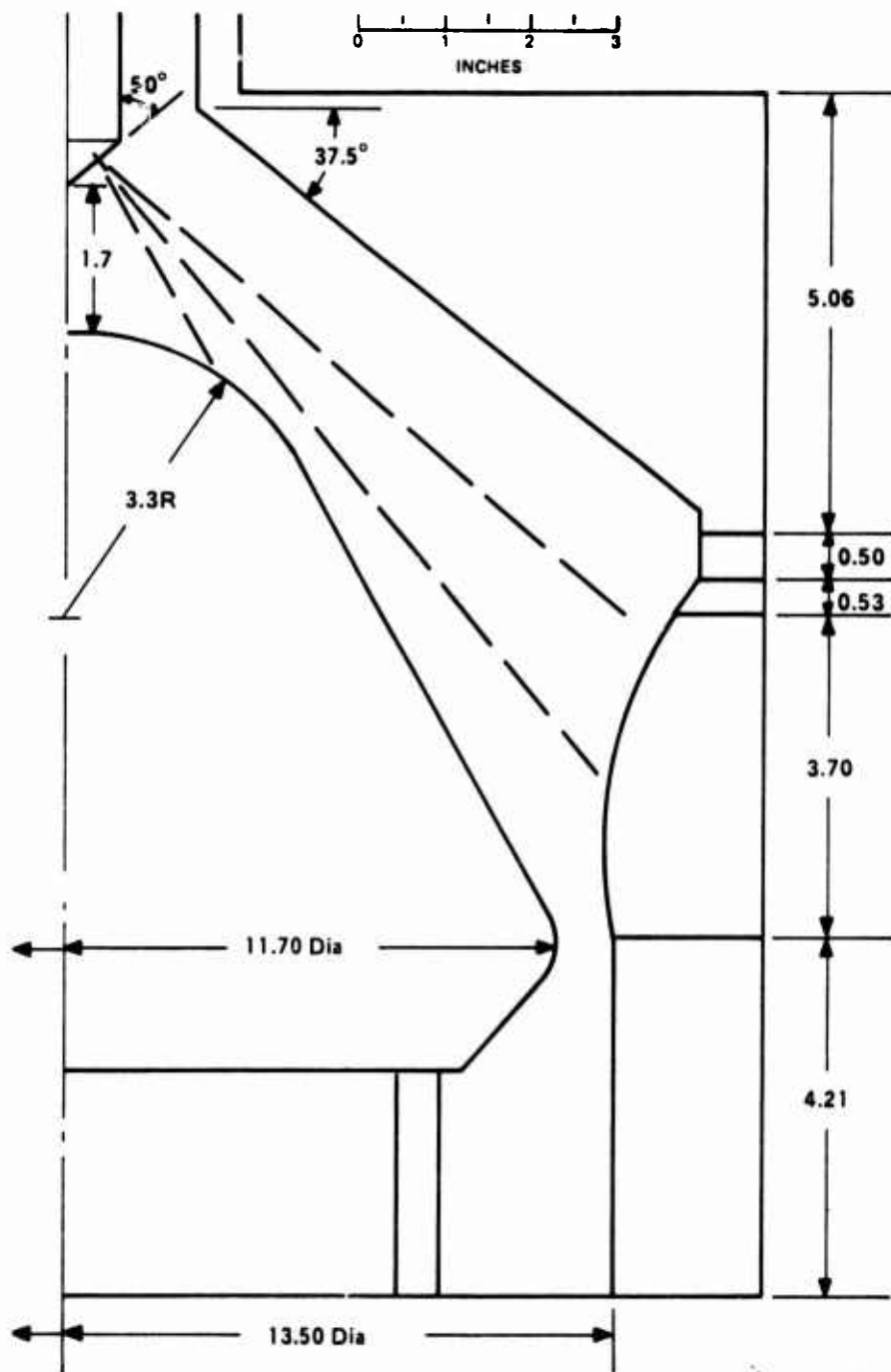


Figure 60. Deposition Chamber Geometry of Run No. 8300-23.

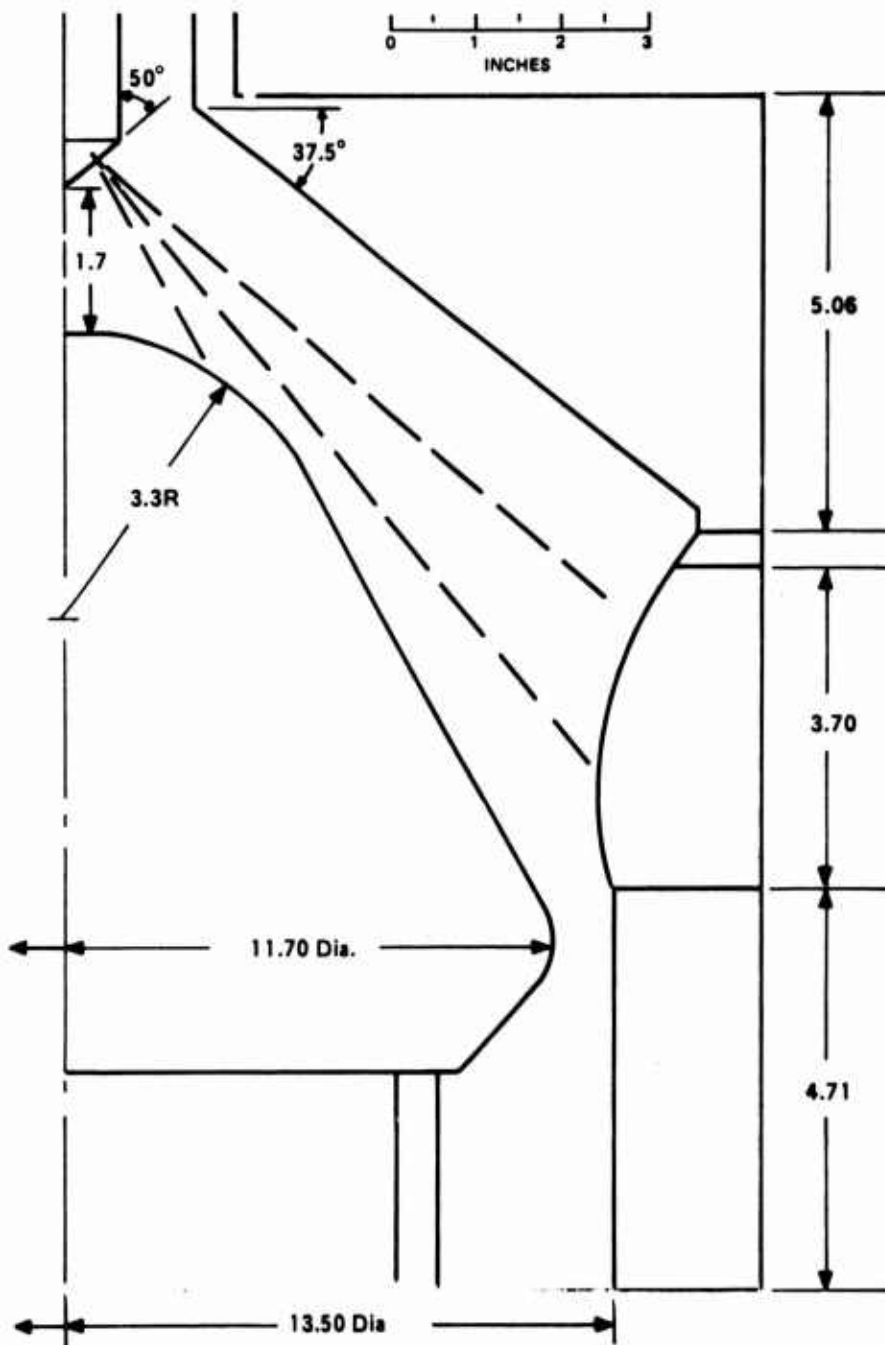


Figure 61. Deposition Chamber Geometry of Run No's. 8300-24, 8300-25 and 8300-26 (Injector lowered 1/4 inch).

as a result, the deposition temperature dropped 400°F. Post-deposition examination showed the coating to be gray in color and rather rough in texture. The coating inner surface contained two longitudinal cracks extending from the entrance to the exit end. At the coating ends these cracks radiated into circumferential delaminations within the coating. These coating defects were a direct result of the extreme drop in the deposition temperature and, with the possible exception of the coating roughness, would not have occurred if the deposition temperature had remained at the desired level. The coating deposition rate increased by 21 percent at the entrance end, 42 percent at the throat and 25 percent at the exit end.

Run 8300-26, the last of the 12.45-inch series, was conducted using the same deposition gas flow rates as the previous run and for the same purpose. The deposition chamber geometry (Figure 61) was unchanged with the exception of the injector which was lowered 1/4 inch. After four hours of deposition, the gas exhaust tube clogged and forced termination of the run. Post-deposition examination showed the coating to be rough and gray in color. The appearance indicated that the deposition temperature was too low. The coating deposition rate decreased by 29 percent at the entrance end and 10 percent at the throat and increased by 4 percent at the exit end.

SECTION VII

DISCUSSION

Nominal deposition parameters were established for all three nozzle throat insert sizes. These are shown in Table XII.

The last fourteen 7.0-inch deposition runs were conducted using similar process conditions and the same deposition chamber geometry. The standard deviation of the coating deposition rate was calculated at the entrance, throat and exit planes for these runs and is included in Table XII. This variation was acceptable considering that no significant effort was expended in achieving more uniform rates, and the fact that these 14 runs were conducted over a time span of 11 months.

Although the last of the three 10.6-inch deposition runs did yield a marginally acceptable coating, the deposition conditions utilized were not considered to be optimum. An increase in the process nitrogen rate on the order of 50 to 100 percent would be expected to yield coatings with a more uniform coating thickness profile. Such an increase would have been utilized had additional runs been conducted at this size.

The parameters used for Run 8300-24 were quite suitable for the 12.45-inch size. Although the deposition rates were somewhat lower than desired, they would be considered acceptable unless very thick coatings and, therefore, longer deposition times were required.

The various deposition chamber geometries used for large nozzle deposition runs indicate that the deposition rate is increased significantly by the utilization of a mandrel body in the center of the deposition chamber. In those cases where a mandrel was not used, the coating deposition rate and proportional thickness at the ends were both severely reduced.

The injector tip configuration was established by utilizing the fact that a turbulent gas jet expands from an orifice at an included angle of 20 degrees. The injector orifices were angled toward the substrate and the injector was positioned so that the expanding gas cone completely enveloped the substrate surface. Nozzle substrates, coated with the injector tip located so near the part that the gas cone could not expand fully, had an excessive deposition rate in the area of impingement and, as a result, these parts had an unacceptable coating thickness profile.

Process nitrogen flow rates were established as a function of the amount of sooting in the gas phase. In general, if the inside surface of the deposition chamber was found to contain soot or carbon growths, an increase in the process nitrogen rate was used to eliminate the problem. Increasing the gas flow rate reduces the deposition gas temperature by reducing the dwell time in the chamber. This prevents the formation of soot particles in the gas phase which, if present, lodge on the coating surface forming nuclei for flowerlike carbon growths and large nodules.

Table XII. Nominal Process Conditions for Large Nozzle Deposition Runs.

Nozzle Throat Insert Code	Annulus Nitrogen Rate (SCFH)	Process Nitrogen Rate (SCFH)	CH ₄ Concentration (volume percent)	Expected Deposition Rate (mils/hr)			Deposition Chamber Geometry
				At Entrance	At Throat	At Exit	
6300 ^a	100	480	2.5	9.3	10.2	7.9	Figure 35
		Standard Deviation		0.8	0.7	0.6	
7300 ^b	80	448	4.5	8.0	10.8	5.4	Figure 39
8300 ^c	100	1452	1.9	6.8	6.5	6.4	Figure 61

^aData derived from last 14 deposition runs.

^bData derived from Run No. 7300-3.

^cData derived from Run No. 8300-24.

Although coatings up to 60 mils in thickness readily survived the deposition cycle, they did not survive during the 7.0-inch nozzle throat insert test firings (see Volume I). The expansion of the substrate outside diameters after deposition indicates that AGSR is not a particularly good substrate material for large diameter AG coated parts. A substrate material with a hoop direction CTE similar to that of PG in the "ab" plane would yield a system with greatly reduced stress levels, both in the coating and the substrate, and increase their likelihood of surviving the firing cycle.